



UNIVERSITI TEKNOLOGI PETRONAS

Approval by Supervisor (s)

The undersigned certify that they have read, and recommend to The Postgraduate Studies Programme for acceptance, a thesis entitled “Switching Time Optimization via Time Optimal Control for Natural Gas Vehicle Refueling” submitted by Mahidzal Dahari for the fulfillment of the requirements for the Degree of Masters of Science in Electrical & Electronic Engineering.

Date: 30<sup>th</sup> June 2006

Signature: \_\_\_\_\_



Main Supervisor: Dr. Nordin Saad

Date: \_\_\_\_\_

26 June 2006

Signature: \_\_\_\_\_



Co-Supervisor: A. P. Dr. Mohamed Ibrahim Abdul Mutalib

Date: \_\_\_\_\_

27 June 2006

UNIVERSITI TEKNOLOGI PETRONAS

Switching Time Optimization via Time Optimal Control  
for Natural Gas Vehicle Refueling

By

MAHIDZAL DAHARI

A THESIS  
SUBMITTED TO THE POSTGRADUATE STUDIES PROGRAMME  
AS A REQUIREMENT FOR THE  
Degree of Masters of Science  
In Electrical & Electronic Engineering

BANDAR SERI ISKANDAR,  
PERAK,

JUNE, 2006

Title of Thesis

Switching Time Optimization via Time Optimal Control for  
Natural Gas Vehicle Refueling

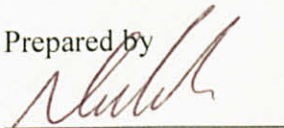
I, MAHIDZAL DAHARI hereby allow my thesis to be placed at the Information Resource Center (IRC) of Universiti Teknologi PETRONAS (UTP) with the following conditions:

1. The thesis becomes the property of UTP
2. The IRC of UTP may make copies of the thesis for academic purposes only.
3. This thesis is classified as

Confidential

Non-confidential

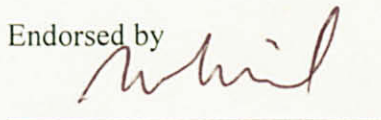
Prepared by



Mahidzal Dahari  
1936 Jalan E5/11,  
Taman Ehsan, 52100,  
Kepong,  
Kuala Lumpur,

Date: 30<sup>th</sup> June 2006

Endorsed by



Dr. Nordin Saad  
Electrical & Electronics  
Engineering Programme,  
Universiti Teknologi PETRONAS,  
Bandar Seri Iskandar,  
31750 Tronoh,  
Perak.

Date: 30<sup>th</sup> June 2006

I, hereby declare that the thesis is based on my original work except for quotations and citations which have been duly acknowledged. I also declare that it has not been previously or concurrently submitted for any other degree at UTP or other institutions.

Signature: \_\_\_\_\_



Name: \_\_\_\_\_

MAHIDZAL BIN DAHARI

Date: \_\_\_\_\_

30 JUNE 2006

## ACKNOWLEDGEMENT

The present research work which was funded by IRPA of Ministry of Science Technology and Innovation (MOSTI) was carried out from January 2004 to April 2006 under the supervision of Dr. Nordin Saad from the Electrical & Electronic Engineering Programme and Assoc. Prof. Dr. Mohamed Ibrahim Abdul Mutalib from the Chemical Engineering Programme of Universiti Teknologi PETRONAS. I would like to thank my supervisor and co-supervisor for providing the guidance and advices needed to complete this research.

I would also like to thank everyone who has directly or indirectly contributed towards this research work especially my family members, colleagues, Compressed Natural Gas Direct Injection (CNGDI) project members, PETRONAS Natural Gas Vehicle (PNGV) staff members, Petronas Research and Scientific Services (PRSS) staff members, Research Enterprise Office (REO) staff members, Postgraduate Study Programme staff members, Electrical & Electronic Engineering (E&E) Programme staff members and others.

Mahidzal Dahari

JUNE 2006

## ABSTRACT

The implementation of Natural Gas Vehicle (NGV) refueling system using multi-pressure storage source requires a suitable controller to be developed. In this thesis, a refueling algorithm using Time Optimal Control (TOC) technique is proposed as a basis for determining the optimal switching time in NGV refueling using the mass and mass flowrate as the state variables, measured using Coriolis flowmeter. In order to implement TOC in actual NGV refueling process, a fully instrumented NGV laboratory test facility was designed and commissioned which includes three main parts: the NGV test rig, the Data Acquisition (DAQ) & Control System using FieldPoint, and the LabVIEW programming model. Performance measurements for experiments conducted at NGV test rig are based on two criteria, i.e., the refueling time and the total mass of natural gas stored. These become the performance measurements used to evaluate the performance of TOC and other NGV controller currently applied in the commercial NGV dispenser i.e., Kraus refueling algorithm. The performance of the refueling algorithms are evaluated based on three experiments: the first experiment is the performance of valves switching and refueling time transitions; the second experiment is the performance of refueling when the storage pressures are set to 3600 psig while the receiver tank is varied from 20 to 2000 psig; and the third experiment is the performance of refueling when the storage pressures are set to different pressures while the receiver tank is maintained at 20 psig. In conclusion, the results from the third experiment verifies the viability of TOC refueling compared to Kraus refueling to be used in NGV refueling using multi-pressure storage source, which average difference for refueling time and total mass loss are 25.33 seconds and 0.95 kg, respectively. By implementing the refueling algorithm in actual NGV refueling stations, it is expected to provide saving in term of the energy consumed by the compressor and contributing to the reduction in the NGV station congestion problem in the country.

## ABSTRAK

Penggunaan sistem pengisian untuk kenderaan gas asli dari tangki simpanan berlainan tekanan memerlukan satu alat kawalan yang sesuai. Dalam tesis ini, satu algoritma pengisian menggunakan teknik Kawalan Masa Optimal berdasarkan jisim dan kadar aliran jisim gas asli yang disukat oleh alat sukatan Coriolis dicadangkan untuk menentukan masa yang tepat bagi mengubah pengisian dari satu tekanan ke tekanan yang lain. Untuk menguji teknik pengisian ini, sebuah alat dibuat dan terbahagi kepada tiga bahagian penting iaitu alat uji kenderaan gas asli, alat untuk menyukat data dan mengawal sistem pengisian, dan model pengaturcaraan sistem menggunakan LabVIEW. Teknik pengisian diuji berpandukan dua kriteria iaitu tempoh masa yang diambil dan jumlah jisim gas asli yang dapat disimpan sehingga pengisian gas asli didalam tangki kenderaan gas asli penuh. Keputusan teknik pengisian dibandingkan dengan teknik pengisian yang lebih komersil antaranya, algoritma pengisian oleh Kraus. Perbandingan dengan Kraus dibuat berdasarkan tiga eksperimen iaitu eksperimen pertama ialah perbandingan masa perubahan injap dan masa yang diambil untuk pengisian dari sesebuah tangki simpanan, eksperimen kedua ialah perbandingan pengisian dengan kesemua tekanan ditangki simpanan ditetapkan pada 3600 psig dan tekanan di tangki kenderaan ditetapkan daripada 20 sehingga 2000 psig, dan eksperimen ketiga ialah perbandingan pengisian dengan kesemua tekanan di tangki simpanan ditetapkan pada tekanan yang berlainan dan tekanan di tangki kenderaan ditetapkan pada 20 psig. Kesimpulannya, keputusan daripada eksperimen ketiga mengesahkan pengisian teknik Kawalan Masa Optimal adalah lebih baik berbanding pengisian Kraus untuk digunakan dalam sistem pengisian gas asli berlainan tekanan dengan purata perbezaan bagi masa pengisian dan jumlah kehilangan jisim ialah sebanyak 25.33 saat dan 0.95 kg. Penggunaan algoritma pengisian ini di stesen pengisian NGV yang sebenar dapat menjimatkan penggunaan elektrik kompresor dan mampu mengurangkan masalah kesesakan kenderaan gas asli di stesen di seluruh negara.



## LIST of PUBLICATIONS

1. V.R. Radhakrishnan, N.A. Hisam, M.I.A. Mutalib, **M.Dahari**, N.B Mellon, M.A. Abdullah, J. Mengat, "*Calculation of Mass of Gas Using Equation of State for NGV Refueling Equipment*" Paper presented in ANGVA 2005 Conference, Kuala Lumpur, July 2005
2. **M. Dahari**, N.Saad, M.I.A. Mutalib, "*Modeling of Natural Gas Vehicle (NGV) Refueling System using LabVIEW*" Paper presented in Technical Postgraduate Symposium (Techpos'04) Universiti Malaya, Petaling Jaya, Oct 2004
3. **M. Dahari**, N.Saad, M.I.A. Mutalib, "*Development of a Controller for NGV Refueling System*" Paper presented for 1<sup>st</sup> Biannual Postgraduate Research Symposium Universiti Teknologi PETRONAS, Sri Iskandar, Jan 2005
4. **M. Dahari**, N.Saad, M.I.A. Mutalib, "*Optimal Switching Time Design and Implementation for NGV Refueling Station*" Paper presented for 2<sup>nd</sup> Biannual Postgraduate Research Symposium Universiti Teknologi PETRONAS, Sri Iskandar, Jan 2006

## TABLE of CONTENTS

<b>ACKNOWLEDGEMENT.....</b>	<b>i</b>
<b>ABSTRACT.....</b>	<b>ii</b>
<b>ABSTRAK.....</b>	<b>iii</b>
<b>LIST OF PUBLICATIONS.....</b>	<b>iv</b>
<b>TABLE OF CONTENTS.....</b>	<b>v</b>
<b>LIST OF FIGURES .....</b>	<b>ix</b>
<b>LIST OF TABLES.....</b>	<b>xiii</b>
<b>LIST OF ABBREVIATIONS.....</b>	<b>xv</b>
<b>NOMENCLATURES.....</b>	<b>xvi</b>
<b>1.0 INTRODUCTION.....</b>	<b>1</b>
1.1 Background.....	1
1.2 Problem Statement.....	3
1.3 Motivation.....	4
1.4 Objectives and contribution of research.....	5
1.5 Outline of the thesis.....	6
<b>2.0 LITERATURE REVIEW.....</b>	<b>7</b>
2.1 Introduction.....	7
2.1.1 Malaysian Standard (MS) for the NGV Industry.....	9
2.2 NGV Vehicle Safety Standards.....	9
2.2.1 NGV Vehicle Technology.....	9
2.2.2 Safety in NGV Conversion Kit System.....	9
2.2.3 Onboard NGV Storage in Vehicle.....	10
2.2.4 NGV Flow within the Vehicle.....	11
2.2.5 NGV Vehicle Combustion.....	13
2.2.6 NGV Driving.....	13
2.3 NGV Refueling System - Research Challenges.....	14

2.3.1	Compressor.....	14
2.3.2	Storage Cascade.....	15
2.3.3	Dispenser.....	17
2.3.3.1	Temperature Pressure Compensation.....	18
2.3.3.2	Coriolis Flowmeter.....	18
2.4	Related Research Work on NGV Refueling System Research.....	19
2.4.1	NGV Cascade Fast Fill Process.....	21
2.4.2	Limitations of the Current System.....	22
2.4.3	Conceptual Model of CNG Filling Process.....	23
2.4.4	Pressure Variation along the Dispenser Pipe.....	26
2.4.5	Filling rate of the NGV Tank.....	28
2.4.6	Pressure Discontinuity and Energy Loss.....	29
2.5	Switching Time Issues.....	31
2.6	Related research work on time optimization problems.....	35
2.7	Strategies.....	43
2.8	Summary.....	44
<b>3.0</b>	<b>METHODOLOGY.....</b>	<b>45</b>
3.1	Introduction.....	45
3.2	Defining the implementation model.....	47
3.3	Development of optimal switching time equation.....	49
3.3.1	Step I - Designing governing equations.....	49
3.3.2	Step II - Applying Pontryagin's Minimum Principle.....	51
3.3.3	Step III - Designing Forced Trajectory.....	54
3.3.4	Step IV - Derivation of Optimal Switching and Total Minimum Time.....	62
3.3.5	Step V - Modeling of forced trajectory using Matlab Simulink.....	64
3.4	Results of simulation model.....	66
3.5	Development of experimental hardware.....	69
3.5.1	NGV test rig.....	69
3.5.1.1	Cascaded storage system.....	70

3.5.1.2	Flow metering system.....	70
3.5.1.3	Receiver system.....	71
3.5.1.4	Recycle system.....	71
3.5.1.5	Sequencing system.....	72
3.5.1.6	Dispensing system.....	72
3.5.1.7	Refueling system.....	73
3.5.1.8	Control panel system.....	73
3.5.2	DAQ & Control System.....	74
3.5.3	Programming Implementation Model.....	75
3.5.3.1	Cascaded storage model.....	75
3.5.3.2	Flow metering model.....	76
3.5.3.3	Receiver model.....	76
3.5.3.4	Recycle model.....	76
3.5.3.5	Sequencing model.....	76
3.5.3.6	Dispensing model.....	77
3.5.3.7	Refueling model.....	77
3.5.3.8	Control panel model.....	77
3.6	Validation of model.....	78
3.7	Summary.....	85
<b>4.0</b>	<b>RESULTS AND DISCUSSION .....</b>	<b>86</b>
4.1	Introduction.....	86
4.2	Performance of valves switching and refueling time transitions.....	86
4.2.1	Comparison of NGV refueling performance for Experiment 1.....	88
4.3	Performance of refueling by varying initial pressure inside receiver tank.....	89
4.3.1	Test model 2 (a): Performance of TOC refueling.....	89
4.3.2	Test model 2 (b): Performance of Kraus refueling.....	92
4.3.3	Comparison of NGV refueling performance for Experiment 2.....	96

4.4 Performance of refueling using multi-pressure storage source.....	98
4.4.1 Test model 3 (a): Performance of TOC refueling.....	98
4.4.2 Test model 3 (b): Performance of Kraus refueling.....	100
4.4.3 Comparison of NGV refueling performance for Experiment 3.....	103
4.5 Summary.....	104
<b>5.0 CONCLUSIONS AND FUTURE WORK.....</b>	<b>105</b>
5.1 Conclusion.....	105
5.2 Direction of Future Work.....	106
<b>REFERENCES.....</b>	<b>109</b>
<b>APPENDIX.....</b>	<b>113</b>

## LIST of FIGURES

Figure 1.1:	Fuel of choice for power generation.....	1
Figure 1.2:	NGV stations and vehicle population in Malaysia.....	2
Figure 2.1:	NGV diamond shape.....	10
Figure 2.2:	Bi-fuel NGV.....	12
Figure 2.3:	Schematic of NGV refueling system.....	14
Figure 2.4:	A typical NGV compressor.....	15
Figure 2.5:	A typical NGV storage cascade.....	16
Figure 2.6:	A typical NGV dispenser.....	17
Figure 2.7:	A typical NGV filling station.....	19
Figure 2.8:	NGV refueling method.....	20
Figure 2.9:	Frequency distribution of initial tank pressure of NGV.....	22
Figure 2.10:	Conceptual model of the dispenser.....	23
Figure 2.11:	Pressure distribution in pipeline for difference entrance Mach numbers.....	26
Figure 2.12:	Pressure distribution in pipeline for different source pressure.....	27
Figure 2.13:	Pressure distribution and duration of choked flow condition.....	28
Figure 2.14:	Pressure discontinuity in choked flow.....	29
Figure 2.15:	Variation of receiver pressure with time.....	30
Figure 2.16:	Variation of receiver pressure with time at source pressure of 102 psig.....	31
Figure 2.17:	Variation of receiver pressure with time at source pressure of 508 psig.....	31
Figure 2.18:	Receiver's filling time with different pressure source switching.....	32
Figure 2.19:	Graph of flowrate versus pressure for a CNG fill.....	33
Figure 2.20:	The strategy and plan of this research work.....	43

Figure 3.1:	Methodology of research work.....	46
Figure 3.2:	Implementation of TOC in NGV refueling with multi-level pressure source.....	47
Figure 3.3:	The motion of mass in a pipeline with force and initial state of mass and mass flowrate $(x_1, x_2)$ measured using Coriolis flowmeter.....	49
Figure 3.4:	The four possible 'shapes' of $p_2(t) = \pi_2 - \pi_1 t$ and the corresponding controls $u(t) = -\text{sgn}\{\pi_2 - \pi_1 t\}$ .....	55
Figure 3.5:	The forced (phase plane) trajectories in the state plane, the solid trajectories are generated by $u = 1$ and the dashed trajectories are generated by $u = -1$ .....	57
Figure 3.6:	Switch curve.....	59
Figure 3.7:	Various trajectories generated by four possible control sequences.....	60
Figure 3.8:	Closed-Loop implementation of Time-Optimal Control Law.....	64
Figure 3.9:	Simulink implementation of Time Optimal Control Law.....	65
Figure 3.10:	(a) Phase-Plane Trajectory for $\gamma_+$ with Initial State $(2, -2)$ .....	66
	(b) Total Time of Switching with Initial State $(2, -2)$ .....	66
Figure 3.11:	(a) Phase-Plane Trajectory for $\gamma_-$ with Initial State $(-2, 2)$ .....	66
	(b) Total Time of Switching with Initial State $(-2, 2)$ .....	66
Figure 3.12:	(a) Phase-Plane Trajectory for $R_+$ with Initial State $(-1, -1)$ .....	67
	(b) Total Time of Switching with Initial State $(-1, -1)$ .....	67
Figure 3.13:	(a) Phase-Plane Trajectory for $R_-$ with Initial State $(1, 1)$ .....	67
	(b) Total Time of Switching with Initial State $(1, 1)$ .....	67
Figure 3.14:	(a) Phase-Plane Trajectory for $R_-$ with Initial State $(0.018, 1)$ .....	68
	(b) Total Time of Switching with Initial State $(0.018, 1)$ .....	68
Figure 3.15:	NGV refueling test rig.....	69
Figure 3.16:	Cascaded storage system.....	70
Figure 3.17:	Flow metering system.....	70
Figure 3.18:	Receiver system.....	71

Figure 3.19:	Recycle system.....	71
Figure 3.20:	Sequencing system.....	72
Figure 3.21:	Dispensing system.....	72
Figure 3.22:	Refueling system.....	73
Figure 3.23:	Control panel for UTP NGV test rig.....	73
Figure 3.24:	FieldPoint system with I/O modules.....	74
Figure 3.25:	Programming implementation model for NGV test rig using LabVIEW.....	75
Figure 3.26:	Graph of mass flowrate for TOC refueling.....	78
Figure 3.27:	Graph for mass flowrate for TOC refueling by opening the valves within 15, 10, 8, 5 and 3 seconds during the initialization process.....	79
Figure 3.28:	Graph of mass flowrate for Kraus refueling.....	81
Figure 3.29:	Flowchart of TOC refueling algorithm.....	83
Figure 3.30:	Flowchart of Kraus refueling algorithm.....	84
Figure 4.1:	Graph of mass flowrate for TOC refueling.....	87
Figure 4.2:	Graph of mass flowrate for Kraus refueling.....	87
Figure 4.3:	Graph of mass flowrate for TOC refueling with all storage pressures set to 3600 psig and receiver tank varies from 20 to 100 psig.....	90
Figure 4.4:	Graph of mass flowrate for TOC refueling with all storage pressures set to 3600 psig and receiver tank varies from 200 to 2000 psig.....	91
Figure 4.5:	Graph of mass flowrate for Kraus refueling with all storage pressures set to 3600 psig and receiver tank varies from 20 to 100 psig.....	93
Figure 4.6:	Graph of mass flowrate for Kraus refueling with all storage pressures set to 3600 psig and receiver tank varies from 200 to 2000 psig.....	94



Figure 4.7:	Graph of mass flowrate for TOC refueling using different storage pressures with receiver tank initially at 20 psig.....	99
Figure 4.8:	Graph of mass flowrate for Kraus refueling using different storage pressures with receiver tank initially at 20 psig.....	101
Figure 5.1:	Optimization study for NGV refueling system.....	107
Figure A:	Process and Instrumentation Diagram of NGV test rig.....	115

## LIST of TABLES

Table 2.1:	Comparison of pollutants levels emitted by different automotive fuels.....	7
Table 2.2:	Retail price of different automotives fuels as of March 2006.....	8
Table 2.3:	Types of vehicles storage cylinders.....	10
Table 3.1:	Values and definitions of parameters and variables for Figure 3.2.....	47
Table 3.2:	Maximum and minimum values of mass and mass flowrate for Coriolis flowmeter used at UTP NGV test rig.....	68
Table 3.3:	The results of total time taken and total mass stored for Figure 3.27.....	79
Table 4.1:	Comparison of refueling performance based on valves switching time.....	88
Table 4.2:	Comparison of refueling performance based on refueling time transitions.....	88
Table 4.3:	Total time taken and total mass stored for TOC refueling with all storage pressures set to 3600 psig and receiver tank varies from 20 to 100 psig.....	90
Table 4.4:	Total time taken and total mass stored for TOC refueling with all storage pressures set to 3600 psig and receiver tank varies from 200 to 2000 psig.....	91
Table 4.5:	Total time taken and total mass stored for Kraus refueling with all storage pressures set to 3600 psig and receiver tank varies from 20 to 100 psig.....	93
Table 4.6:	Total time taken and total mass stored for Kraus refueling with all storage pressures set to 3600 psig and receiver tank varies from 200 to 2000 psig.....	93

Table 4.7:	Analysis of comparison for total time taken between Kraus and TOC refueling when initial pressure inside receiver tank varies from 20 to 100 psig.....	96
Table 4.8:	Analysis of comparison for total mass stored between Kraus and TOC refueling when initial pressure inside receiver tank varies from 20 to 100 psig.....	96
Table 4.9:	Analysis of comparison for total time taken between Kraus and TOC refueling when initial pressure inside receiver tank varies from 200 to 2000 psig.....	97
Table 4.10:	Analysis of comparison for total mass stored between Kraus and TOC refueling when initial pressure inside receiver tank varies from 200 to 2000 psig.....	97
Table 4.11:	Total time taken and total mass stored for TOC refueling using different storage pressures with receiver tank initially at 20 psig.....	99
Table 4.12:	Total time taken and total mass stored for Kraus refueling using different storage pressures with receiver tank initially at 20 psig.....	101
Table 4.13:	Analysis of comparison for total time taken between Kraus and TOC refueling using different storage pressures with receiver tank initially at 20 psig.....	103
Table 4.14:	Analysis of comparison for total mass stored between Kraus and TOC refueling using different storage pressures with receiver tank initially at 20 psig.....	103
Table A:	Bill of Material.....	117

### LIST of ABBREVIATIONS

Words	Abbreviation
Natural Gas Vehicle	(NGV)
Universiti Teknologi PETRONAS	(UTP)
Compressed Natural Gas	(CNG)
Input-Output	(I/O)
Time Optimal Control	(TOC)
Data Acquisition	(DAQ)
Compressed Natural Gas Direct Injection	(CNGDI)
PETRONAS Natural Gas Vehicle	(PNGV)
Research Enterprise Office	(REO)
Department of Occupational Safety and Health	(DOSH)
PETRONAS Research and Scientific Service	(PRSS)

## NOMENCLATURES

$A$	:	Area, $m^2$
$c$	:	Speed of sound, $ms^{-1}$
$C_p$	:	Specific heat capacity at constant pressure, $kJ.kg^{-1}.K^{-1}$
$C_v$	:	Specific heat capacity at constant volume, $kJ.kg^{-1}.K^{-1}$
$f$	:	Friction factors
$G$	:	Mass velocity, $kg.m^{-2}.s^{-1}$
$H$	:	Enthalpy, kJ
$L$	:	Length of pipe, m
$L_{max}$	:	Maximum length of pipe, m
$M$	:	Mach number
$m$	:	Mass, kg
$M_a$	:	Upstream Mach number
$M_b$	:	Downstream Mach number
$M_o$	:	Pipe entrance Mach number
$M_w$	:	Molecular weight
$\nu$	:	Specific volume, $m^3.kg^{-1}$
$P$	:	Pressure, kPa
$P_a$	:	Upstream pressure, kPa

$P_b$	:	Downstream pressure, kPa
$P_c$	:	Critical pressure, kPa
$P_r$	:	Reduced pressure, kPa
$Q$	:	Heat, kJ
$R$	:	Gas constant, $\text{kPa}\cdot\text{m}^3\cdot\text{kmol}^{-1}\cdot\text{K}^{-1}$
$r_H$	:	Hydraulic radius, m
$T$	:	Temperature, K
$t$	:	Time, s
$T_a$	:	Upstream temperature, K
$T_b$	:	Downstream temperature, K
$T_c$	:	Critical temperature, K
$T_r$	:	Reduced temperature, K
$u$	:	Speed of fluid, $\text{ms}^{-1}$
$V$	:	Volume, $\text{m}^3$
$\omega$	:	Eccentric factor
$Z$	:	Compressibility factor
$\gamma$	:	Isentropic exponent
$\rho$	:	Density, $\text{kg}\cdot\text{m}^{-3}$

# CHAPTER 1

## INTRODUCTION

### 1.1 Background

As efforts are made to reduce motor vehicle exhaust emissions and to reduce air pollution, automobile manufacturers have turned towards the development of alternate fuel sources for motor vehicles. One of these fuel sources is the compressed natural gas (CNG), an abundant, yet relatively inexpensive, and clean burning fuel. There is no real differentiation amongst fuels as they serve the same purpose, transportation. Hence, the only driving force world-wide for the market development of natural gas vehicle (NGV) is the price differential between natural gas and conventional fuels, which may have different reasons in the various countries. Figure 1.1 shows the breakdown of the major alternative fuels available in Malaysia.

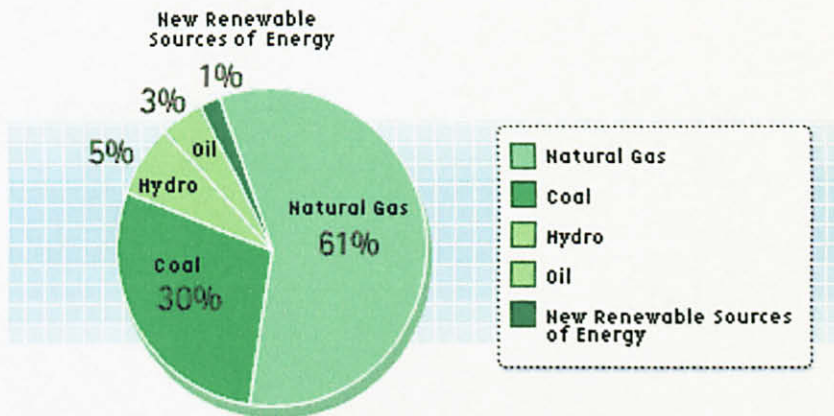


Figure 1.1: Fuel of choice for power generation [1]

Clearly, the figure shows that Malaysia has an abundant natural gas reserves. As of January 2004, Malaysia has the 12th largest gas reserves in the world, which contains about 97.6 trillion cubic feet.

This translates to about 66.8 years of natural gas availability based on the current production rate, hence there is an opportunity to promote the use of the natural gas as an alternative fuel for vehicles [1]. CNG is natural gas that has been compressed for storage aboard an NGV, a vehicle in which its engine is fueled by the natural gas. It has many overwhelming advantages against traditional means of transportation using gasoline or diesel [2].

Firstly, natural gas brings environmental benefits due to the fact that it is completely burnt in comparison to gasoline or diesel. Thus NGV emits less pollutant, such as nitrous oxides (NO<sub>x</sub>), carbon dioxide (CO<sub>2</sub>) and especially carbon monoxide (CO). In the case of leakage, as natural gas is lighter than air, it dissipates into the atmosphere, thereby reducing the risk of explosions and fires [2]. Secondly, the natural gas resource is available in more abundance than petroleum which makes it costs lower than gasoline. PETRONAS through its wholly owned subsidiary, PETRONAS NGV Sdn Bhd (PNGV), have been making NGV available to Malaysian motorists through its expanding chain of NGV outlets in the Klang Valley and other major urban areas in the country. The aim has been to commercialize and promote the use of natural gas as a cleaner fuel for the transportation sector. Figure 1.2 shows the growth on NGV vehicles and refueling stations in Malaysia.

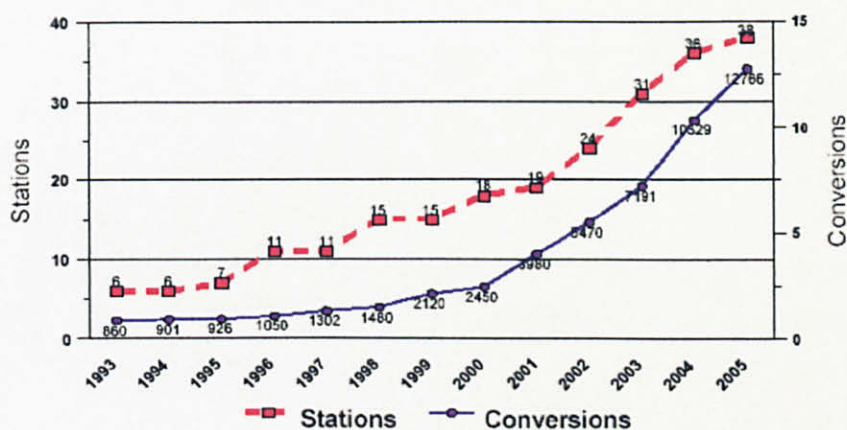


Figure 1.2: NGV stations and vehicle population in Malaysia [3]



Currently, there are about 15,600 NGV operating in the country, with a total of 40 NGV stations to cater for NGV users, all of which were set up by PNGV. The number is expected to increase rapidly, as the Malaysian Government is keen to promote the use of NGV as it is environmental-friendly with lower emissions. In Malaysia, the Ministry of Transportation is planning to increase the number of public vehicles using natural gas by about 10%, whilst the use of NGV for public transport is also among the proposals of the Cabinet Committee in view to the impact of the price increase of fuel and petroleum products on the economy [3].

## 1.2 Problem Statement

The NGV refueling station stores natural gas temporarily in three banks of storage tanks. Each bank of the storage tanks are termed as low, medium and high based on the quantity of natural gas it holds, but of the same initial pressure of 3600 psig. The arrangement of the tanks is to increase the utilization of the storage and also serves to speed up the filling rate when switching from one storage tank to another. In practice, when the pressure inside storage tanks has dropped to a certain pressure, it will be refilled by trailers (mother-daughter concept) or directly from natural gas pipeline.

A limited availability of natural gas pipelines in strategic areas has been identified as a main problem in ensuring a continuous and sustainable growth of the industry in Malaysia [3]. This has impeded the development of more refueling facilities, and as a result, has contributed to the congestions at NGV stations at several locations within the city limits. A strategy that has been proposed to reduce the congestion at the stations was to upgrade the dispensing facilities within the station where permissible. In an NGV station, the natural gas is transferred into vehicle cylinders by pressure differential. If only the differential storage pressure was used to transfer the gas, then the flow of gas would cease when the storage pressure and vehicle pressure has been equalized. According to Radhakrishnan *et al.*, during the refueling there was a limit of mass flow rate called choking of the flow [4].

At this condition it was found that the pipe exit pressure was much higher than the tank pressure and the resulting abrupt pressure drop was a major cause of the energy loss. Most of the NGV vehicles come to the station for filling will have its storage tank at a very low pressure. When an empty NGV tank is connected to the dispenser maintained at nearly 3600 psi, sonic flow could take place in the refueling hose, and there will be pressure discontinuity at the tip of the dispenser. This irreversible energy loss has contributed considerably to the filling rate of an automobile tank.

### 1.3 Motivation

One of the alternative solutions to reduce the time and energy losses during refueling is by introducing an optimum filling schedule using a series of sources with increasing pressures proposed by Radhakrishnan *et al.* [4]. However the problem lies in finding the suitable method that could automatically and optimally switch the refueling source from lower to higher pressure bank sequentially as the vehicle storage pressure increases. Alternatively, the optimum filling could be done by using a variable discharge pressure compressor to compress the natural gas directly to the NGV vehicle. The compressor is capable of varying its discharged pressure to ensure optimal pressure drive while achieving optimum usage of electricity. Nevertheless, with the current infrastructure in place, modifying the refueling station in order to accommodate variable pressure compressor may lead to high cost. A more sensible solution is to introduce system and devices that could improve the refueling process with reasonable cost to ensure return on investment could be made. Given the scenario above, the motivation behind the research is to develop a system using commercially available devices to address the problem. In doing so, the major challenge is to develop the heart of the system which is the refueling algorithm that will control the refueling process to achieve optimal time and energy consumption.

#### 1.4 Objectives and contribution of the research

The objectives of the research are;

- **to develop a new NGV refueling algorithm based on Time Optimal Control to achieve minimum time for refueling of NGV.**
- **to implement the NGV refueling algorithm on an experimental rig which resembles the set up available at NGV refueling station.**
- **to compare NGV refueling performance using the developed algorithm against an established one i.e., Kraus refueling.**

In achieving the objectives of the research, the contribution of the research work involves;

- Introducing an approach for switching time optimization using Time Optimal Control (TOC) method. The features of this approach is similar to the approach used in [11], [12], [13], [14] and [15] by considering the switching time optimization as bang-bang control.
- Developing a simulation model using MATLAB to represent an NGV refueling system which is used as a tool for evaluating and re-designing the optimal switching time to achieve optimal performance.
- Designing the TOC algorithm for NGV refueling system switching time optimization on LABVIEW, and embedding it on FieldPoint for actual testing on an experimental rig.
- Investigating the effectiveness of the TOC algorithm using various possible refueling cases/scenarios.

## 1.5 Outline of the thesis

This thesis could be mainly divided into two parts. In part I, consisting of chapter 1 and 2, an introduction of NGV refueling station with highlights on the importance of the approach used in the research work is presented. A review on the analysis of the problem is also made with the intend of setting the scope for the research work. Part II, consisting of chapter 3 to 5, presents the approach of designing an optimal control model for the time switching minimization of NGV refueling system, including the model analysis and design, model implementation, performance and analysis, and the experimental work.

Following the introduction made in Chapter 1, Chapter 2 focuses the research to NGV filling efficiency by describing a pressure discontinuity at the tip of the dispenser. A series of sources with increasing pressures has been proposed which requires an optimal time switching control i.e., Time Optimal Control (TOC). With several literature reviews on TOC covered in Chapter 2, Chapter 3 focuses the research on the development of TOC refueling algorithm for NGV refueling system with multi level pressure source. In order to test the TOC refueling algorithm in actual NGV refueling process, Chapter 4 discusses a fully instrumented NGV laboratory test facility which consists of three main parts: the NGV test rig, the Data Acquisition (DAQ) & Control System and the LabVIEW programming model. The performance of TOC refueling algorithm is compared to a commercially used NGV refueling controller i.e., the Kraus refueling using two performance measures: time of refueling, and the total mass of natural gas stored. Based on these performance measures, experiments are conducted on the test rig which the results shown the benefits of TOC refueling algorithm in providing optimum time for NGV refueling. Finally, Chapter 5 gives the conclusion of this thesis and suggests future research direction relevant to the switching time design and implementation for an NGV refueling.

## CHAPTER 2

### LITERATURE REVIEW

This chapter is intended to introduce a selection of research activities in the field of NGV refueling system to provide a view of what are the elements for NGV refueling system, problems and opportunities. As with the choice of coverage, the reference are selected from a large number of sources but is not meant to provide a comprehensive review.

#### 2.1 Introduction

NGV vehicles provide an economical solution to air quality, energy security and public health concerns. Natural gas, the least polluting fossil fuel, burns more cleanly as compared to other traditional fuels such as petrol and diesel [2], see Table 2.1.

Table 2.1: Comparison of pollutants levels emitted by different automotive fuels [2]

Fuel	Carbon Monoxide (CO)	Nonmethane Hydrocarbon (NMHC)	Nitrogen Oxides (NO)
Petrol	Base	Base	Base
LPG	- 20%	- 10%	+ 20%
NGV	- 60%	- 90%	- 10%
Diesel	- 40%	- 10%	+ 700%

NGV consists primarily of methane ( $\text{CH}_4$ ), a gas formed by decomposing organic material. Methane in its normal state is odourless, colourless and tasteless which makes it difficult to be detected by an ordinary person. To overcome this, an odouriser (mercaptan sulphur) is added to NGV, giving it a distinctive odour. NGV used in vehicles is the same as the natural gas used in power stations. In Malaysia, it is transported from the Petronas Gas Processing Plant (GPP) in Kerteh through pipelines to the NGV refueling stations. NGV generally carries an octane rating of between 122 and 130.

Octane rating measures a fuel's resistance to burn. A higher rating indicates an ability to burn more efficiently, and thus improving engine power and performance. The weight of a molecule of NGV is 70% lighter than a molecule of air, meaning that NGV dissipates quickly into the surrounding when released into the atmosphere, mixing with surrounding air rather than pooling on the ground [2].

As a safety advantage, natural gas also combusts over a narrow range flammability limits that is when the natural gas to air mixture is between 5 to 15%. Outside this range of flammability limit, combustion will not take place. NGV naturally ignites at 630°C, a critical factor that further reduces the probability of accidental combustion. In Malaysia, NGV is supported by the government with incentives and legislations to encourage vehicles owner to use NGV. Currently, NGV price is only 68.0 cents/liter equivalent of petrol, is cheaper than other fuels, see Table 2.2. NGV conversion kits are also exempted from import duty and sales tax [2].

Table 2.2: Retail price of different automotives fuels as of March 2006 [2]

Fuels	Pump Price/Litre
NGV	RM 0.68
Petrol (Unleaded)	RM 1.92
Petrol (Leaded)	RM 1.88
Diesel	RM 1.58
LPG	RM 1.75

As noted, major factors for potential vehicle owners to consider when making their vehicle fuel choices, have been identified. Interestingly, NGV vehicles safety record compares favourably to other traditional fuels or alternatives fuels available today. This is due to the superior and still improving technology, higher safety standards and the physical properties of NGV itself which makes it safer to use than petroleum based fuels [2].

### ***2.1.1 Malaysian Standard (MS) for the NGV Industry***

NGV Conversion kits and cylinders must meet various safety standards, rules and regulations. The construction of NGV refueling station and the installation of NGV conversion kits in vehicles must comply with MS 1204 and MS 1096 respectively. These two Malaysian Standards are the basic references for local NGV industry [5].

## **2.2 NGV Vehicle Safety Standards**

NGV offers significant safety advantages over many of its competitors in the vehicle fuel market. As noted in section 2.1, in the case of leak, natural gas poses little danger because it dissipates rapidly into the air. Yet even within its good safety record, as shown in Table 2.1 and 2.2, NGV possesses several unique physical, chemical and usage characteristics that require those handling it to exercise care and adopt good safety habits. This section will elaborate the basic practices and procedures, addressing areas such as NGV fueling components and how to operate an NGV vehicle [2].

### ***2.2.1 NGV Vehicle Technology***

NGV vehicles come in monofuel, bi-fuel, and dual-fuel models. Monofuel vehicles use only NGV, bi-fuel vehicles operate on either NGV or petrol, while dual fuel vehicles burn both diesel and NGV simultaneously in a proportion that usually varies from 5% to 20% diesel (as an initial starter), with NGV accounting for the remaining portion [6].

### ***2.2.2 Safety in NGV Conversion Kit System***

NGV conversion kits and cylinders must meet various safety standards, rules and regulations developed and implemented at the national and international levels. Compliance to these standards assures NGV users that the minimal safety issues are already being addressed from the manufacturing stage of the NGV system. It also indicates that the products they buy, meet basic safety requirements. In Malaysia, the NGV conversion kits must comply with MS 1906. This Malaysian Standard is the basic reference for the NGV industry for the conversion kits. [2].



Figure 2.1: NGV diamond shape [2]

The NGV diamond-shaped label as shown in Figure 2.1 helps the safety and emergency response officials such as fire-brigade and police to identify an NGV vehicle. According to MS 1906, NGV vehicles must have two durable labels to indicate the use of NGV in the vehicles [5].

### 2.2.3 Onboard NGV Storage in Vehicle

Once natural gas reaches the refueling station via the underground pipes, it flows to a compressor, then to a storage cascade and finally to a dispensing system. During refueling, NGV flows from the dispenser into the high pressure storage cylinders installed in the onboard cylinder of the vehicle. The onboard NGV storage cylinders consist of high pressure vessels approved by DOSH. Cylinders can be made of various materials, including composites. However, the cylinders currently used in bi-fuel vehicles are made of 100% metal. They commonly come in cylindrical shapes. NGV storage components have to be designed, manufactured and tested to rigid specifications. Four types of cylinders that conform to current standards for installations on NGV vehicles are listed in Table 2.3 [2].

Table 2.3: Types of vehicles storage cylinders [2]

Type	Material
Type 1	Steel
Type 2	Metal liner reinforced with resin impregnated continuous filament (hoop wrapped)
Type 3	Metal liner reinforced with resin impregnated continuous filament (fully wrapped)
Type 4	Metal liner reinforced with resin impregnated continuous filament (all wrapped)



In applications that require increased vehicle driving range as well as improved mileage per litre equivalent of NGV, users tend to use lighter-weight cylinders. Cylinders manufactured to standard specifications have a 20 years usage life with no requirement for retesting except visual inspection. Although cylinders are designed to exceed the limits of normal operation, they should not be filled above the designated pressure, a necessary precaution in ensuring the integrity of the NGV fueling system [5].

#### *2.2.4 NGV Flow within the Vehicle*

NGV filling receptacles can be located at various points on the vehicle. As for the retrofitted bi-fuel vehicles shown in Figure 2.2, it is normally located in the engine compartment. NGV flows from the dispenser, through the receptacle into a high pressure tubing connected to the onboard storage cylinders. Both the filling nozzle at the dispenser and the vehicle fueling receptacle is constructed of spark-resistant material for additional safety. Both also have built-in check valves to prevent the back-flow of natural gas should an incident occur while fueling. When an NGV user disengages the nozzle from the vehicle receptacle, any NGV remaining between the valves and fittings are vented harmlessly into the atmosphere [6]. There are 2 master shut-off valves, one in the engine compartment and the other at the onboard cylinder valve. The following section shows the main components in bi-fuel NGV vehicle.



### **2.2.5 NGV Vehicle Combustion**

Once the gas mixes with air and flows into the combustion chamber, NGV ignites and burns to power the engine. NGV can burn in high-compression engines with ratios up to 15.5:1, a favorable performance characteristic relative to other fuels, which may only burn efficiently in engines with lower compression ratios. NGV fueling system is designed for carburetor and fuel injection systems. Some of the latest NGV models use electronic fuel controls to monitor and adjust the flow of fuel in the engine. Monofuel vehicles are able to take the full advantage of the octane difference between petroleum based fuels and NGV because they are built to run only on NGV. This results in the reduction of engine piston rings and engine cylinder valves and hence limits oil contamination [6].

### **2.2.6 NGV Driving**

The actual operation of an NGV is remarkably similar to driving a petrol or diesel-powered vehicle, with just a few minor exceptions. A monofuel NGV, for example, typically has more power than a vehicle running on a traditional fuel, particularly when climbing hills, and would start more easily in cold weather compare to a petrol vehicle. In fact, it is nearly impossible to distinguish between the driving performance of an NGV and a petroleum powered vehicle. It is important to note that if the odour of NGV is detected in or around a vehicle, the engine should not be started. Instead, the quarter-turn safety shut-off valve and the NGV cylinder valve are turned to the “off” position and maintenance personnel should be notified that leak has been detected [2].

The following section is intended to provide a brief overview of the current research activities in the field of NGV and to give an indication of the type of research, applications and directions being investigated.

### 2.3 NGV Refueling System – Research Challenges

In Malaysia, the construction of NGV refueling station must comply with MS 1204. There are two basic methods of refueling: the fast-fill and slow-fill method, see Figure 2.3. The fast fill method allows NGV to be filled into a vehicle between 3 to 5 minutes. The slow-fill method is generally used by fleets whose vehicles are parked for a longer span, such as overnight. A slow-fill facility refuels a vehicle by drawing directly from a compressor while a fast-fill station draws from a storage cascade. A storage cascade is a grouping of cylinders that stores natural gas supplied by the compressor [2].

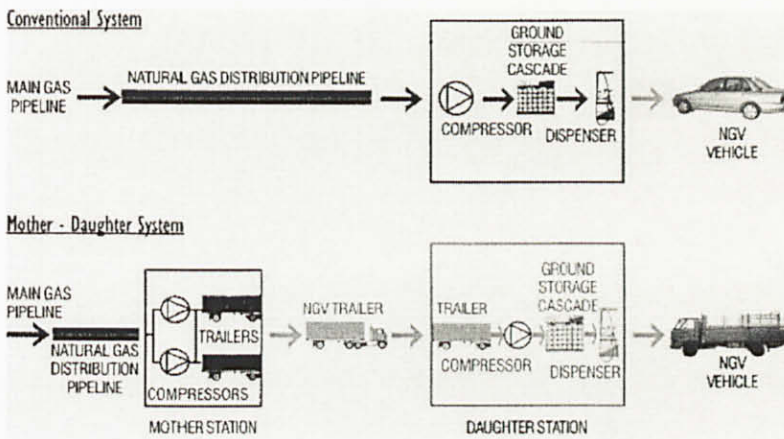


Figure 2.3: Schematic of NGV refueling system [2]

#### 2.3.1 Compressor

Once natural gas reaches the fueling facility either via pipeline or trailers, it flows into an underground welded steel pipe that connects to a series of filters, to remove impurities. The compressor takes natural gas out of the line after it passes through the filters and dryer, compresses the gas so it can be stored in high-pressure cylinders of the storage cascade. The compressor typically runs on either electricity or natural gas and has different compression settings. Each of the individual compressor components usually are separated by check valves. Check valve is a self-activating safety valve that prevents natural gas flow from reversing and in this case is to automatically limit the flow in a piping system to a single direction. Figure 2.4 shows a typical compressor for NGV refueling station [2].

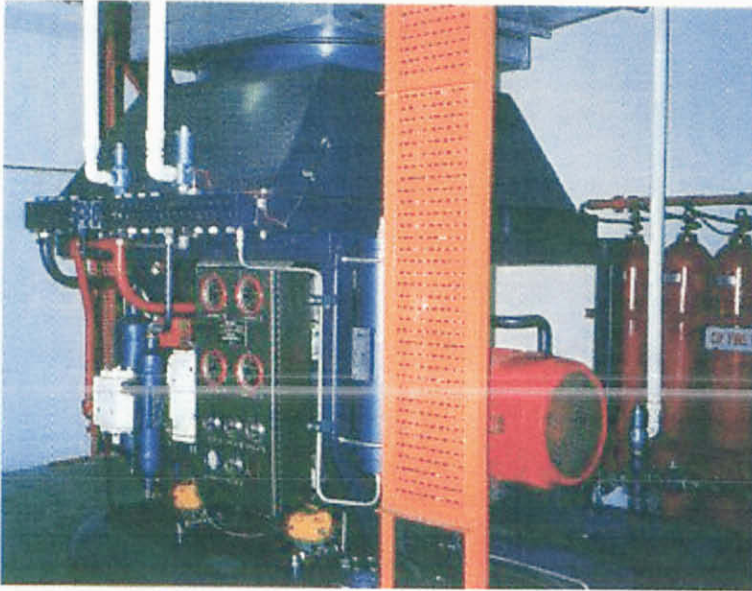


Figure 2.4: A typical NGV compressor [2]

Natural gas leaves the compressor through seamless, stainless steel high pressure pipe, entering another series of filters to further eliminate impurities as well as carrying over oil from the compressor unit. It is then sent into a series of cylinders group together to form a storage cascade [2].

### 2.3.2 *Storage Cascade*

Natural gas is stored in high pressure cylinders usually in the shape of cylinders. Natural gas fueling functions on the concept of pressure equalization, i.e., using stationery storage cylinders grouped together into a cascade and mounted on a plinth or concrete slab. The storage cascade filled with natural gas would later be supplying natural gas to a vehicle's storage system via the dispenser. The cylinders that make up a cascade are usually arranged in banks, with the containers in each bank connected by manifolds. Banks are separated by automatic valves connected to a controller that automatically switches these source banks as natural gas contents deplete. Just as the compressor has relief valves for each stage of compression, each vessel in a cascade has a pressure-relief valve to release the pressure harmlessly into the atmosphere in case of the unusual event of over compression. Figure 2.5 shows a typical arrangement of the storage cascade [2].

In general, not more than one-third of a cascade's capacity can be withdrawn, a level that allows the cascade to retain adequate pressure to inject fuel into a vehicle. When a vehicle with a lower pressure is connected to a fueling station, natural gas flows from one of the banks of the cascade until the pressure between the vehicle and the bank begins to equalize. When this occurs, the flow of natural gas slows and the controller switches to another bank until the pressure begins to equalize. Most fueling stations have three banks operating at the maximum pressure of 3,600 psi [2].



Figure 2.5: A typical NGV storage cascade [2]

### 2.3.3 Dispenser

NGV dispensers come in two types i.e., the Fast Fill and the Time Fill. In Malaysia, the Fast Fill type as shown in Figure 2.6 has been widely used. The main function of a dispenser is to safely transfer gas into the vehicle cylinder and measure the quantity of gas delivered. Natural gas dispensing systems closely resemble those used for fueling petrol and diesel vehicles, with a hose, nozzle and a meter. Natural gas flows from the storage vessels through steel underground pipes, with an individual line to carry gas from each bank. Natural gas flows through another filter, built-in into the dispenser. NGV dispenser hoses are equipped with breakaway couplings that allow the hose to separate from the dispenser in the event a driver attempts to leave while fueling or before returning the hose and nozzle to the dispenser. Breakaway couplings causes the check valves on both the dispenser and the vehicle to seat, assuring that the NGV in the hose safely contained and preventing any additional release of gas from the dispenser or vehicle. Currently, some dispensers use programmed software to compensate for temperature variation as another system safeguard. This allows the natural gas to expand when the fuel heats up on a warm day or in a warm area after filling a vehicle on a cold day. The safety filling is based on temperature pressure compensation method which used the signal reading acquired from a Coriolis flowmeter [2].



Figure 2.6: A typical NGV dispenser [2]

### ***2.3.3.1 Temperature Pressure Compensation***

Like all gases, natural gas expands and contracts with temperature. When under pressure, this results in a corresponding change in pressure, which can sometimes be dramatic. For example, natural gas with a specific gravity of 0.6 can be stored at 3000 psig at 30°C. If the temperature of the gas in the cylinder falls to -40°C, the resulting gas pressure is approximately 1600 psig. If the temperature was to rise to 49°C, the resulting gas pressure would be approximately 3600 psig. If, however, a vehicle were filled to 3000 psig on a cold day of -40 °C, and then immediately brought inside to a parking garage at room temperature 30°C, the pressure in the cylinder would rise to 4430 psig, which is beyond the design pressure of most cylinders. For this reason, the dispenser must adjust the end of fill pressure to correct for the ambient temperature. The quantities of fuel delivered, and therefore the vehicles range, are still the same, but the dispenser has made this adjustment to correct the final fill pressure for ambient temperature. This function is known as Temperature Pressure Compensation system which is embedded in a controller inside the dispenser [7].

### ***2.3.3.2 Coriolis Flowmeter***

Coriolis meter is used in CNG measurement because it can measure the flow of natural gas in true mass. It relies on measurement of certain vibration characteristics of a tube through which gas is flowing. The vibrations are dependent on the mass flow rate of the gas in the tube and hence the meter provides a true mass measurement. In addition, the natural frequency of the tube can be used to measure gas density and therefore the meter can also be used to calculate volumetric flow. The meter is also able to respond to rapid changes in flow and unaffected by gas composition or pressure. A temperature sensor can be embedded inside the flowmeter to measure temperature signal that can be used in Temperature Pressure Compensation system. For these reasons, Coriolis meters have become the most commonly used meter in NGV dispenser [8].



## 2.4 Related Research Work on NGV Refueling System Research

A report carried out by Advantica and National Weights and Measures Laboratory (NWML) shows that a typical NGV filling station consists of a compressor, storage vessels and a dispenser [9].

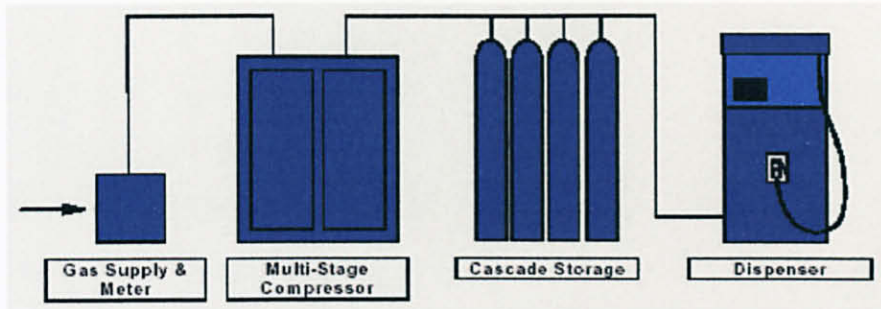


Figure 2.7: A typical NGV filling station [9]

Gas from the distribution pipeline, usually at low pressure of 14.7 psig or medium pressure of 14.7-102 psig, is compressed using a large multi-stage compressor into a cascaded storage system as shown in Figure 2.7. This system is maintained at a pressure higher than that in the vehicle's on-board storage so that the gas flows to the vehicle under differential pressure. Typically, the cascaded storage will operate at 3600 psig, while the vehicle's maximum on board storage pressure is 3000 psig. In some countries, notably USA and Europe, higher cascade storage and vehicle pressures are used and are becoming more common for heavy-duty vehicle applications. In order to make the utilization of the compressor and buffer storage more efficient, CNG stations usually operate using a three-stage cascaded storage system. The buffer storage is divided into three "banks" – termed as the low, medium and high pressure banks using valves controlled by the dispenser system. During refueling the vehicle is first connected to the low-pressure bank. As the pressure in the bank falls and that in the on-board storage rises, the flow of gas decreases. When the flow rate has declined to a pre-set level the system switches to the medium pressure bank, then finally to the high-pressure bank to complete the fill. The cascaded system results in a more complete "fill" rather than if the whole buffer storage was maintained at one pressure because it can utilize the compressor and storage with maximum efficiency [9].

In addition, when the compressor is automatically switched on to refill the banks it fills the high pressure bank to 3600 psig first, and then switches to the medium and the low banks. This is to ensure that the high-pressure bank (used to complete the fill) is maintained at maximum pressure, thus ensuring that vehicles are always supplied with the maximum amount of gas available. Figure 2.8 is a depiction of three types of refueling methods such as time fill, buffer fast fill, and cascade fast fill. The system complexity increases from time fill, to buffer fast fill, to cascade fast fill system operation. Time fill and buffer fast fill will not be discussed in detail because Malaysia's existing refueling is using the cascade fast fill type [9].

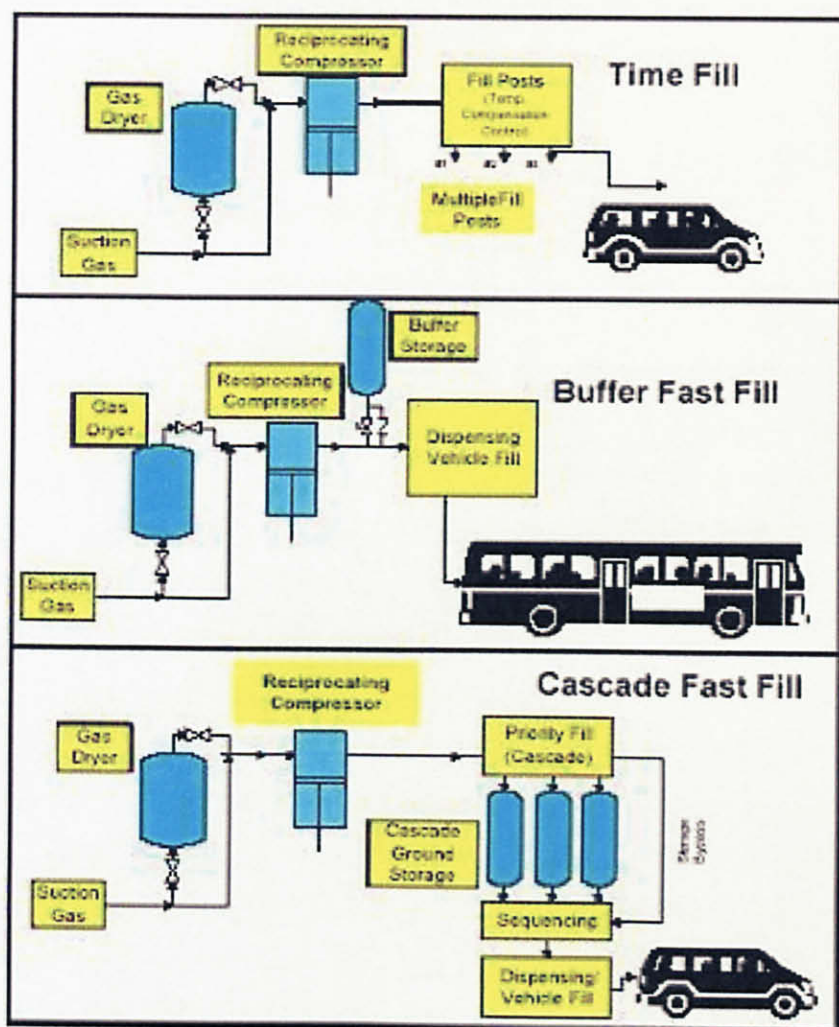


Figure 2.8: NGV refueling method [7]

### 2.4.1 *NGV Cascade Fast Fill Process*

A useful review of the NGV cascade fast fill process has been given in Jordair Technical Exchange Presentation [7]. Typically, gas is compressed and stored at 3600 psig and dispensed to 3000 psig at 30°C. This means that if only the differential storage pressure was used to transfer the gas, the flow of gas would cease when the storage pressure and vehicle pressure have equalised. This can occur at any pressure from atmospheric (14.7 psig) to 3600 psig, but to get a full fill of 3000 psig, the storage pressure could not drop below 3000 psig. This means that only 600 psig of the 3600 psig available could possibly be transferred into the vehicle before the flow of gas would stop. Since there is no pump or other form of forced withdrawal used, the remaining 3000 psig is essentially unavailable for transfer into the vehicle. The number 600/3600, or approximately 15%, is referred to as the utilization of the storage, the quantity of storage that is actually usable to transfer into the vehicle. The system is relatively inefficient, as it can only use approximately 15% of the available storage capacity for refueling [7].

To get higher utilization from a given volume of storage, a system referred to as a 3-bank cascade filling scheme is employed. In this system, the given quantity of storage is divided into three individual banks fully separate from each other labeled as high, medium and low bank. This is not a description of their pressures but rather of their filling priority. When full, all the three banks start at the same pressure of 3600 psig. The dispenser first draws gas from the low bank into the vehicle cylinder during the refueling. Once this pressure begins to equalize (the flow drops off to an unacceptably slow rate), the dispenser control system switches the dispenser gas source to the mid bank. As before, the filling is by pressure differential until the flow drops off. This is followed by the high bank. Finally, once the flow from the high bank drops off, the compressor is turned on to compress natural gas directly from the main pipeline of the NGV gas station, until the vehicle's tank is finally full. Certain storage configurations are able to divide the storage banks into unequal volumes. It has been reported in [7] that a common storage ratio of approximately 50% low bank, 30% medium bank and 20% high bank can further increase the effective utilization of the storage and also speed up the filling rate [7].

### 2.4.2 Limitations of the Current System

From the development point of view, NGV refueling facility has gone through several stages of improvement to make it economical in terms of compressor's utilization. It has evolved from a single line dispensing system which dispenses gas from a single source into a 3-banks cascaded storage to maximize the compressor utilization that leads to the reduction in the compression energy. Due to the importance of empirical data on vehicle initial fuel tank pressure, a survey was conducted at NGV refueling station, Shah Alam, Selangor from 13<sup>th</sup> January 2005 to January 18<sup>th</sup> January 2005. Figure 2.9 shows the results of the survey which involves 1000 NGV vehicles and it is found that NGV vehicles coming for refueling have various initial fuel tank pressures that range between 20 to 2000 psig.

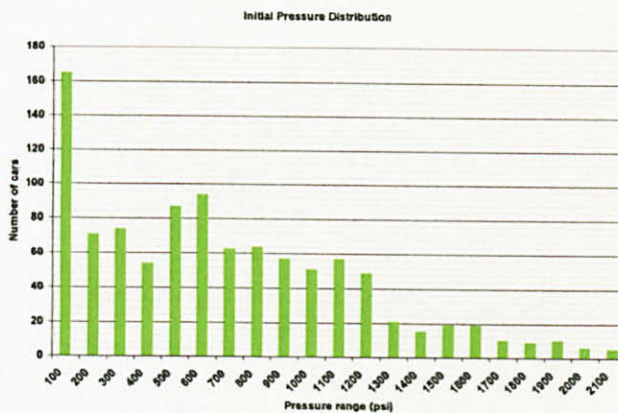


Figure 2.9: Frequency distribution of initial fuel tank pressure of NGV

This wide range of initial pressure, if fed with higher single source pressure, will cause a pressure discontinuity at the tip of the dispenser. Pressure discontinuity causes internal energy of gas to reduce and the lost energy will be dissipated into heat causing temperature rise to the fuel tank system. With existing refueling station, this leads to reduction in filling efficiency because a lot of energy has been lost. Radhakrishnan *et al.* [4] proposed a conceptual model for a dispenser system and uses it to study theoretically the compressible gas flow phenomena during the filling of the NGV vehicle from the storage banks. It is found that the energy lost can be reduced if the filling is done using multiple source pressure, and this phenomenon will be explained in the next section.

### 2.4.3 Conceptual Model of CNG Filling Process

Figure 2.10 shows the simplified model for process modeling study to duplicate existing NGV refueling system. It consists of a reservoir, a straight horizontal pipeline and a receiver [4].

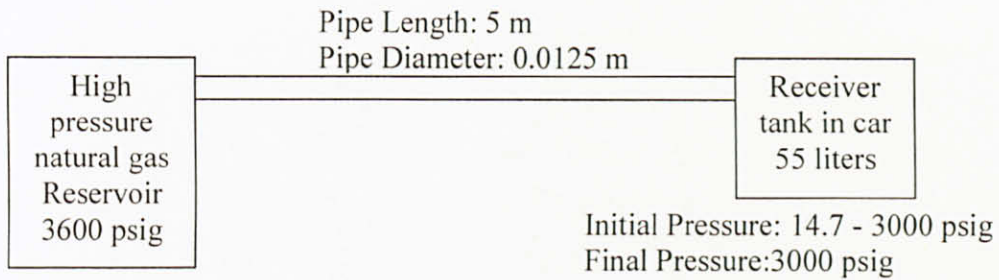


Figure 2.10: Conceptual model of the dispenser [4]

The reservoir's pressure is assumed to be constant at 3600 psig and temperature at 30°C. The pipeline is horizontally straight with length of 5 meters and diameter of 0.0125 meters. These are the actual size of the piping system of the current NGV refueling equipment in Malaysia. The cross sectional area of the pipe is constant. Friction effect along the pipeline is taken into account since the flow is irreversible. It is assumed that NGV with an empty tank 14.7 psig is being filled. The NGV tank varies from the initial value of 14.7 psig to full fill pressure of 3000 psig. These sets of conditions are chosen as the extreme values. Depending on the initial quantity of gas inside the tank and the required final fill pressure, other conditions may apply and can be easily substituted. The volume of the tank is 0.055 m<sup>3</sup> which is the standard value in the Malaysia's NGV. The initial temperature of the tank is assumed to be 30°C and temperature rise is expected due to gas compression effects. The flow of natural gas between the source and the receiver is modeled as a Fanno Flow system. It is an adiabatic frictional flow and also a flow of a compressible fluid with frictional pressure drop. Flow through a straight pipe of constant cross section is adiabatic when heat transfer through pipe wall is negligible [4].

The typical situation is a long pipe into which gas enters at a given pressure, temperature and flow at a rate determined by the length and diameter of the pipe and the pressure maintained at the outlet. A realistic equation of state to relate the state properties of the gas must be assumed. The initial Mach number,  $M_0$  was assumed to be zero since the source cross sectional area is very large compared to that of the pipe. With the source at high pressure and the sink at low pressure the flow rate has to be determined using a trial and error procedure such that the Mach number becomes 1 at the pipe exit. This is because in a long pipeline with a very low exit pressure, the speed of the gas may reach the sonic velocity. It is not possible, however, for a gas to pass through the sonic barrier from the direction of either subsonic or supersonic flow. If the gas enters the pipe at a Mach number less than 1, the Mach number will increase but will not become greater than 1. If an attempt is made to maintain the constant discharge pressure and lengthening the pipe to force the gas to change from subsonic to supersonic flow (or vice versa), there is a maximum gas flow limit that occurs when Mach number is equal to one. The limiting of the mass flow rate is called 'choking' of the flow. At this condition it was found that the pipe exit pressure is much higher than the tank pressure and the resulting abrupt pressure drop is a major cause of the energy loss. Based on compressible gas flow dynamics and Fanno flow conditions, the following equations could be derived from fundamental principles. An equation of state using compressibility factor was found to be the most appropriate for natural gas [4].

In summary, the important parameters constituted to the model of the NGV filling is defined in equation 2.4.1 to equation 2.4.7. The description of the symbol used is described in the nomenclature, see page xvi to xvii. To determine the effect of different operating conditions, the system was simulated under various conditions of the source and sink pressures. This corresponds to NGV coming with different initial tank conditions as well as different amount of purchase requirements.

Upstream Mach number:

$$\frac{fL_{\max}}{r_H} = \frac{1}{\gamma} \left( \frac{1}{M_o^2} - 1 - \frac{\gamma+1}{2} \ln \frac{2 \left\{ 1 + [(\gamma-1)/2] M_o^2 \right\}}{M_o^2 (\gamma+1)} \right) \quad (2.4.1)$$

Downstream Mach number:

$$\frac{fL}{r_H} = \frac{1}{\gamma} \left( \frac{1}{M_{n-1}^2} - \frac{1}{M_n^2} - \frac{\gamma+1}{2} \ln \frac{M_n^2 \left\{ 1 + [(\gamma-1)/2] M_{n-1}^2 \right\}}{M_{n-1}^2 \left\{ 1 + [(\gamma-1)/2] M_n^2 \right\}} \right) \quad (2.4.2)$$

Upstream pressure (pipe entrance):

$$\frac{P}{P_o} = \frac{1}{\left\{ 1 + [(\gamma-1)/2] M_o^2 \right\}^{1/(1-1/\gamma)}} \quad (2.4.3)$$

Downstream pressure:

$$\frac{P_{n-1}}{P_n} = \frac{M_n}{M_{n-1}} \sqrt{\frac{1 + [(\gamma-1)/2] M_n^2}{1 + [(\gamma-1)/2] M_{n-1}^2}} \quad (2.4.4)$$

Downstream temperature:

$$\frac{T_{n-1}}{T_n} = \frac{1 + [(\gamma-1)/2] M_n^2}{1 + [(\gamma-1)/2] M_{n-1}^2} \quad (2.4.5)$$

Mass velocity:

$$G = M \sqrt{\rho \gamma P} \quad (2.4.6)$$

Calculate pressure in receiver:

$$P = \frac{mRTz}{M_w V} \quad (2.4.7)$$

### 2.4.4 Pressure Variation along the Dispenser Pipe

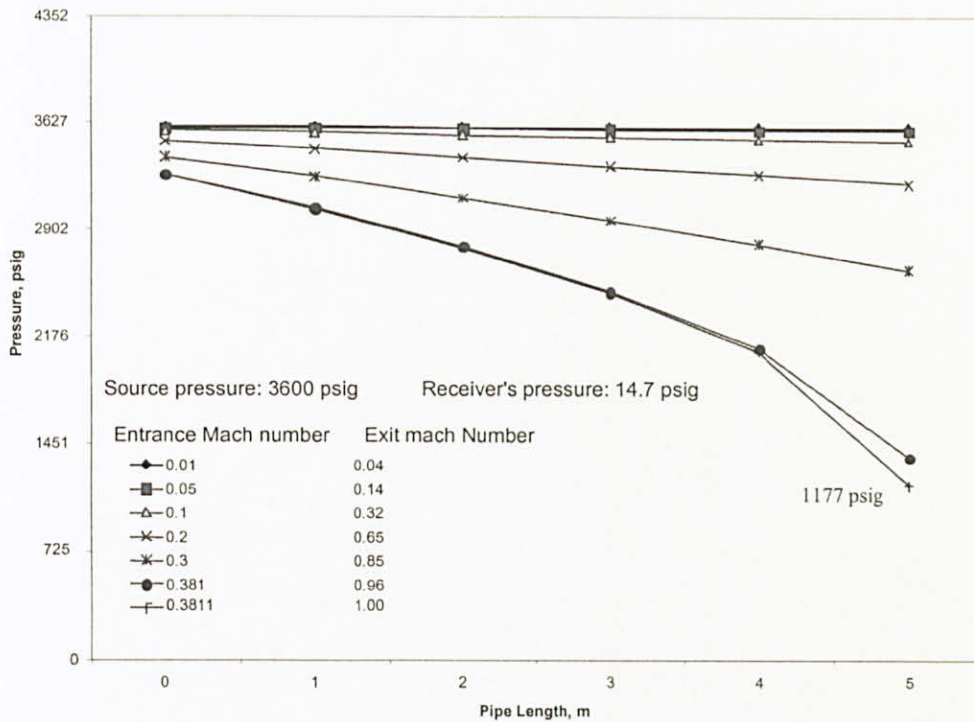


Figure 2.11: Pressure distribution in pipeline for difference entrance Mach numbers [4]

Figure 2.11 shows a set of simulation results for a given source pressure and sink pressure, and with different entrance Mach numbers. The source pressure was chosen to be 3600 psig while the sink pressure equals 14.7 psig. As depicted, the pressure decreases as the medium flows along the pipeline. A higher mass velocity that corresponds to higher entrance Mach numbers, the pressure drops is higher. However, the exit pressure is much higher than the tank pressure and there will be a pressure discontinuity. The exit Mach number is less than one and will be higher as the entrance Mach number is increased. Ultimately, at an entrance mach number of 0.3811 the exit Mach number is exactly equal to one. A higher entrance Mach number than 0.3811 is not possible since the exit Mach number will be higher than one, which is thermodynamically erroneous as explained in details by Radhakrishnan *et al.* [4]. Hence the maximum entrance Mach number is 0.3811 to give the exit Mach number exactly equal to one [4]. This corresponds to receiver pressure of less than 1177 Psig for a choking flow to take place.



With the entrance Mach number fixed at 0.3811 a series of simulations runs were conducted to determine the pressure at the exit of the dispenser. The sink pressure was again assumed to be 14.7 psig. Figure 2.12 shows the exit pressure for a given source pressure along the pipeline. It can be seen that the pressure at the end of the dispenser is much higher than at the sink pressure. The difference between the two pressures is more for much higher source pressures. This explains the rise in the pressure discontinuity between the tip of the dispenser and the automobile gas storage tank [4].

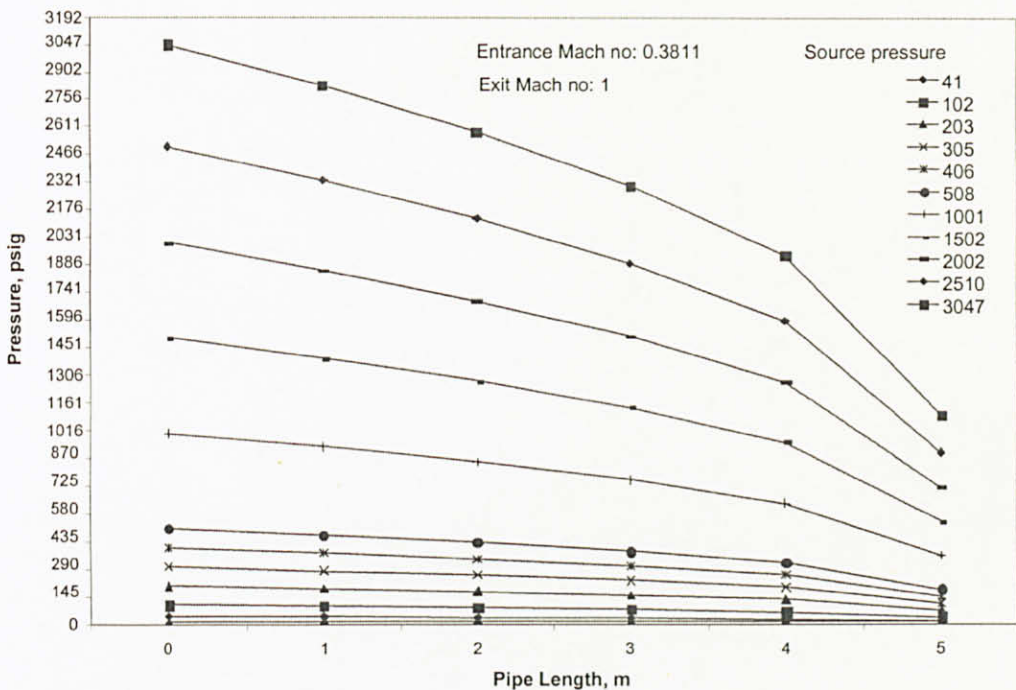


Figure 2.12: Pressure distribution in pipeline for different source pressure [4]

### 2.4.5 Filling rate of the NGV Tank

For a constant source pressure of 3600 psig and an initial vehicle tank pressure of 14.7 psig, the simulation for the filling of the tank is shown in Figure 2.13. Initially during the start of the filling, the flow regime is under choked flow conditions since the tank pressure is very low. This situation continues for the first 300 seconds when the exit Mach number equals to one. From 300 to 340 seconds the flow turns to normal flow since the Mach number at the exit is less than 1. It is found that the vehicle tank requires 340 seconds to fill pressure until 3000 psig [4].

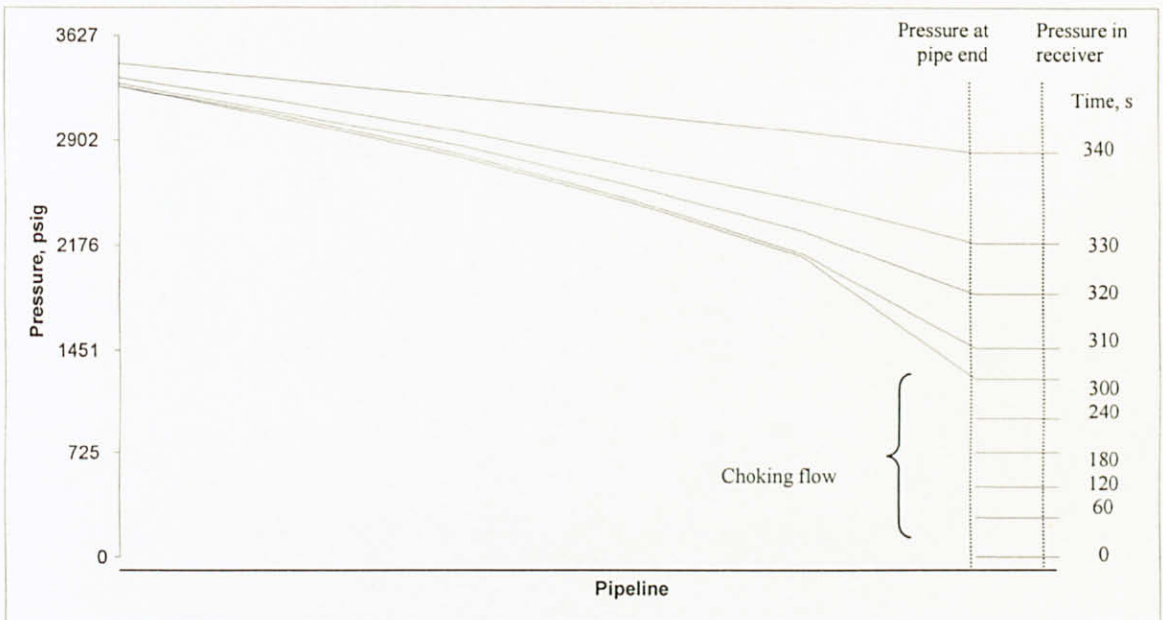


Figure 2.13: Pressure distribution and duration of choked flow condition [4]

### 2.4.6 Pressure Discontinuity and Energy Loss

When the source pressure is high and sink pressure is low, the dispenser exit pressure is much higher than the sink pressure. This leads to the pressure discontinuity as shown in Figure 2.14. The figure shows the variation of the receiver pressure with loss that can be avoided [4].

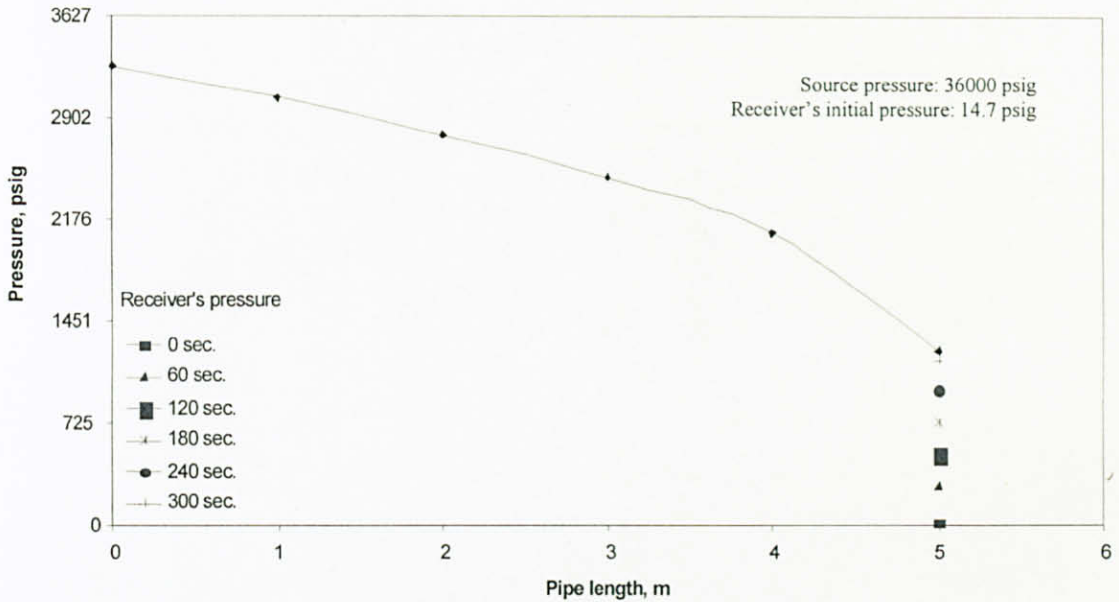


Figure 2.14: Pressure Discontinuity in choked flow [4]

Figure 2.15 shows the result obtained for a simulation under constant source pressure and various receivers' pressure. The source pressure was 3600 psig while the receiver's initial pressures were 14.7 psig, 102 psig, 508 psig, 1016 psig, 1523 psig and 2031 psig. Selection of the receiver's initial pressure is made by estimating the remaining fuel content of vehicles that comes for refueling [4].

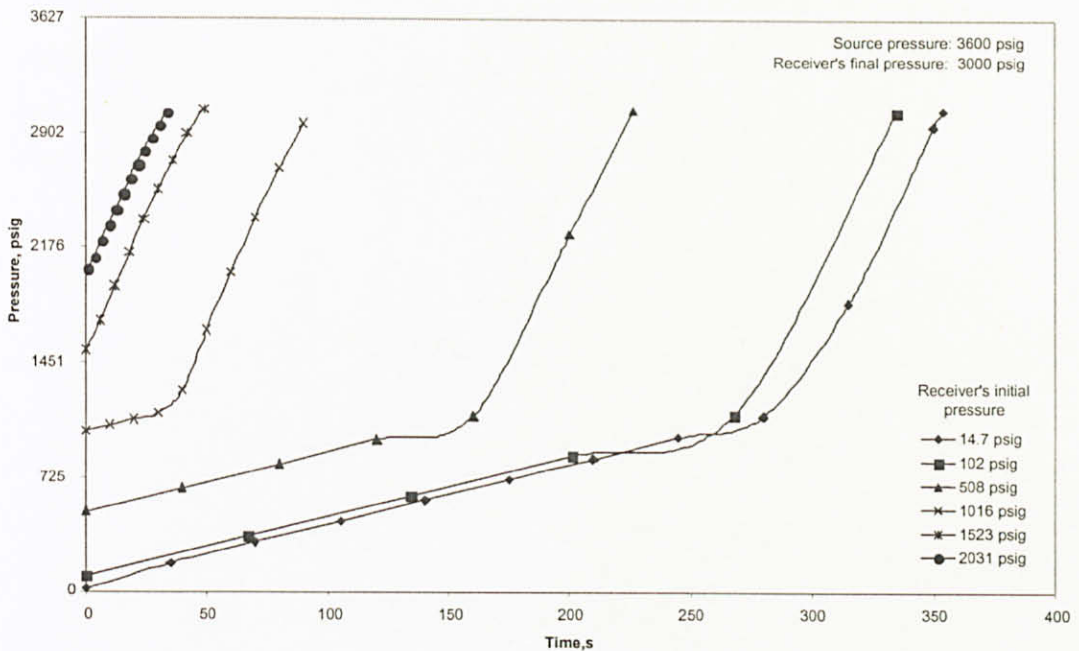


Figure 2.15: Variation of receiver pressure with time [4]

From the 14.7 psig, 102 psig, 508 psig, 1016 psig lines, the lines are divided into 2 sections of different slopes. The initial section of lower slope represents the “choked flow” while the later section of the higher slope represents “normal flow”. During a choking flow, pipe exit Mach number is equal to 1. At source pressures of 1523 psig and 2031 psig, it could be observed that there is no choked flow section. This indicates that if the refueling is done for a tank with initial pressure of 1523 psig and above, no choking flow would occur [4].

## 2.5 Switching Time Issues

It is shown that energy losses occur if the dispensing is performed under choked flow conditions. If the dispensing were performed using low values of the source pressure, the refueling time may become unacceptably high. To understand the interaction of these two conflicting requirements, a series of simulation studies were conducted with different source pressures and different initial sink pressures. Figure 2.16 and Figure 2.17 show the rate of filling with respect to time for source pressure of 102 psig and 508 psig [4].

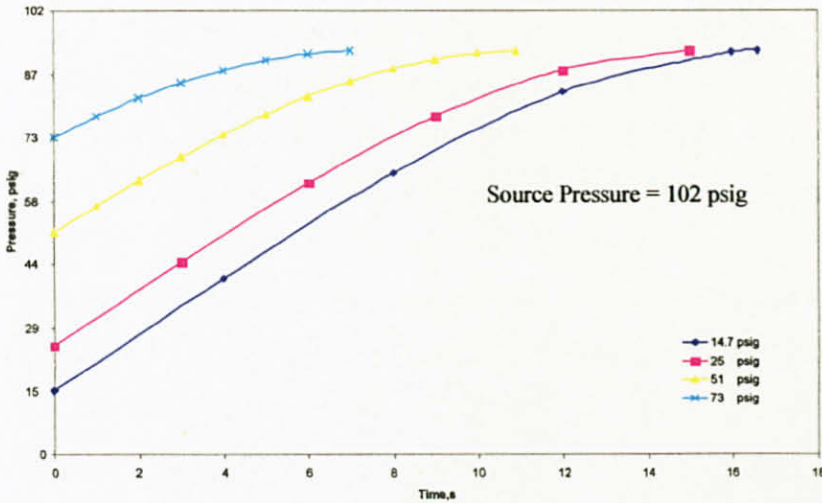


Figure 2.16: Variation of receiver pressure with time at source pressure of 102 psig [4]

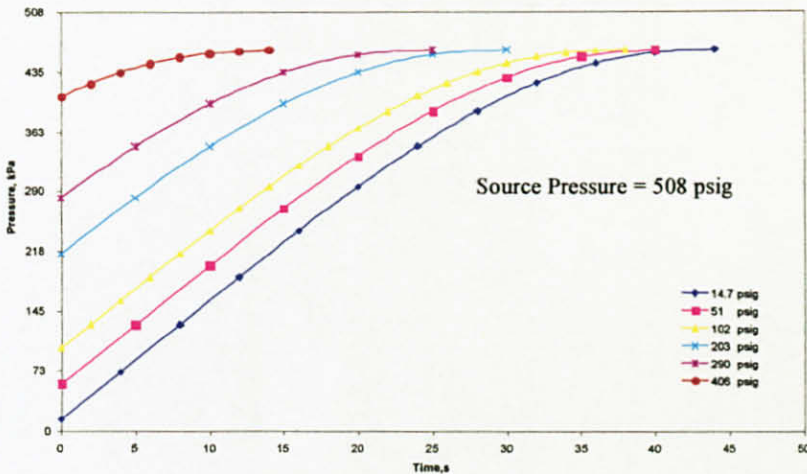


Figure 2.17: Variation of receiver pressure with time at source pressure of 508 psig [4]

If the source pressure is 102 psig and initial sink pressure is 14.7 psig, a fast filling rate will be developed at the initial period. However, in this case, there is no choked flow. The rate of filling is also reduced as the sink pressure increases. Based on reduction of the filling rate, a value of 92 psig was established as the final sink pressure. This is achieved at time of refueling equals 35 seconds (the graph in Figure 2.16 only shows until 16 seconds). Once the sink pressure reaches the value of 92 psig, the filling is switched to higher pressure source. A source pressure of 508 psig is chosen as the next value as shown in Figure 2.17. The filling is continued until the receiver pressure is equal to 462 psig. The next choice of the source pressure is 1016 psig which takes the sink pressure to 925 psig. This follows by a source pressure of 2031 psig which takes the sink pressure to 1850 psig. Finally, a source pressure of 3600 psig is chosen which takes the sink pressure to the value of 3000 psig. The filling rate curves for all these source pressures show the same trend as Figure 2.16 and 2.17 with no choked flow and a gradual reduction in the rate of filling. These simulation results indicate that to achieve minimum compression energy and filling time, a series of source pressures should be used with gradual switching from a low source pressure to a higher source pressure, see Figure 2.18 [4].

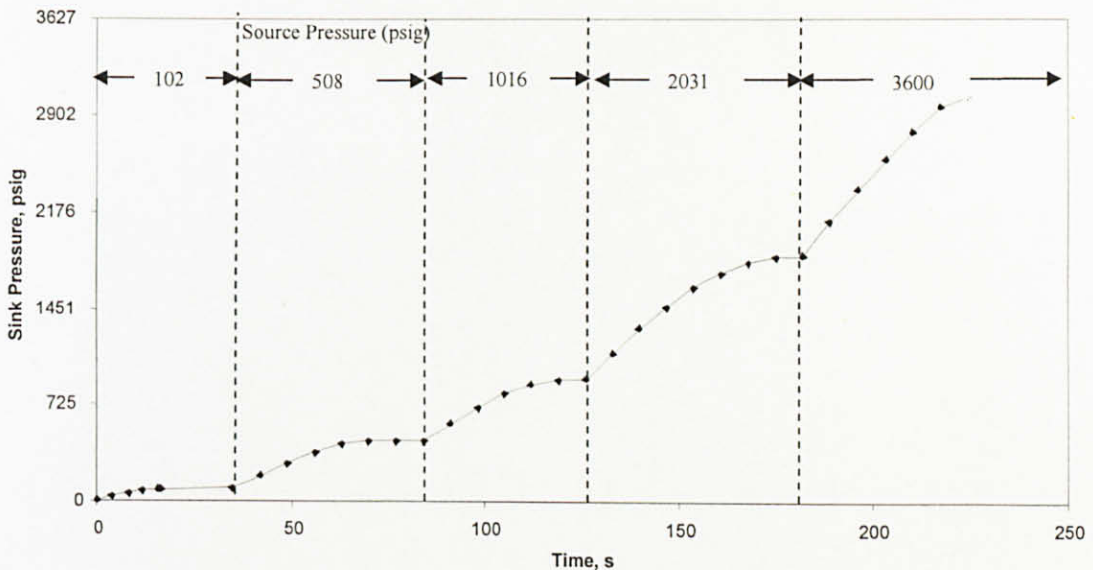


Figure 2.18: Receiver's filling time with different pressure source switching [4]

From the proposed switching schedule, it is assumed when the NGV vehicle arrives at the filling station, it has a tank pressure of 14.7 psig. The dispensing starts with the lowest source pressure of 102 psig and proceeds until the sink pressure approaches 92 psig. At this point, the source is switched to 508 psig and the filling proceeds until the sink pressure reaches 462 psig. At this point the source is switched to 1016 psig and the filling will continue until the sink pressure reaches 925 psig. The next source pressure is 2031 psig and the filling proceeds until the sink pressure approaches 1850 psig. Finally, the maximum source pressure of 3600 psig is used and will be filling the sink to a final pressure of 3000 psig, which corresponds to the “full tank” pressure. The figure shows that, the complete filling has shortened to 220 seconds compares to 300 seconds under the previous refueling method as described in section 2.4.6.

Currently, different control methodologies are used by the NGV manufacturers for NGV refueling. One of the methods is by applying a flowmeter in the cascade fast fill refueling type which provides flowrate signal that can be used as a threshold to change from one bank to another. A typical graph of flowrate during refueling of an NGV vehicle is shown in Figure 2.19.

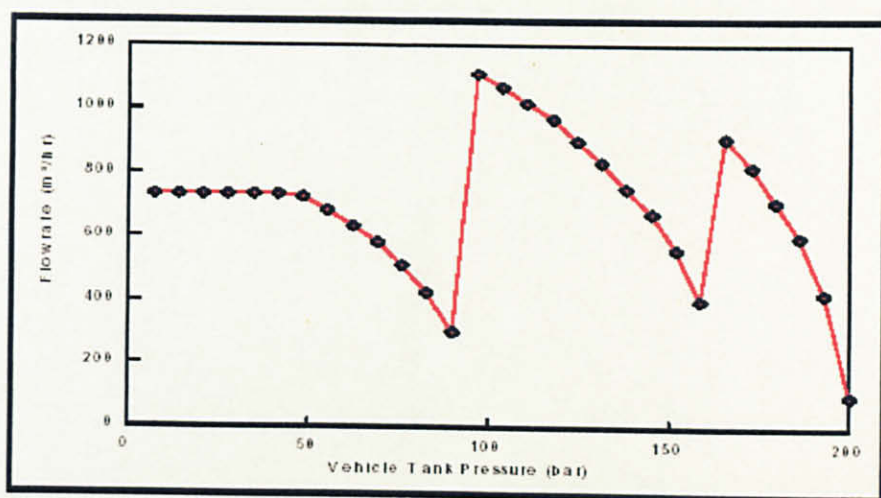


Figure 2.19: Graph of flowrate versus pressure for a CNG fill [9]

The sequences of the refueling process depicted in Figure 2.19 can be described as follows. Initially, the system measures the starting pressure in the vehicle and injects a known volume of gas into the NGV vehicle storage. Control software calculates the storage volume. This information gives the required quantity of gas needed to fill the system to 3000 psig. Control algorithms consider the heating effects as the in-cylinder gas pressure rises and compensate for factors such as ambient temperature and non-ideal gas behavior such as compressibility factor. The system also allows a more rapid fill and helps to smooth out the flow rate spikes [9]. One of the controllers that use this algorithm and has been widely installed in the NGV dispensers in Malaysia is Kraus controller, developed by Kraus Company Inc, Canada. To implement the NGV refueling via different pressure storages as suggested by Radhakrishnan *et al.* [4], a suitable controller needs to be developed since the existing controller starts the refueling with a storage pressures at about 3600 psig. Apart from that, the measurement also was based on pressure and temperature which should be compensated to accommodate for changes in pressure and temperature of the gas being measured to arrive at standard volume units. Therefore, a suitable controller is needed i.e., Time Optimal Controller (TOC).

The following section mainly discusses on the optimal control theory by placing emphasis on the TOC technique in resolving a representative survey of engineering applications. The purpose is to give detailed information on TOC, which forms a background for the development of an NGV refueling algorithm using multi-level pressure source.



## 2.6 Related research work on time optimization problems

A representative survey of applications of the Time Optimal Control is provided in this section. These have been selected on the basis of the diversity of areas that could be solved using TOC and the successful implementation of this method in many engineering problems.

Turnau *et al.* [16] described an experiment in practical implementation of simulated Time Optimal Control in a laboratory cart pendulum system. The simulation results are compared with two types of measured trajectories of the real system: firstly generated by an implementation of the time-optimal control, and secondly generated by a rule-based algorithm. The technologies of rapid prototyping, real-time simulation and hardware-in-the-loop simulation are used for direct synthesis of control algorithms. The feasibility of construction of time-optimal controller in the real system has been proposed.

In another paper, Furuta *et al.* [17] described the computation of time optimal swing up control of single pendulum. The paper presents a computational strategy to obtain the Time Optimal Control for nonlinear systems and discrete time control under input bound. The swing up control of a single pendulum from pendant stable equilibrium to upright unstable equilibrium is used to illustrate their approaches. For the simplified model of the single pendulum, which is a second-order system, an approach based on Linear Programming method is introduced, while for the actual single pendulum, an approach based on Nonlinear Optimization is introduced. Simulation results show the feasibility of the computational approaches.

In an interesting paper, Eker and Malmborg [18] described the design and implementation of a hybrid controller for a double-tank system for a heating or ventilation process. The results show that a hybrid controller consisting of a time-optimal controller combined with a PID controller gives very good performance.

A nonlinear control law to achieve a robust Time Optimal Control over the full range of operation conditions for level controls of a two tank system has been developed, as described by Heckenthaler and Engell [19]. The development is based on fuzzy control, but in contrast to the usual fuzzy controller designs, most of the rules were not derived from heuristics but rather from the mathematical formulas. This approximation is improved by heuristic rules which were gained from the observation of the behaviour of the controlled plant. The resulting nonlinear control law exhibits a performance which is neither attainable with standard linear control nor with classical Time Optimal Control.

A number of problems in control can be reduced to finding suitable real solutions of algebraic equations. In particular, such a problem arises in the context of switching surfaces in optimal control. Recently, a methodology for doing symbolic manipulations with polynomial data has been developed and tested, namely the use of Gröbner bases. Walther *et al.* [20] have applied the Gröbner basis technique to find effective solutions to the classical problem of Time Optimal Control.

A research work by Hol *et al.* [21] introduces an optimization algorithm for singular and non-singular digital Time Optimal Control for robots. A new algorithm that enables computation of both bang-bang and singular Time Optimal Controls for robots has been discussed. The algorithm uses both the conjugate gradient and Gauss Newton method to enhance its efficiency, which does not require state parameterization. The algorithm is used to compute Time Optimal Controls for an industrial 5 link robot model.

Galicki [22] addressed a computer example involving a planar redundant manipulator of three revolute kinematic pairs with geometric constraints using Time Optimal Control. The task is to move the end-effector along a prescribed geometric path (state equality constraints). It is proved that if the dynamics of a manipulator are defined by  $n$  actuators and  $m$  path-constrained equations, where  $m < n$ , then at most  $n-m+1$  actuators are saturated, provided that the time-optimal manipulator trajectory is regular with respect to a prescribed geometric path given in the work space.

Reynolds and Meckl [23] use hybrid optimization scheme for solving general optimization problems to a Time Optimal Control problem. By applying both constrained optimization and linear programming techniques to a particular problem, the benefits and drawbacks of each method can be easily described. While some of the results are relative to the problem of interest, some guidelines for solving general optimization problem is presented. Solutions of the Time Optimal Control problem for a standard two-mass spring-damper system show some interesting properties that illustrate the difficulty of applying constrained optimization exclusively.

In a recent paper, Penev and Christov [24] explained a fast time-optimal control synthesis algorithm for a class of linear systems. It is based on the decomposition of the Time Optimal Control problem into a class of decreasing order problems, and the properties and relations between problems within this class. The emphasis in this paper is on the optimal control synthesis stage of the approach proposed. A property of the considered class of problems is studied which enables development of a fast algorithm for synthesis of Time Optimal Control without using switching hyper surface.

One of the earliest efforts dealing with closed loop, approximately Time Optimal Control of a class of linear systems with a total effort constraint is credited to Melsa and Shultz [25]. This method is based on a special class of solutions of the Hamilton-Jacobi equation, called eigenvector scalar products. In designing a closed-loop system using this method, the controller-computer must only solve algebraic equations, and hence the control can be computed continuously.

In another recent paper, Gao [26] derived mathematical derivation of a closed form discrete optimal control law. A Time Optimal Control law is constructed in the form of state feedback for a discrete time, double integral plant by using the Isochronic Region method. This closed form nonlinear state feedback clearly demonstrates that Time Optimal Control in discrete time makes the new control law advantageous in engineering applications.

Ailon and Langholz [27] developed a study of controllability and Time Optimal Control of a robot model with drive train compliances and actuator dynamics. Conditions that ensure the existence of a Time Optimal Control are demonstrated, and controllability of the augmented model (robot and actuator) in open and closed-loop form is established. A procedure is described for the derivation of easily computable functional inequalities which represent upper bounds on the norm of the augmented system's time response.

Newman [28] introduced a robust control algorithm for a realization of nearly Time Optimal Control of double integrator plants that involves the combination of traditional bang-bang Time Optimal Control with the methods of sliding-mode control. The approach is nearly time optimal rather than exactly time optimal, since the bang-bang control components are restricted to values below full actuator saturation, thus reserving some actuator effort for compensation of disturbances and model imperfections. The algorithm blends smoothly into a linear controller near a stable goal location.

Shiller [29] presented a general necessary condition for singular Time Optimal Control of robotic manipulation moving along specified paths and has shown that the Time Optimal Control can be singular if one of the equations of motion reduces to a velocity constraint. The paper derives a more general necessary condition for singular control. It is also proven that singular control cannot exist if the set of admissible controls is strictly convex, as is demonstrated for a two-link planar manipulator with elliptical actuator constraints.

In their paper, Ebrahimi *et al.* [30] designed a minimum Time Optimal Control of flexible spacecraft for rotational maneuvering. The spacecraft is modeled as a linear undamped elastic system, which yields an appropriate model for analysis of planar rotational maneuvers. The developed control law is applied on an Iranian satellite "Sepehr" during a slewing maneuver, and the simulation results show that the control input with just few switching times can significantly lessen the vibrating motion of the flexible appendage.

Sakagami and Kawamura [31] implemented the Time Optimal Control for underwater robot manipulators based on iterative learning control and time-scale transformation. The paper presents a new Time Optimal Control method without parameter estimation, and is based on iterative learning control and time-scale transformation. To realize Time Optimal Control, a class of motions is considered which spatial paths were fixed but time trajectories (speed patterns) were changed. By using time-scale transformation, the feedforward input pattern is formed from the basic torque patterns obtained through iterative learning control. The effectiveness of the proposed method is verified by several experiments.

Brown *et al.* [32] considered a free end velocity Time Optimal Control of a bifilar-wound hybrid step motor. The necessary conditions for the optimal control are derived from motor, load, and driver circuit models using Pontryagin's minimum principle. A reduced order relaxation method, involving forward or backward integrations, is developed for the solution to the nonlinear two-point boundary value problem specified by the necessary conditions. A driver model for the inverse-diode drive circuit is introduced, and the Time Optimal Control for the hybrid step motor with drive circuit is found. Example solutions and comparisons to lead angle controls are presented.

Clark and Stark [33] used Time Optimal Control for analyzing the behavior of human saccadic eye movement. Time Optimal control theory takes into account constraints such as energy and time economies which are relevant to the understanding of biological design. A sixth-order nonlinear representation model which considers reciprocal innervation and the asymmetrical force velocity relationship of the agonist-antagonist muscle pair that moves the eye was developed. Simulations were done by digital computer and responses of the model to first, second, and third order Time Optimal Control signals were observed; the major portions of the response trajectories were essentially the same. It was concluded that the saccadic eye movements studied are accurately depicted by a model that yields time optimal responses.

A novel approach on detecting multiple objects is proposed by Steiner *et al.* [34]. It is based on Time Optimal Control of the transmitting transducer. The optimal control sequence is determined by quadratic programming. The resulting pulse signal has a considerably shorter decay time compared to a conventional burst excitation. This allows a better resolution for the recognition of objects that are close to each other.

Furukawa *et al.* [35] reported a solution to a real-time control of cooperative unmanned air vehicles (UAVs) that engage multiple targets in a time-optimal manner. Techniques to dynamically allocate vehicles to targets and to find the Time Optimal Control actions of vehicles are proposed. The effectiveness of the Time Optimal Control technique is demonstrated through numerical examples. The proposed strategy is applied to a practical battlefield problem where ten vehicles are required to engage four targets, and numerical results show the efficiency of the proposed strategy.

Several examples will now be given to indicate how TOC methodology has been used in the area of time optimal switching problems. There are quite a number of reports on the time optimal switching problem using TOC. These include Kuo *et al.* [11], Chang and Chow [12], Park and Cho [13], Danbury [14], and Moon *et al.* [15].

One of the pioneering works dealing with the Time Optimal switching problem dates back to Kuo *et al.* [11]. A controller with phase position feedback is designed and built for the minimum time control of the motor. Experimental results showed that the controlled motor is capable of traveling a prescribed number of steps in near minimum time by the injection of one or two single pulses and the proper adjustment of the lead angle of the feedback sensors. High-speed responses such as 300 steps in 100 ms from start to stop have been achieved experimentally.

Chang and Chow [12] proposed a Time Optimal Control of switchable series or shunt capacitors requiring only a single switching for damping power system swings resulting from large disturbances. The strategy is useful for a switchable series capacitor with a high compensation rating relative to the transmission system. The general case of Time Optimal Control of series capacitors requiring multiple switching is also investigated. The strategy is applicable to a switchable series capacitor with a low compensation rating relative to the transmission system. It is illustrated for a single-machine infinite-bus system and an interconnected system.

Park and Cho [13] used a Time Optimal Control for Nuclear Reactor Power which consists of coarse and fine control stages. During the coarse control stage, the maximum control effort or time optimal is used to direct the system toward the switching boundary which is set near the desired power level. At this boundary, the controller is switched to the fine control stage in which an adaptive proportional-integral-feedforward (PIF) controller is used to compensate for any unmodeled reactivity feedback effects. This fine control is also introduced to obtain a constructive method for determining the (adaptive) feedback gains against the sampling effect. The feedforward control term is included to suppress the over or undershoot. The estimation and feedback of the temperature induced reactivity is also discussed.

Danbury [14] presented a Time Optimal Control of a servomechanism requires a nonlinear control law based on a switching function. The switching function depends on the characteristics of the actuator and on the load. In practical servomechanisms the friction load may be unknown and may slowly vary. In such cases the optimal switching function is unknown prior to the start of each move. A controller is developed which estimates the optimal switching function during each move, thus enabling near Time Optimal Control to be achieved. The controller allows for certain nonlinearities in the actuator and in the friction/velocity function, and avoids the problems of chattering and limit cycling normally associated with Time Optimal Control.

Moon *et al.* [15] designed a fourth-order model for a crane-load system which a Time Optimal Control scheme with input constraints was investigated for transferring the crane load with swing angle regulation. Rather than following a conventional numerical method approach for solving the two point boundary value problem, a rule-based approach inspired by the manual crane operation is proposed. It is shown that the Time Optimal Control problem becomes the determination of the switching times. Based on the heuristics obtained, a set of expert rules is generated for the adjustment of the switching times. A simple iteration method for obtaining the optimal switching times is presented which provides an alternative solution when there is no analytical expression for a solution. From collected data a lookup table is generated. By incorporating an interpolation algorithm, it is possible to transfer the crane load an arbitrary distance without load pendulation at the destination in minimum time.

Notably, there is substantial literature on engineering related problems adapted to the TOC, and quite a well developed literature in approaching the time optimal switching problems through the TOC. Considering the nature of this research work and the defining benefits of TOC, the choice to use TOC is based on scaling the research on NGV refueling system in the aspect of improving the time switching issue. The following section discusses the strategy used in the research.



## 2.7 Strategies

The strategy used in this research is shown as a flowchart in Figure 2.20. Firstly, the TOC algorithm which includes the derivation of switching equation and simulation of forced trajectory are developed using Matlab Simulink. Next, the results from the Matlab Simulink are used to validate the results produced by the TOC algorithm implemented on an actual NGV test rig. Finally, the performance of refueling based on TOC algorithm will be compared with the Kraus refueling based on several experiments.

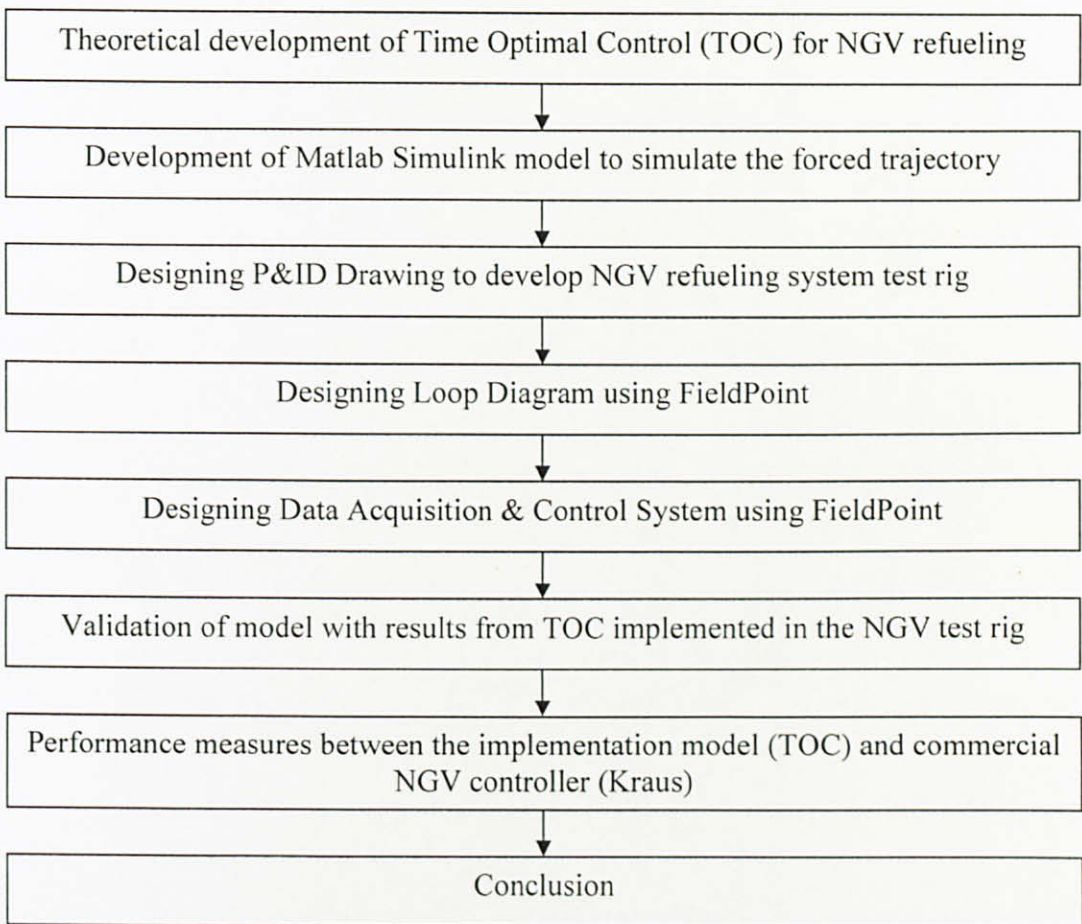


Figure 2.20: The strategy and plan of this research work

## 2.8 Summary

Chapter 2 describes the general background of this research and introduces the benefits of NGV vehicles. This research is focused to NGV refueling, and basically there are three types of refueling methods used: the time-fill, the buffer fast fill and the cascade fast fill. It has been pointed out that, the cascade fast fill resulted in a more complete fill. The refueling of natural gas is done by transferring the natural gas to the NGV vehicle based on pressure differential, in which the storage pressure at the refueling station is initially set at 3600 psig and pressure inside the NGV tank may varied from 20 to 2000 psig. This wide range of initial pressure, if fed with higher single source pressure, would cause a pressure discontinuity at the tip of the dispenser. Pressure discontinuity causes internal energy of gas to be reduced and the lost energy will be dissipated as heat that resulted in the temperature rise of the fuel tank system. This leads to reduction in filling efficiency because a lot of energy has been lost. A conceptual model of a dispenser is developed to allow theoretical study of compressible gas flow phenomena during the filling of the NGV vehicle from the station storage banks. The simulations results indicate that to achieve minimum compression energy and filling time, a series of source pressures should be used, with a gradual switching from a low source pressure to a higher source pressure. The implementation of NGV refueling system using multi-pressure storage source requires a suitable control strategy to be developed. This research will propose a new NGV refueling algorithm based on Time Optimal Control (TOC) technique.

## CHAPTER 3

### METHODOLOGY

This chapter concentrates on development of time switching optimization using TOC for an NGV refueling with multi-pressure storage source. The important point in the design is to ensure that switching algorithm using TOC performs as expected and intended, and establish that the simulation model behavior of switching time validly represents that of the NGV system.

#### 3.1 Introduction

Typically, the main objective of using optimal control in a control system is to determine a control signal that will cause the system to satisfy some physical constraints and at the same time extremize (maximize or minimize) a chosen performance criterion (performance index). The interest is to find the optimal control,  $\mathbf{u}^*(t)$ , ('\*' indicates optimal condition) that will drive the system from initial state to final states,  $\mathbf{x}(t)$  with some constraints on controls,  $\mathbf{u}(t)$  and at the same time extremizing the given performance index indicated by,  $\mathbf{J}^*$ . The statement of boundary conditions for the physical constraints on the controls and states variables, are constrained as equation 3.1.1, where, '+' and '-' indicate the maximum and minimum values these variables can attain.

$$\mathbf{U}_- \leq \mathbf{u}(t) \leq \mathbf{U}_+ \text{ and } \mathbf{X}_- \leq \mathbf{x}(t) \leq \mathbf{X}_+ \quad (3.1.1)$$

For NGV switching system using multi-pressure storage source, the formulation of time optimal control problem requires a mathematical model, generally in state variables form and a specification of the performance index i.e., minimum switching time. The following section introduces the methodology used to solve the problem which could be simplified in a flowchart as shown in Figure 3.1

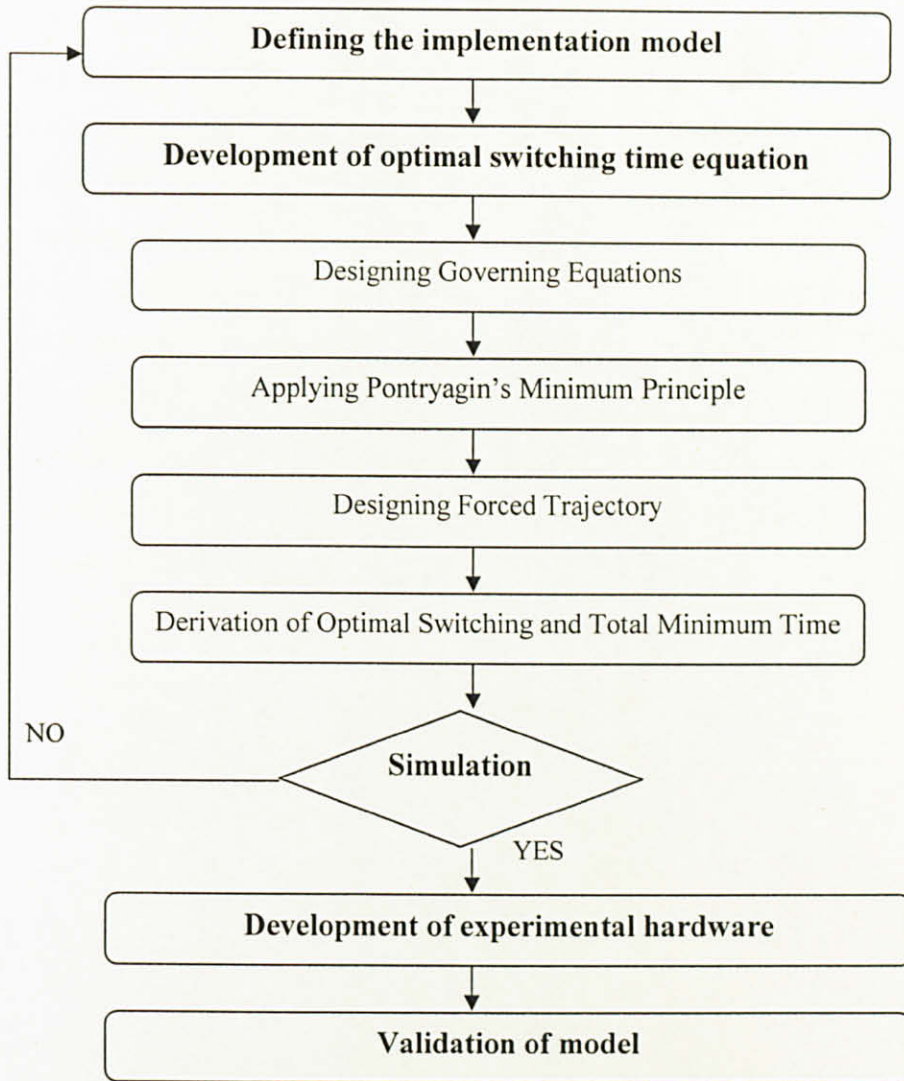


Figure 3.1: Methodology of research work

The problem is solved in a series of steps. In step I, the mathematical model for NGV refueling system is described. In step II, the Pontryagin's Minimum Principle is used to show that the optimal control is bang-bang. The optimal forced trajectory is described in step III. In step IV, the optimal switching time is derived. In step V, the forced trajectories are simulated using Matlab Simulink before its implementation model is tested on an experimental test rig. Finally, the model is validated with a commercially NGV refueling i.e., Kraus. The following section identifies the implementation model of the problem.

### 3.2 Defining the implementation model

The mass flowrate of natural gas will be the main variable to use. The advantage of using mass for measuring natural gas for NGV refueling system is that mass is constant at any area of various pressures and temperatures, hence ideal for Malaysia condition. The technique requires a Coriolis flowmeter to measure the mass flowrate in a pipeline and to determine natural gas in true mass. Newton's 2<sup>nd</sup> Law of Motion are applied to determine the resultant force between the NGV storage source and vehicle tank, as a basis to calculate the switching time to switch from one storage bank to another. Figure 3.2 and Table 3.1 show the conceptual model of NGV refueling system with multi-level pressure source to implement the TOC refueling algorithm with mass and mass flowrate,  $(x_1, x_2)$  as the measurement variables using Coriolis flowmeter.

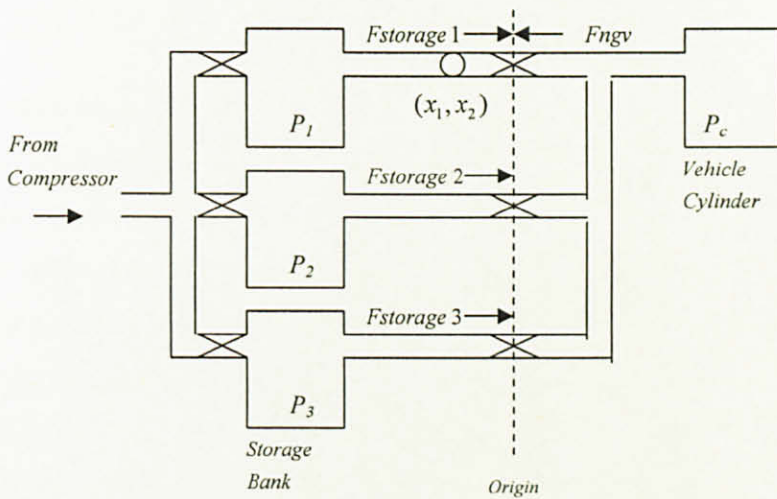


Figure 3.2: Implementation of TOC in NGV refueling with multi-level pressure source

Table 3.1: Values and definitions of parameters and variables for Figure 3.2

Symbol	Description	Units
$m_1$	mass at storage bank 1	$kg$
$m_c$	mass at vehicle cylinder	$kg$
$\dot{m}_{coriolis}$	rate of mass flowrate	$kg\ s^{-2}$
$P_1$	pressure at storage bank 1	$kPa$
$P_c$	pressure at vehicle cylinder	$kPa$
$A$	area of pipeline	$m^2$

From the Newton's 2<sup>nd</sup> Law of Motion, it is known that  $F = ma$ , where  $F$  is the force,  $m$  is the mass, and  $a$  is the acceleration. Pressure from the storage bank and NGV vehicle provide the force,  $F_{storage}$  and  $F_{ngv}$  respectively. There are two forces attracting the load, one at the front (force from the NGV vehicle  $F_{ngv}$ ) and another one at the rear of the load (force from the storage cylinder  $F_{storage}$ )

With higher pressure source at the rear of the load propels the load forward (in a positive direction) whilst higher pressure source at the front of the load propels it backwards (in a negative direction). The total force in a pipeline when both pressures have equalized is

$$F_{storage} + (-F_{ngv}) = F = 0 \quad (3.2.1)$$

At the stage of mass equilibrium, the resultant force inside the pipeline between the NGV cylinder and storage bank is equal. However, to achieve such equilibrium, longer time is required due to declining pressure differential which drives the system towards equilibrium. In the case of the NGV refueling with multi-level pressure source, there are several sources of natural gas source at different pressure level. The refueling starts from lower pressure source and switches over to higher pressure storage wisely as the natural gas car storage tank pressure approaches the source pressure. Therefore, the objective is to determine the right timing for the switch-over to take place. The time of switching can be solved using a forced trajectory developed based on Pontryagin Minimum Principle. From Figure 3.2 and notations from Table 3.1, the governing equations of the system is

$$\frac{m_1 - m_c}{A\rho} (\ddot{m}_{coriolis}) = A(P_1 - P_c) \quad (3.2.2)$$

The equation is used as a basis to determine the optimal switching time in the development of NGV refueling algorithm with multi-level pressure source. The following section explains the first step taken in the optimal switching design.

### 3.3 Development of optimal switching time equation

Detail explanation on how the modeling and simulation via TOC is conducted can be found in [10], [36]. The flow of a mass in natural gas pipeline can be considered as a simple motion of an inertial load in a frictionless pipeline environment as illustrated in Figure 3.3

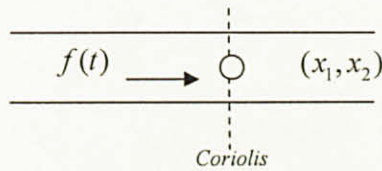


Figure 3.3: The motion of mass in a pipeline with force and initial state of mass and mass flowrate,  $(x_1, x_2)$  measured using Coriolis flowmeter.

#### 3.3.1 Step I – Designing governing equations

The motion is described by

$$m\ddot{y}(t) = f(t) \quad (3.3.1)$$

Where  $m$  is the mass of natural gas,  $y(t)$  be the output (or angular displacement) and  $f(t)$  is the external force applied to the system.

The transfer function  $G(s)$  of the system is

$$G(s) = \frac{y(s)}{f(s)} = \frac{1}{ms^2}$$

The control is defined as  $u(t)$ . By setting  $u(t) = \frac{f(t)}{m}$ , then equation (3.3.1) reduces to the equation

$$\ddot{y}(t) = u(t)$$

The state variables is defined as  $x_1(t)$  and  $x_2(t)$  by

$$\begin{aligned}x_1(t) &= y(t) = \text{output} \\x_2(t) &= \dot{y}(t) = \text{output rate}\end{aligned}$$

In the case of motion of mass for natural gas in a pipeline, the output and output rate are mass and mass flowrate measured using Coriolis flowmeter. The system in state-space representation is obtained as

$$\begin{bmatrix} \dot{x}_1 \\ \dot{x}_2 \end{bmatrix} = \begin{bmatrix} 0 & 1 \\ 0 & 0 \end{bmatrix} \begin{bmatrix} x_1 \\ x_2 \end{bmatrix} + \begin{bmatrix} 0 \\ 1 \end{bmatrix} [u] \quad (3.3.2)$$

$$\begin{aligned}\dot{x}_1(t) &= x_2(t) \\ \dot{x}_2(t) &= u(t)\end{aligned} \quad (3.3.3)$$

This system can be written in the form

$$\dot{x}(t) = f(x(t)) + g(x(t))u(t) \quad (3.3.4)$$

The control  $u(t)$  is assumed to be constrained in magnitude by the relation

$$|u(t)| \leq U(t) \forall t \in [t_0, t_1] \quad (3.3.5)$$

Where

$$U^- \leq u(t) \leq U^+ \rightarrow |u(t)| \leq U \quad (3.3.6)$$

$$U^+(t) = +1 \quad (3.3.7)$$

$$U^-(t) = -1 \quad (3.3.8)$$

The magnitude constraint is the result of physical limitations on the amount of mass flowrate which may be realized in coriolis flowmeter used in NGV test rig. The following section explains the second step taken in the optimal switching design.



### 3.3.2 Step II – Applying Pontryagin’s Minimum Principle

From the mathematical model of NGV refueling system, the objective of the problem can be specified precisely. When NGV tank is empty, pressure from storage bank is higher than pressure inside the NGV. As a result, the force will push the mass towards the NGV tank. Let  $t_1$  be the time taken for the mass to move from storage bank to NGV tank. When the mass inside the NGV tank increases, the pressure will start to increase and the force will push the mass towards storage bank. Let  $t_2$  be the time taken for the mass to move back from NGV tank to storage bank. If the storage bank is assumed to be the location of origin, the objective can be defined as to find the control input  $u(t)$  that minimizes the transition time to the origin. To be admissible each  $u(t)$  must satisfy the three conditions below, see [10] for details.

1) The system is completely controllable, when the matrix

$$G = [B : AB : A^2B : \dots : A^{n-1}B] \quad (3.3.9)$$

$$= \begin{bmatrix} 0 & 1 \\ 1 & 0 \end{bmatrix} = -1 \neq 0$$

is of rank  $n$  or the matrix  $G$  is nonsingular

2) The magnitude of the control  $u(t)$  is constrained as

$$U^- \leq u(t) \leq U^+ \rightarrow |u(t)| \leq U \quad (3.3.10)$$

Or component wise,

$$|u_j(t)| \leq U_j, \quad j = 1, 2, \dots, r \quad (3.3.11)$$

Here  $U^+$  and  $U^-$  are the upper and lower bounds of  $U$ .

But, the constraint relation (3.3.10) can also be written more conveniently as

$$-1 \leq u(t) \leq +1 \rightarrow |u(t)| \leq 1 \quad (3.3.12)$$

Or component wise

$$|u_j(t)| \leq 1 \quad (3.3.13)$$

3) The initial state is  $x(t_0)$  and the final (target) state is 0.

The method of solutions will consist of the following steps:

1) *Step 1*: Performance Index (PI): For minimum time system as shown by (3.3.1), the performance index is

$$J = \int_{t_0}^{t_f} 1 \cdot dt = t_f - t_0 \quad (3.3.14)$$

Where  $t_0$  is fixed and  $t_f$  is free ( $t_0$  is the initial time and  $t_f$  is the final time)

2) *Step 2*: Hamiltonian: From the system (3.3.3) and the PI (3.3.14), the Hamiltonian is

$$H(x(t), p(t), u(t)) = 1 + p_1(t)x_2(t) + p_2(t)u(t) \quad (3.3.15)$$

3) *Step 3*: Minimization of Hamiltonian: According to the Pontryagin Principle, the Hamiltonian is needed to be minimized as

$$\begin{aligned} H(x(t), p(t), u^*(t)) &\leq H(x(t), p(t), u(t)) \\ &= \min_{|u| \leq 1} H(x(t), p(t), u(t)) \end{aligned} \quad (3.3.16)$$

Using the Hamiltonian (3.3.15) in the condition (3.3.16), then

$$1 + p_1(t)x_2(t) + p_2(t)u^*(t) \leq 1 + p_1(t)x_2(t) + p_2(t)u(t) \quad (3.3.17)$$

This leads to

$$p_2(t)u^*(t) \leq p_2(t)u(t) \quad (3.3.18)$$

$$= \min_{|u| \leq 1} \{p_2(t), u(t)\} \quad (3.3.19)$$

If  $p_2(t) > 0$  i.e., (positive) the optimal control must be the smallest admissible control value  $u(t) = -1$ . On the other hand, if  $p_2(t) < 0$  i.e., (negative) the optimal control must be the largest admissible control value  $u(t) = +1$ . Finally, if  $p_2(t) = 0$ , the optimal control  $u(t)$  is indeterminate. Therefore, the time optimal control is given by expression

$$u(t) = -\text{sign}\{p_2(t)\} = \Delta = \pm 1 \quad (3.3.20)$$

This type of control action is also called “Bang-Bang” since it is either at its maximum value or its minimum value. Transitions between the extrema are called switches. The following section explains the third step taken in the optimal switching design.

### 3.3.3 Step III – Designing Forced Trajectory

Now to know the nature of the optimal control, the costate function  $p_2(t)$  needs to be solved.

1) *Step 1: Costate Solutions:* The costate equations along with the Hamiltonian (3.3.15) are

$$\begin{aligned}\dot{p}_1(t) &= -\frac{dH}{dx_1(t)} = 0 \\ \dot{p}_2(t) &= -\frac{dH}{dx_2(t)} = -p_1(t)\end{aligned}\quad (3.3.21)$$

Let  $\pi_1$  and  $\pi_2$  be the initial values of the costate variables

$$\begin{aligned}\pi_1 &= p_1(0) \\ \pi_2 &= p_2(0)\end{aligned}\quad (3.3.22)$$

Then, from equations (3.3.21), it is found that

$$\begin{aligned}p_1(t) &= \pi_1 = \text{constant} \\ p_2(t) &= \pi_2 - \pi_1 t\end{aligned}\quad (3.3.23)$$

2) *Step 2: Time Optimal Control Sequences:* It can be noted that  $p_2(t)-t$  was a straight line in the  $p_2(t)$  plane; the four possible shapes of  $p_2(t)$  and the corresponding shapes of the  $H$ -minimal control  $u(t) = -\text{sign}\{p_2(t)\}$  are shown in Figure 3.4

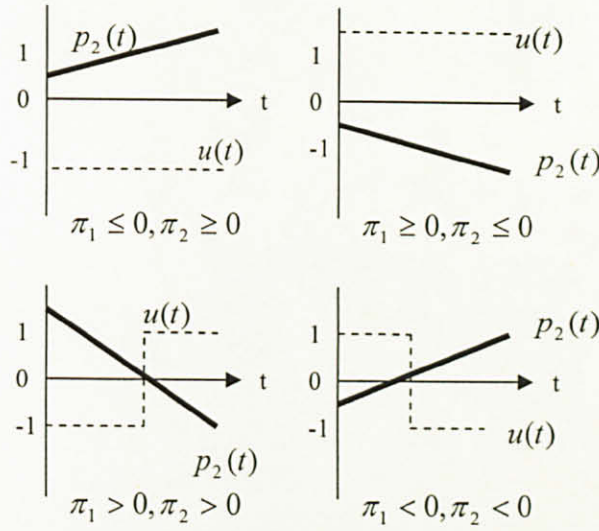


Figure 3.4: The four possible ‘shapes’ of  $p_2(t) = \pi_2 - \pi_1 t$  and the corresponding controls  $u(t) = -\text{sgn}\{\pi_2 - \pi_1 t\}$

The four possible ‘shapes’ of  $p_2(t)$  shown in Figure 3.4 indicates that the optimal control is a piecewise constant and could switch, at most once because the problem was normal. There exists four control sequences i.e,

$$\{+1\}, \{-1\}, \{+1, -1\}, \{-1, +1\} \quad (3.3.24)$$

That could satisfy the time-optimal control problem [equations (3.3.20)]. Equation (3.3.23) has indicated that there were only four possible control sequences. Therefore, the admissible control sequences are given by (3.3.24). However, it is important to note that a control sequences like for example  $\{+1, -1, +1\}$  is not an optimal control sequence. The reason is the control sequence  $\{+1, -1, +1\}$  requires two switching which was in violation of the time optimal theorem (see [10, 36] for details). From Figure 3.4, the optimal control for this second order system (double integral) can be seen as a piecewise constant and could switch only once. In order to arrive at closed-loop realization of the optimal control, the phase  $(x_1(t), x_2(t))$  plane (state) trajectories need to be found.

3) *Step 3: State Trajectories:* Since, over a finite interval of time, the time-optimal control constant  $u(t) = \Delta = \pm 1$ , we can solve (3.3.3) using  $u(t) = \Delta = \text{const}$  with the initial conditions

$$x_1(0) \cong \xi_1, x_2(0) \cong \xi_2 \quad (3.3.25)$$

To obtain the relations

$$x_2(t) = \xi_2 + \Delta t \quad (3.3.26)$$

$$x_1(t) = \xi_1 + \xi_2 t + \frac{1}{2} \Delta t^2 \quad (3.3.27)$$

The time  $t$  is eliminated, and gives

$$x_1(t) = \xi_1 - \frac{1}{2} \Delta \xi_2^2 + \frac{1}{2} \Delta x_2(t)^2 \quad (3.3.28)$$

Where

$$t = \Delta(x_2(t) - \xi_2) = \frac{x_2(t) - \xi_2}{\Delta} \quad (3.3.29)$$

Equation (3.3.28) is the equation of the trajectory in the  $(x_1, x_2)$  plane originating at  $(\xi_1, \xi_2)$  and due to the action of the control  $u(t) = \Delta$ .

If  $u = +1$ , then

$$\begin{aligned} t &= x_2(t) - \xi_2 \\ x_1(t) &= \xi_1 - \frac{1}{2} \xi_2^2 + \frac{1}{2} x_2(t)^2 = C_1 + \frac{1}{2} x_2(t)^2 \end{aligned} \quad (3.3.30)$$

And if  $u = -1$ , then

$$\begin{aligned} t &= \xi_2 - x_2(t) \\ x_1(t) &= \xi_1 + \frac{1}{2} \xi_2^2 - \frac{1}{2} x_2(t)^2 = C_1 - \frac{1}{2} x_2(t)^2 \end{aligned} \quad (3.3.31)$$

Where  $C_1 = \xi_1 - \frac{1}{2}\xi_2^2$  and  $C_2 = \xi_1 + \frac{1}{2}\xi_2^2$  are constant. Now, the relations (3.3.30) and (3.3.31) can be represented as a family of parabolas in  $(x_1, x_2)$  plane as in Figure 3.5

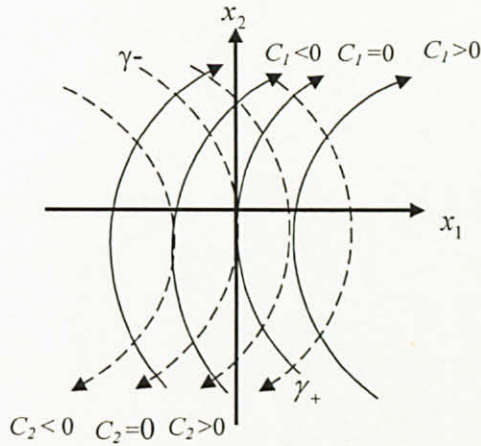


Figure 3.5: The forced (phase plane) trajectories in the state plane, the solid trajectories are generated by  $u = 1$  and the dashed trajectories are generated by  $u = -1$

The objective is to drive any initial state to  $(0,0)$ , that is, to the origin of the state plane.

Then, from (3.3.28), it is found that at  $t = t_f$

$$x_1(t = t_f) = 0; x_2(t = t_f) = 0 \tag{3.3.32}$$

With this, (3.3.28) becomes

$$0 = \xi_1 - \frac{1}{2}\Delta\xi_2^2 + 0 \rightarrow \xi_1 = \frac{1}{2}\Delta\xi_2^2 \tag{3.3.33}$$

Rewrite this for any initial state using  $x_1(t) = \xi_1, x_2(t) = \xi_2, \Delta = u$ , it is found that

$$x_1(t) = \frac{1}{2} u x_2^2(t) \quad (3.3.34)$$

The problem can be restated as to find the time-optimal control sequence to drive the system from any initial state  $(x_1(t), x_2(t))$  to the origin  $(0,0)$  in a minimum time.

4) *Step 4: Switch Curve:* From Figure 3.5, it can be seen that there are two curves labeled  $\gamma_+$  and  $\gamma_-$  which transfer any initial state  $(x_1(t), x_2(t))$  to the origin  $(0,0)$ .

1. The  $\gamma_+$  curve is the locus of all (initial) points  $(x_1(t), x_2(t))$  which can be transferred to the final point  $(0,0)$  by the control  $u = +1$ . That is

$$\gamma_+ = \{(x_1, x_2) : x_1 = \frac{1}{2} x_2^2, x_2 \leq 0\} \quad (3.3.35)$$

2. The  $\gamma_-$  curve is the locus of all (initial) points  $(x_1(t), x_2(t))$  which can be transferred to the final point  $(0,0)$  by the control  $u = -1$ . That is

$$\gamma_- = \{(x_1, x_2) : x_1 = -\frac{1}{2} x_2^2, x_2 \geq 0\} \quad (3.3.36)$$

3. The complete switch curve, or the  $\gamma$  curve, is defined as the union of the partial switch curves  $\gamma_+$  and  $\gamma_-$ . That is

$$\begin{aligned} \gamma &= \{(x_1, x_2) : x_1 = -\frac{1}{2} x_2 |x_2|\} \\ &= \gamma_+ \cup \gamma_- \end{aligned} \quad (3.3.37)$$

where  $\cup$  means the union operation. The switch curve  $\gamma$  is shown in the following section as Figure 3.6.



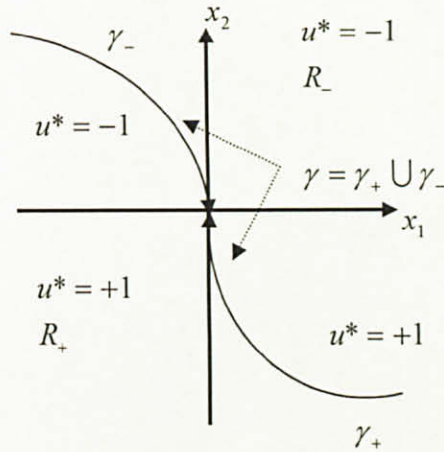


Figure 3.6: Switch curve

5) *Step 5*: Phase Plane Regions: The regions is defined by applying the control  $u = +1$  or  $u = -1$ .

1. Let  $R_+$  be the region of the points such that

$$R_+ = \left\{ (x_1, x_2) : x_1 < -\frac{1}{2} x_2 |x_2| \right\} \quad (3.3.38)$$

That is  $R_+$  consist of the region of the points to the left of the switch curve  $\gamma$ .

2. Let  $R_-$  be the region of the points such that

$$R_- = \left\{ (x_1, x_2) : x_1 > -\frac{1}{2} x_2 |x_2| \right\} \quad (3.3.39)$$

That is  $R_-$  consist of the region of the points to the right of the switch curve  $\gamma$ . The various trajectory generated by the possible control sequences is shown in the following section as Figure 3.7.

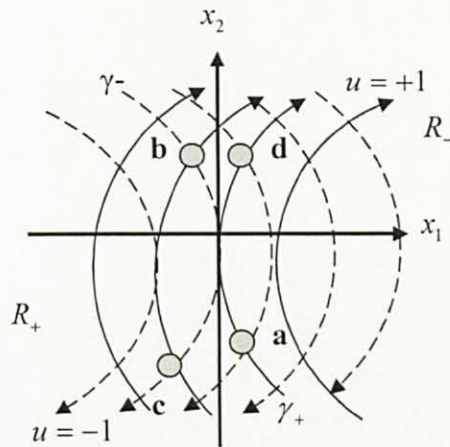


Figure 3.7: Various trajectories generated by four possible control sequences

Figure 3.7 shows four possible control sequences (3.3.24) which drive the system from any initial condition to the origin.

1. If the system is initially anywhere (point **a**) on the  $\gamma_+$  curve, the optimal control is  $u = +1$  to drive the system to origin in minimum time  $t_f$ .
2. If the system at rest anywhere (point **b**) on the  $\gamma_-$  curve, the optimal control is  $u = -1$  to drive the system to origin in minimum time  $t_f$ .
3. If the system is initially anywhere (point **c**) in the  $R_+$  region, the optimal control sequence is  $u = \{+1, -1\}$  to drive the system to origin in minimum time  $t_f$ .
4. If the system is initially anywhere (point **d**) in the  $R_-$  region, the optimal control sequence is  $u = \{-1, +1\}$  to drive the system to origin in minimum time  $t_f$ .

If the system is initially at point  $\mathbf{d}$ , where the control  $u = +1$  and the optimal control sequence  $u = \{-1, +1\}$  were used, the system can also be drove to origin. However, if say a control sequence  $\{+1, -1, +1\}$  is used, which was not a member of the optimal control sequence (3.3.24), then the time  $t_f$  taken is higher than the corresponding time  $t_f$  taken for the system with control sequence  $\{-1, +1\}$ .

6) *Step 6: Control Law:* The time optimal control  $u$  as a function of the state  $[x_1, x_2]$  is given by

$$\begin{aligned} u^* &= u^*(x_1, x_2) = +1 \text{ for } (x_1, x_2) \in \gamma_+ \cup R_+ \\ u^* &= u^*(x_1, x_2) = -1 \text{ for } (x_1, x_2) \in \gamma_- \cup R_- \end{aligned} \quad (3.3.40)$$

Alternatively, if  $z = x_1 + \frac{1}{2}x_2|x_2|$  is defined, then if

$$\begin{aligned} z > 0, u^* &= -1 \quad \text{and} \\ z < 0, u^* &= +1 \end{aligned} \quad (3.3.41)$$

The following section explains the forth step taken in the optimal switching design.

### 3.3.4 Step IV – Derivation of Optimal Switching and Total Minimum Time

#### 1) Step I: Optimal Switching Time

Let say the initial point  $(\xi_1, \xi_2)$  is at regional  $R_-$ . Therefore  $\Delta = u = -1$ ,

$$x_1 = \xi_1 - \frac{1}{2}x^2 + \frac{1}{2}\xi_2^2 = \xi_1 + \frac{1}{2}(\xi_2^2 - x_2^2) \quad (3.3.42)$$

This intersect  $\gamma_+$  at a point  $(x_1, x_2)$  where  $x_1$  is positive and  $x_2$  is negative that satisfies

$$\begin{aligned} \xi_1 + \frac{1}{2}(\xi_2^2 - x_2^2) &= \frac{1}{2}x_2^2 \\ x_2^2 &= \xi_1 + \frac{1}{2}\xi_2^2 \end{aligned} \quad (3.3.43)$$

Since  $x_2 < 0$  at all points of  $\gamma_+$ , the switch occurs at the point where

$$x_2 = -\sqrt{\xi_1 + \frac{1}{2}\xi_2^2} \quad (3.3.44)$$

The equation for the intersection in region  $\gamma_+$  is  $x_1 = \frac{1}{2}x_2^2$ . Therefore

$$x_1 = \frac{1}{2}\xi_1 + \frac{1}{4}\xi_2^2 \quad (3.3.45)$$

The time from start to switch with  $\Delta = u = -1$  is

$$\begin{aligned} t_1 &= \xi_2 - x_2 \\ t_1 &= \xi_2 + \sqrt{\xi_1 + \frac{1}{2}\xi_2^2} \end{aligned} \quad (3.3.46)$$

With similar reasoning, the time from switch to start with  $\Delta = u = +1$  is  $t_2 = x_2 - \xi_2$ .

With  $x_2 = 0$ , the time is

$$t_2 = \sqrt{\xi_1 + \frac{1}{2}\xi_2^2} \quad (3.3.47)$$

Therefore, the minimum total time taken for the flow to be equalized at the point of coriolis (origin) is

$$T = t_1 + t_2 = \xi_2 + \sqrt{\xi_1 + \frac{1}{2}\xi_2^2} + \sqrt{\xi_1 + \frac{1}{2}\xi_2^2} = \xi_2 + 2\sqrt{\xi_1 + \frac{1}{2}\xi_2^2} \quad (3.3.48)$$

2) *Step 2: Total Minimum Time:* The time taken for the system starting at any position in state space and ending at the origin can be calculated by using the set of equation (3.3.28) and (3.3.29) for each portion of the trajectory. It can be shown that the minimum time  $t_f$  for the system starting from  $(x_1, x_2)$  and arriving at  $(0,0)$  is given by

$$t_f = \begin{cases} x_2 + \sqrt{4x_1 + 2x_2^2} & \text{If } x_1 > -\frac{1}{2}x_2|x_2| \\ -x_2 + \sqrt{-4x_1 + 2x_2^2} & \text{If } x_1 < -\frac{1}{2}x_2|x_2| \\ |x_2| & \text{If } x_1 = -\frac{1}{2}x_2|x_2| \end{cases} \quad (3.3.49)$$

The following section explains the fifth step taken in the optimal switching design i.e., simulation of forced trajectory using Matlab Simulink.

### 3.3.5 Step V – Modeling of forced trajectory using Matlab Simulink

1) Step I: Engineering Implementation of Control Law

Figure 3.8 shows the implementation of the optimal control law (3.3.40).

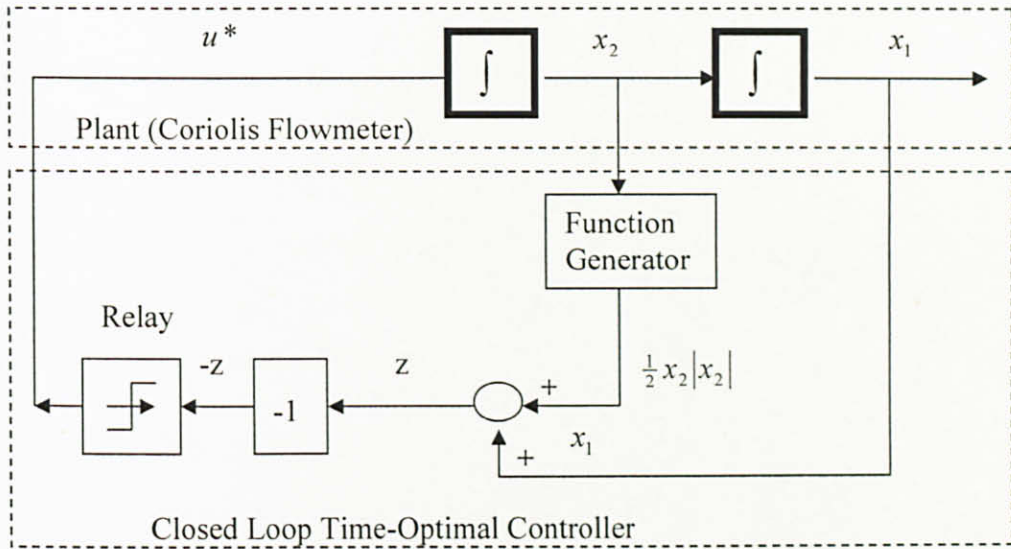


Figure 3.8: Closed-Loop implementation of Time-Optimal Control Law

Note that the closed-loop (feedback) optimal controller nonlinear (control  $u$  is a nonlinear function of  $x_1$  and  $x_2$ ) although the system is linear. The state variables  $x_1$  (output) and  $x_2$  (output rate) are measured at each instant of time. The signal  $x_2$  is introduced to the nonlinearity (function generator), whose output is  $\frac{1}{2}x_2|x_2|$ . The signal  $z(t)$  is given as

$$z(t) = x_1(t) + \frac{1}{2}x_2(t)|x_2(t)| \quad (3.3.50)$$

and after a sign reversal, a relay can be controlled. Basically, the relay is the engineering realization of the signum operation. The relay output  $u^*(t)$  is the time optimal control.

1. If the system is initially at  $(x_1, x_2) \in R_-$ , then  $x_1 > -\frac{1}{2}x_2|x_2|$ , this means  $z > 0$  and hence the output of the relay is  $u = -1$ .
2. If the system is initially at  $(x_1, x_2) \in R_+$ , then  $x_1 < -\frac{1}{2}x_2|x_2|$ , this means  $z < 0$  and hence the output of the relay is  $u = +1$ .

A basic difficulty occurs when the state  $(x_1(t), x_2(t)) \in \gamma$ , then  $z(t) = 0$ . In this case, the input signal to the relay is zero: however, since a relay is a physical element with small (but nonzero) inertia, the relay will not switch precisely at the  $\gamma$  curve but some distance away. Hence, by the time the relay actually switches, the state is no longer on the  $\gamma$  curve and the input to the relay is nonzero. For this reason the system of Figure 3.5 is also called an engineering realization of the control law.

## 2) Step 2: Matlab Simulink Model

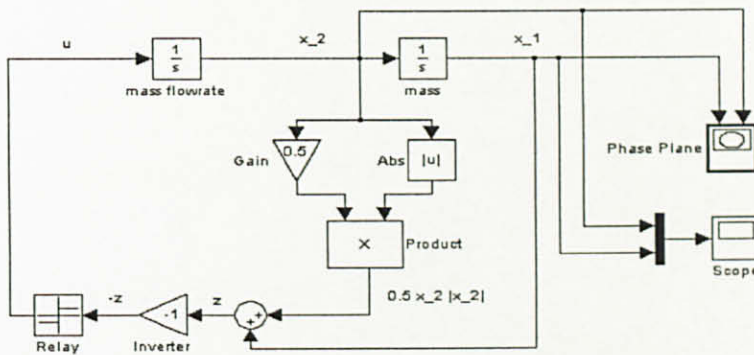
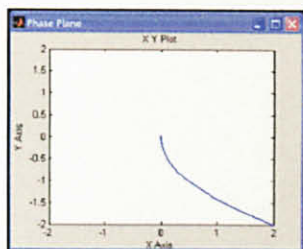


Figure 3.9: Simulink implementation of Time Optimal Control Law

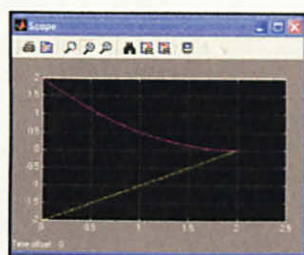
The implementation of time-optimal control model is obtained by using *abs* and *signum* function block as shown in Figure 3.9. The model is tested with four different initial conditions of output,  $x_1$ , and output rate,  $x_2$ , to simulate the  $(x_1, x_2)$  phase-plane trajectories belonging to  $\gamma_+$ ,  $\gamma_-$ ,  $R_+$  and  $R_-$ , and compare that with equations (3.3.46) and (3.3.47) to valid  $t_1$  and  $t_2$ . The following section shows several examples of forced trajectory simulated from the Matlab Simulink model.

### 3.4 Results of simulation model

Figure 3.10 (a) shows the forced trajectory for an initial state of (2, -2). Figure 3.10 (b) shows the switching time only occurs for  $t_1$  and the total time taken to the origin is  $t_f = 2s$ . This can be validated by equation (3.3.49) under  $t_f = |x_2|$  if  $x_1 = -\frac{1}{2}x_2|x_2|$ .



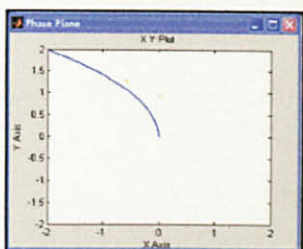
(a) Phase-Plane Trajectory



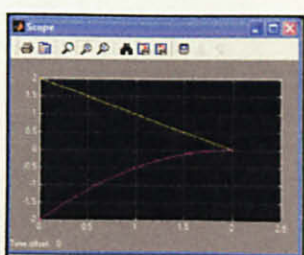
(b) Time of Switching,  $t_1$

Figure 3.10: (a) Phase-Plane Trajectory for  $\gamma_+$  with Initial State (2, -2)  
(b) Total Time of Switching with Initial State (2,-2)

Figure 3.11 (a) shows the forced trajectory for an initial state of (-2, 2). Figure 3.11 (b) shows the switching time also occurs for  $t_1$  and the total time taken to the origin is  $t_f = 2s$ . This can also be validated by equation (3.3.49) under  $t_f = |x_2|$  if  $x_1 = -\frac{1}{2}x_2|x_2|$ .



(a) Phase-Plane Trajectory

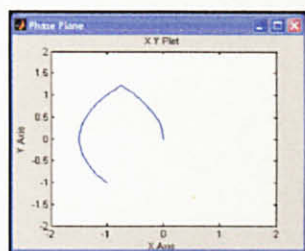


(b) Time of Switching,  $t_1$

Figure 3.11: (a) Phase-Plane Trajectory for  $\gamma_-$  with Initial State (-2, 2)  
(b) Total Time of Switching with Initial State (-2, 2)



Figure 3.12 (a) shows the forced trajectory for an initial state of  $(-1, -1)$ . Figure 3.12 (b) shows the switching time occurs for  $t_1$  and  $t_2$  with total time taken to the origin is  $t_f = 3.45s$ . This is validated by equation (3.3.49) under  $t_f = -x_2 + \sqrt{-4x_1 + 2x_2^2}$  if  $x_1 < -\frac{1}{2}x_2|x_2|$ .



(a) Phase-Plane Trajectory

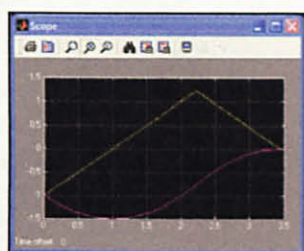
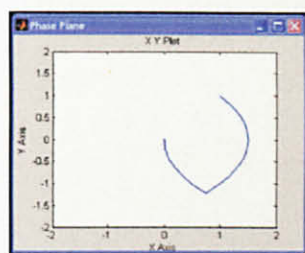
(b) Time of Switching,  $t_1$  and  $t_2$ 

Figure 3.12: (a) Phase-Plane Trajectory for  $R_+$  with Initial State  $(-1, -1)$   
 (b) Total Time of Switching with Initial State  $(-1, -1)$

Figure 3.13 (a) shows the forced trajectory for an initial state of  $(1, 1)$ . Figure 3.13 (b) shows the switching time occurs for  $t_1$  and  $t_2$ . More precisely, equations (3.3.46), (3.3.47) and (3.3.48) can be used to calculate the time for switching, time from switching to origin and total time which are  $t_1 = 2.225s$ ,  $t_2 = 1.225s$  and  $t_f = 3.45s$ . The total time can be validated by equation (3.3.49) under  $t_f = x_2 + \sqrt{4x_1 + 2x_2^2}$  if  $x_1 > -\frac{1}{2}x_2|x_2|$ .



(a) Phase-Plane Trajectory

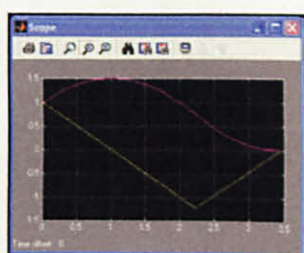
(b) Time of Switching,  $t_1$  and  $t_2$ 

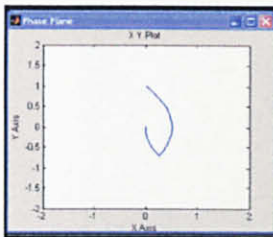
Figure 3.13: (a) Phase-Plane Trajectory for  $R_-$  with Initial State  $(1, 1)$   
 (b) Total Time of Switching with Initial State  $(1, 1)$

Before implementing the TOC refueling algorithm in an executable program, the equations of switching is used to validate its performance with range of signals from the actual Coriolis flowmeter of the NGV test rig. Practically, the value of mass and mass flowrate measured by the coriolis flowmeter cannot be negative, and this is only true for range of  $0 \leq x_1(t) \leq x_1(t)^+$  and  $0 \leq x_2(t) \leq x_2(t)^+$ . Therefore, the input initial states for the actual system are only valid at region  $R_-$  as shown in Figure 3.14

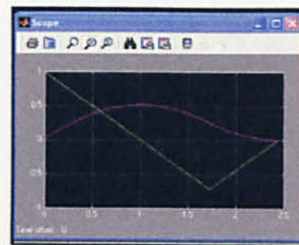
Table 3.2: Maximum and minimum values of mass and mass flowrate for Coriolis flowmeter used at UTP NGV test rig.

State Variable	Minimum	Maximum	Unit
Mass Flowrate	0	24	kg/min
Mass at Coriolis	0	0.4	kg

The values need to be scaled down so that the trajectory can be fully shown on the Simulink model. Initial state of 20 kg/min and 0.365 kg are equal to 1 kg/min and 0.018 kg in the Simulink.



(a) Phase-Plane Trajectory



(b) Time of Switching,  $t_1$  and  $t_2$

Figure 3.14: (a) Phase-Plane Trajectory for  $R_-$  with Initial State (0.018, 1)  
(b) Total Time of Switching with Initial State (0.018, 1)

The time of switching is  $t_1 = 1.72s$ . The time taken from switching point to the origin is  $t_2 = 0.72s$ . The total minimum time taken is  $t_f = 2.44s$ . Therefore, the actual time for initial state of (0.365, 20) is  $t_1 = 34.4s, t_2 = 14.4s$  and  $t_f = 48.8s$ .

### 3.5 Development of experimental hardware

One of the main tasks in this research work is to implement TOC refueling algorithm in an actual NGV refueling system, and hence, a fully instrumented NGV laboratory test facility was designed and constructed. This enables simulation of TOC during the fillings to be performed using real NGV system. The need to simulate the various conditions of NGV vehicles in Malaysia demand a test rig that able to provide a wide variety of initial pressures as required in the simulations and experiments. A number of main components that are required in the NGV refueling system test rig should be clearly explained to facilitate discussion.

The development of NGV test rig includes three main parts: NGV test rig, Data Acquisition (DAQ) & Control System using FieldPoint, and LabVIEW programming model. The test rig is designed such that it should be able to replicate the actual filling condition of the existing refueling station. Figure 3.15 shows the actual test rig located at NGV laboratory of Universiti Teknologi PETRONAS (UTP). In order to understand the detail process flow of the test rig, P&ID diagram is attached in the Appendix.

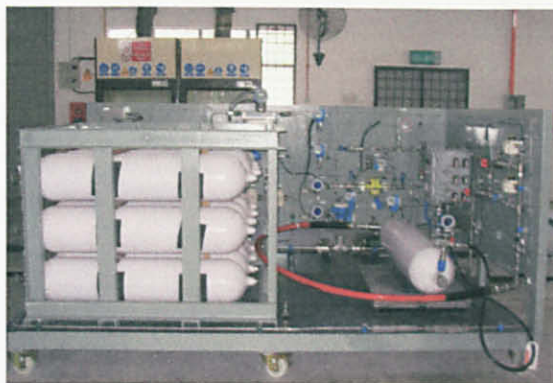


Figure 3.15: NGV test rig

#### 3.5.1 NGV test rig

The test rig consists of eight major components: the cascaded storage system, flow metering system, receiver system, recycle system, sequencing system, dispensing system, refueling system and control panel system. The purposes of these components are described in the following section.

### 3.5.1.1 Cascaded storage system

A three stage cascade storage supply of nine 5000 psig rated cylinders as shown in Figure 3.16 has been arranged in a 4-3-2 arrangement representing the low, medium and high pressure configuration. Each cylinder has a capacity of 55 liters at 5000 psig rated pressure. The cylinder cascade banks were assembled with motorized ball valves which were remotely activated during the testing from the laboratory computer control system.



Figure 3.16: Cascaded storage system

### 3.5.1.2 Flow metering system

A gas mass flowmeter was installed in the test rig to measure the flow of gas in the NGV cylinder during the relatively high flow, rapid charging tests. The system shown in Figure 3.17 has also been equipped with three types of volumetric flowmeter: turbine, vortex and differential flowmeter for the purpose of analyzing the flow measurement of natural gas.

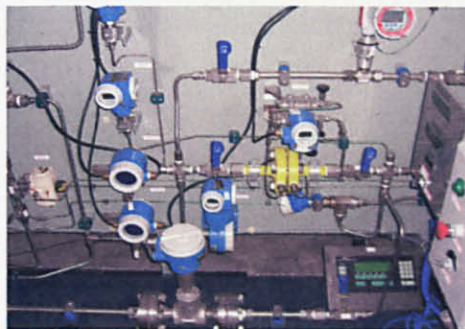


Figure 3.17: Flow metering system

### ***3.5.1.3 Receiver system***

The receiver system is a replication of an actual car storage tank, and is shown in Figure 3.18. It has one 55 liters cylinder tank at the 5000 psig rated pressure, equipped with an embedded thermocouple and a load cell to measure the actual filling weight.



Figure 3.18: Receiver system

### ***3.5.1.4 Recycle system***

The system needs to recover and recycle the natural gas from the receiver system back to the cascaded storage system. It consists of recycling piping and two compressors, as shown in Figure 3.19. Since a small amount of natural gas from receiver system is expected to be lost during each experiment, therefore the system is equipped with three 55 liters ‘make-up’ cylinders to compensate for the losses.



Figure 3.19: Recycle system

### 3.5.1.5 Sequencing system

The sequencing system is to set the low, medium and high pressure at cascaded storage system using ball valves shown in Figure 3.20. A ball valve is a valve that opens by turning a handle attached to a ball inside the valve. The ball has a hole, through the middle, thus when the hole is in line with both ends of the valve, the gas flow will take place. When the valve is closed, the hole is perpendicular to the ends of the valve, and the gas flow is blocked. If the natural gas at the cascaded storage system has reached the set pressure, the balance is restored in the temporary cylinders.



Figure 3.20: Sequencing system

### 3.5.1.6 Dispensing system

The system is to display the total sale, the total volume in liter and the price per liter on a panel as shown in Figure 3.21, during the refueling. The mass flowrate as measured by the coriolis flowmeter is translated into the sale value.



Figure 3.21: Dispensing system

### 3.5.1.7 Refueling system

The system is to test the process of refueling natural gas using a refueling algorithm based on Kraus Global Inc Company [37] which was embedded in a PCI card shown by Figure 3.22. It has built in sequencing control, totalized features for NGV refueling and located in an explosion proof housing.



Figure 3.22: Refueling system

### 3.5.1.8 Control panel system

The system housed the FieldPoint and LEDs, used to indicate the conditions of power source of the NGV test rig and the condition of compressors. There are six switches as shown in Figure 3.23, i.e., ‘SYSTEM CHANGEOVER’ to test refueling using Kraus controller or TOC, ‘COMP START’ and ‘COMP RESET’ to start and reset the compressors, ‘GAS DETECTOR’ to trigger the gas detector system, ‘DISP START’ to activate the refueling and ‘DISP SWITCH’ to turn on the dispensing system.



Figure 3.23: Control panel for UTP NGV test rig

### 3.5.2 DAQ & Control System

The development of DAQ & Control System for the NGV test rig is designed using a FieldPoint from National Instrument [38]. All the signal data produced by the transmitters and instrumentations used in the test rig are monitored and controlled remotely from a computer located in a control room via an ethernet connection and the FieldPoint. The TOC algorithm is developed using LabVIEW programming which was embedded on the FieldPoint for reliable distribution or stand-alone deployment. Figure 3.24 shows the FieldPoint system assembled with input/output (I/O) modules.

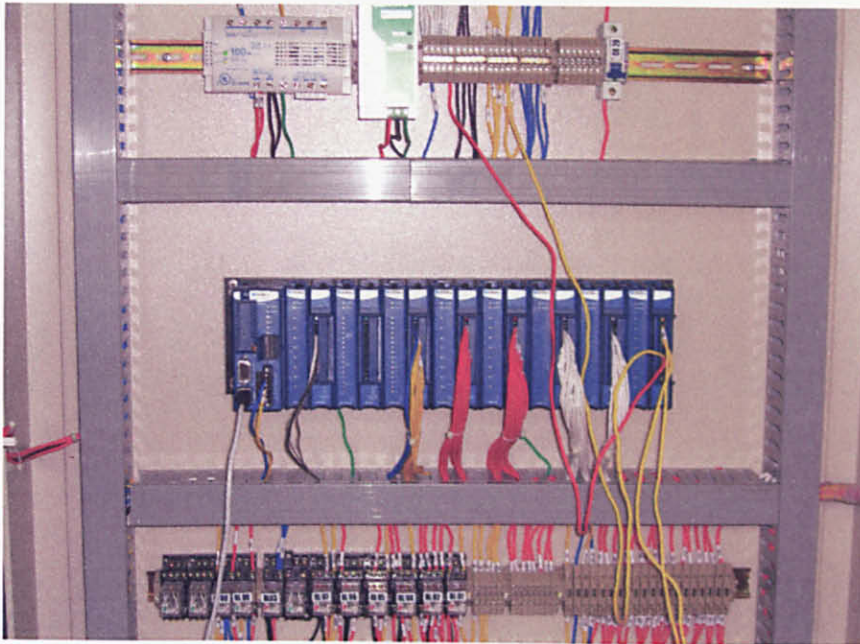


Figure 3.24: FieldPoint system with I/O modules

The modules used in the test rig are the controller, the thermocouple module, the counter module, the digital input module, the relay modules, the analog input modules and the analog output module. To simplify the installation, the plug-and-play is utilized so that the module can be automatically detected and identified by the computer.



### 3.5.3 Programming Implementation Model

Figure 3.25 shows the programming implementation model of NGV test rig developed using LabVIEW software.

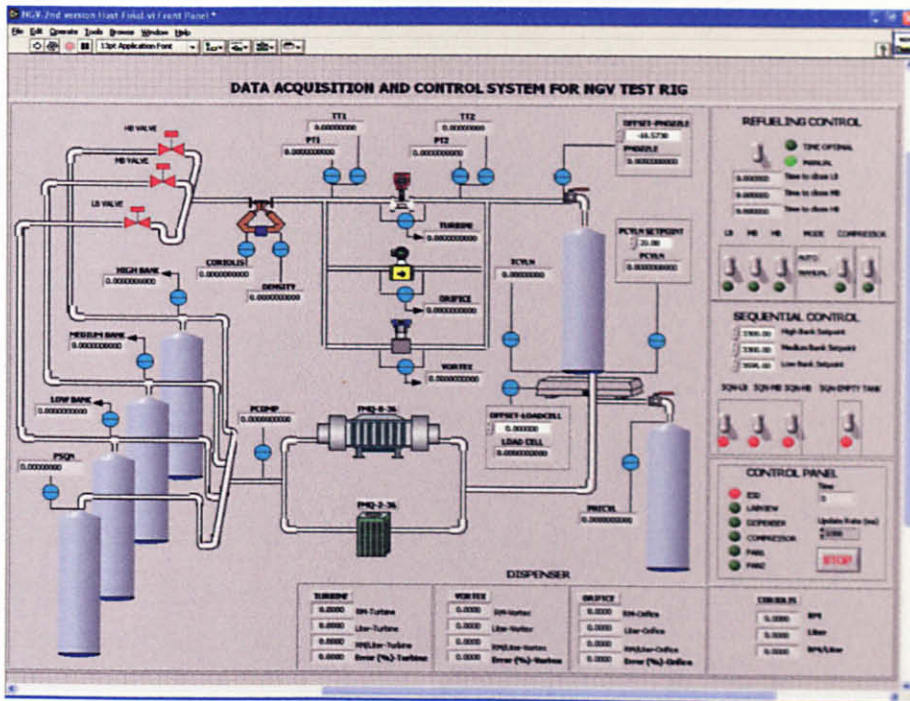


Figure 3.25: Programming implementation model for NGV test rig using LabVIEW

The LabVIEW models for NGV test rig are divided into eight major components: the cascaded storage model, flow metering model, receiver model, recycle model, sequencing model, dispensing model, refueling model and the control panel model.

#### 3.5.3.1 Cascaded storage model

The low, medium and high pressure configuration in the cascaded storage system is indicated by 'LOW BANK', 'MEDIUM BANK' and 'HIGH BANK'. The flow of natural gas to the receiver system is activated by 'LB', 'MB' and 'HB' toggle switch buttons which would change the 'LB VALVE', 'MB VALVE' and 'HB VALVE' to green color.

### ***3.5.3.2 Flow metering model***

The flowrate produced by flowmeters in the flow metering system is specified by 'TURBINE', 'ORIFICE', 'VORTEX' and 'CORIOLIS'. The density from the actual coriolis flowmeter is shown by 'DENSITY'. Pressure and temperature before and after the system are indicated by 'PT1', 'TT1' and 'PT2', 'TT2'.

### ***3.5.3.3 Receiver model***

The actual pressure, temperature, pressure inside the nozzle and actual filling weight of the receiver system are indicated by 'PCYLN', 'TCLYN', 'PNOZZLE' and 'LOAD CELL'. The value set at 'OFFSET-PNOZZLE' and 'OFFSET-LOADCELL' is used to compensate with the actual values of pressure inside the nozzle and filling weight of the NGV cylinder.

### ***3.5.3.4 Recycle model***

The compressors in the recycle system are specified by 'FMQ-8-36' and 'FMQ-2-36' which are activated by the 'COMPRESSOR' toggle switch button. The pressure during recycling process is shown by 'PCOMP' and pressure inside the 'make-up' cylinders is shown by 'PRECYL'. The recycling process stops until the pressure inside the NGV cylinder reaches the set value at 'PCYLN SETPOINT'.

### ***3.5.3.5 Sequencing model***

The 'temporary' cylinders in the sequencing system are specified by 'PSQN' which is activated by ball valve represented by 'SQN-EMPTY TANK' toggle switch button. The toggle switch button at 'MODE' determines the two type of recycling process that is the 'MANUAL' or 'AUTO'. If 'MANUAL' is chosen, the ball valves represented by 'SQN-LB', 'SQN-MB' and 'SQN-HB' toggle switch buttons are activated manually to set the pressure values at 'LOW BANK', 'MEDIUM BANK' and 'HIGH BANK'. If 'AUTO' is chosen, these buttons are activated automatically at the same time when the pressure indicated by the 'LOW BANK', 'MEDIUM BANK' and 'HIGH BANK' reaches the reference values set at 'Low Bank Setpoint', 'Medium Bank Setpoint' and the 'High Bank Setpoint'.

### ***3.5.3.6 Dispensing model***

The total sale, total volume in liter and price per liter in the dispensing system are represented by 'RM', 'Liter' and 'RM/Liter' using four dispensing models such as 'TURBINE', 'ORIFICE', 'VORTEX' and 'CORIOLIS'. The total volume in liter for actual turbine, orifice and vortex flowmeters is compared with the coriolis flowmeter based on percentage error shown by 'Error (%)'.

### ***3.5.3.7 Refueling model***

The refueling system is represented by "REFUELING CONTROL" and there are two types of refueling model represented by toggle switch button such as 'TIME OPTIMAL', and 'MANUAL'. If 'MANUAL' is activated, the refueling is tested based on Kraus refueling and if 'TIME OPTIMAL' is activated, the refueling is tested using time optimal control algorithm which has three indicators such as 'Time to close LB', 'Time to close MB' and 'Time to close HB'.

### ***3.5.3.8 Control panel model***

The control panel system is represented by 'CONTROL PANEL' and in addition contains six virtual LEDs such as 'ESD', 'LABVIEW', 'DISPENSER', 'COMPRESSOR', 'FAN1' and 'FAN2' to indicate the status of actual switches i.e., 'EMERGENCY STOP', 'SYSTEM CHANGOVER', 'DISP SWITCH', 'COMP START' and 'GAS DETECTOR'.

Sections 3.5.1 to 3.5.3 have been to describing three main components that are required in NGV laboratory test facility: NGV test rig; DAQ control system using FieldPoint; LabVIEW programming model, respectively. The following section explains the actual NGV refueling process based on TOC model conducted on the NGV test rig.

### 3.6 Validation of model

Figure 3.26 shows graph of mass flowrate for TOC refueling. The graph is obtained from series of experimentation which could be divided into 4 stages of refueling process i.e., the initialization of refueling, the filing using the low bank (LB), the filling using the Medium Bank (MB) and the filling using the high bank (HB).

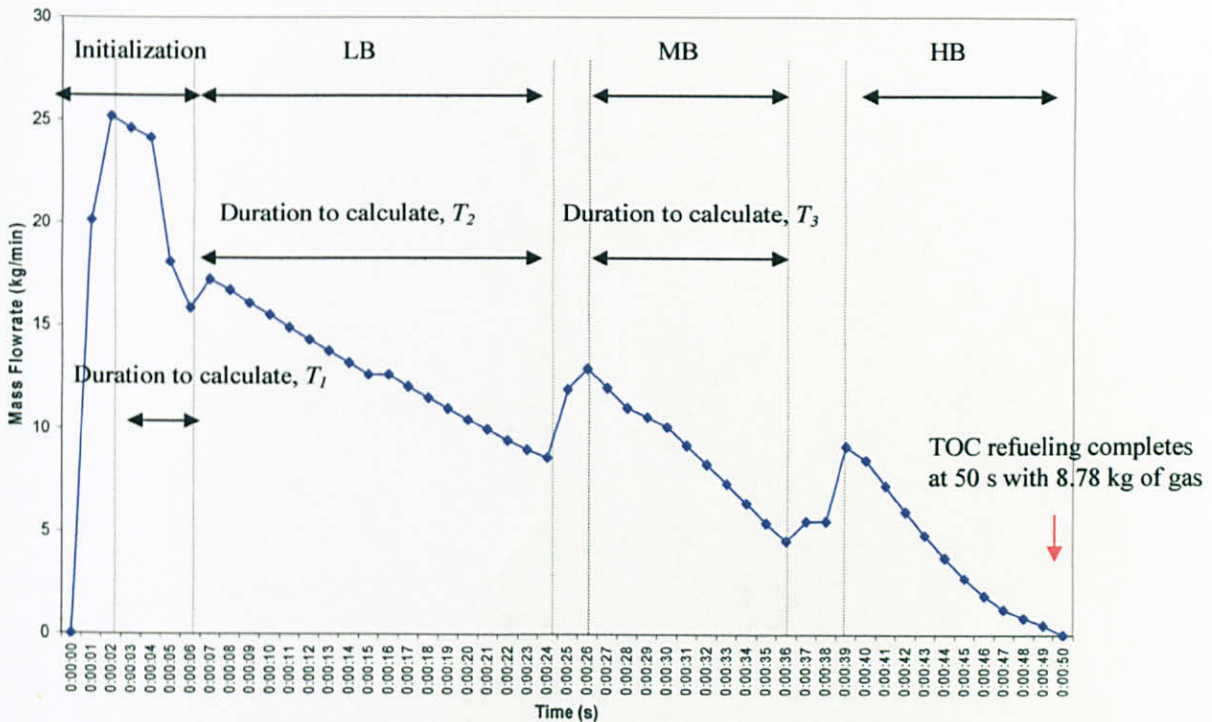


Figure 3.26: Graph of mass flowrate for TOC refueling

In the initialization stage, all the solenoid valves at the cascaded storage system i.e., the low bank valve, medium bank valve and high bank valve are initially in the close position. When the dispenser switch button at the control panel is turned on to start refueling, these valves are automatically open for three seconds for the natural gas to flow to the receiver tank. The opening is three seconds because it is the minimum time for Coriolis flowmeter to detect the mass and mass flowrate in the pipeline.

Several experiments have been conducted to verify the suitable time to open the three valves during the initialization stage as shown in Figure 3.27. Whilst, Table 3.3 shows the results of the experiments based on the total time taken and total mass of natural gas stored. Figure 3.27 shows the graphs of mass flowrates based on TOC refueling algorithm by varying the opening of valves within 15, 10, 8, 5 and 3 seconds at the initialization stage.

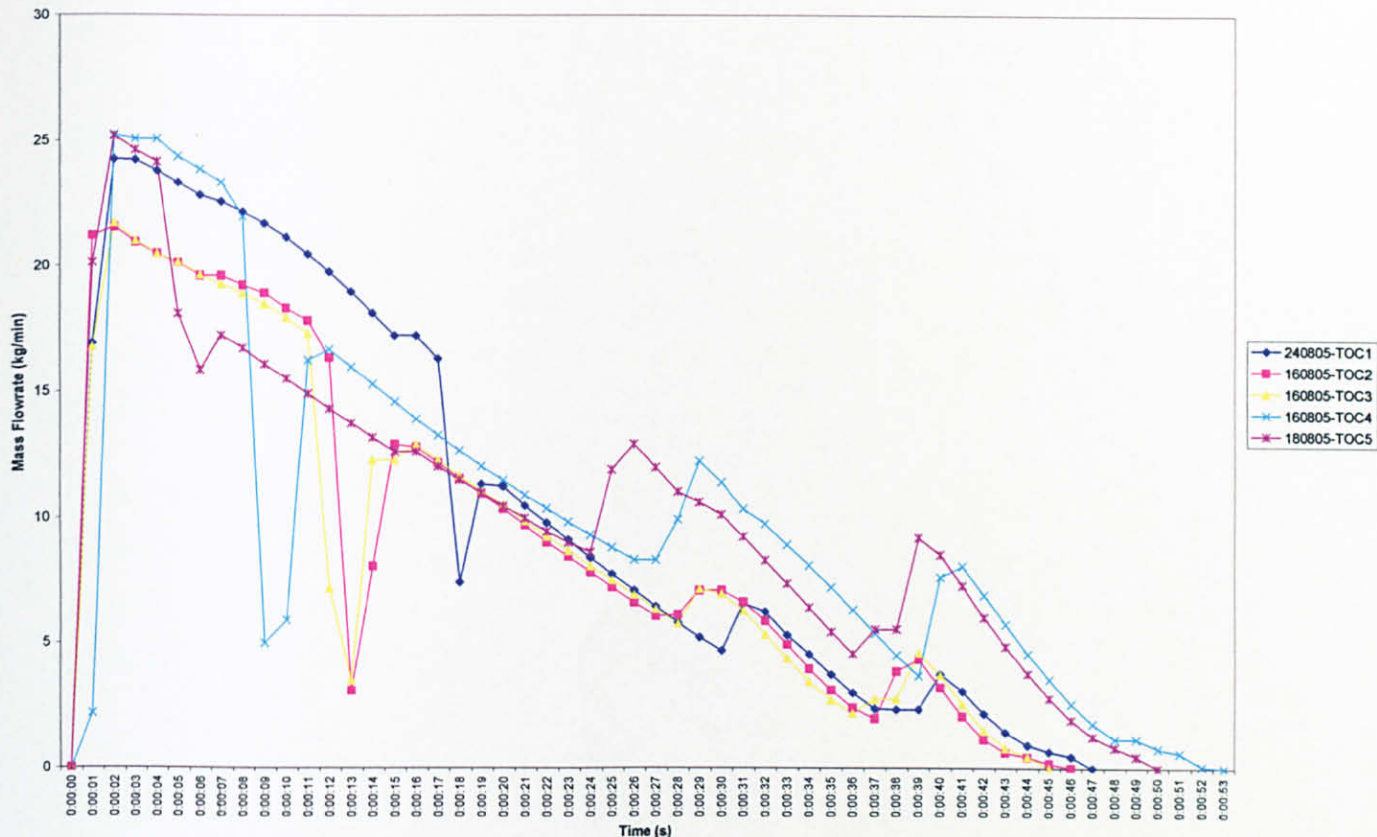


Figure 3.27: Graph for mass flowrate for TOC refueling by opening the valves within 15, 10, 8, 5 and 3 seconds during the initialization process

Table 3.3: The results of total time taken and total mass stored for Figure 3.27

Experiment	Time for opening the valves	Total time taken to complete refueling	Total mass stored after complete refueling
	(s)	(s)	(kg)
TOC1	15	47	8.41
TOC2	10	46	7.27
TOC3	8	45	7.09
TOC4	5	53	8.78
TOC5	3	50	8.87

Noted that, the total mass could be increased when the valves are opened for a shorter periods. Therefore, the experiments have verified that the suitable time to open the valves for the initialization stage is 3 seconds.

Within the three seconds, the time to switch from the low bank to the medium bank is predicted and the value is stored in the FieldPoint as ' $T_1$ '. After three seconds, all valves are closed and only the low bank valve is open to start the refueling from the low bank. During the refueling from the low bank, the time to switch from the medium bank to the high bank is determined and the value is stored in the FieldPoint as ' $T_2$ '.

As the refueling from the low bank continues and when the refueling time has reached ' $T_1$ ', the medium bank valve is open to initiate the refueling from the medium bank. During the refueling of the medium bank, the time to close all the valves is calculated and the value is stored in the FieldPoint as ' $T_3$ '.

As the refueling from the medium bank continues and when the refueling time has reached ' $T_2$ ', the high bank valve is open to initiate the refueling from the high bank. The refueling from the high bank continues until the refueling time has reached ' $T_3$ '. All valves are closed to indicate that the TOC refueling is completed.

To validate TOC as a method to optimize refueling time of current NGV refueling, graph of mass flowrate from Figure 3.26 is compared with graph of mass flowrate from a commercially NGV refueling i.e., Kraus as shown in the following section.

Figure 3.28 shows the graph of mass flowrate for Kraus refueling. The graph is also obtained from series of experimentation which could also be divided into 4 stages of refueling process i.e., the initialization of refueling, the filling using the low bank (LB), the filling using the Medium Bank (MB) and the filling using the high bank (HB). The following section explains the description for Kraus refueling which is based on [37].

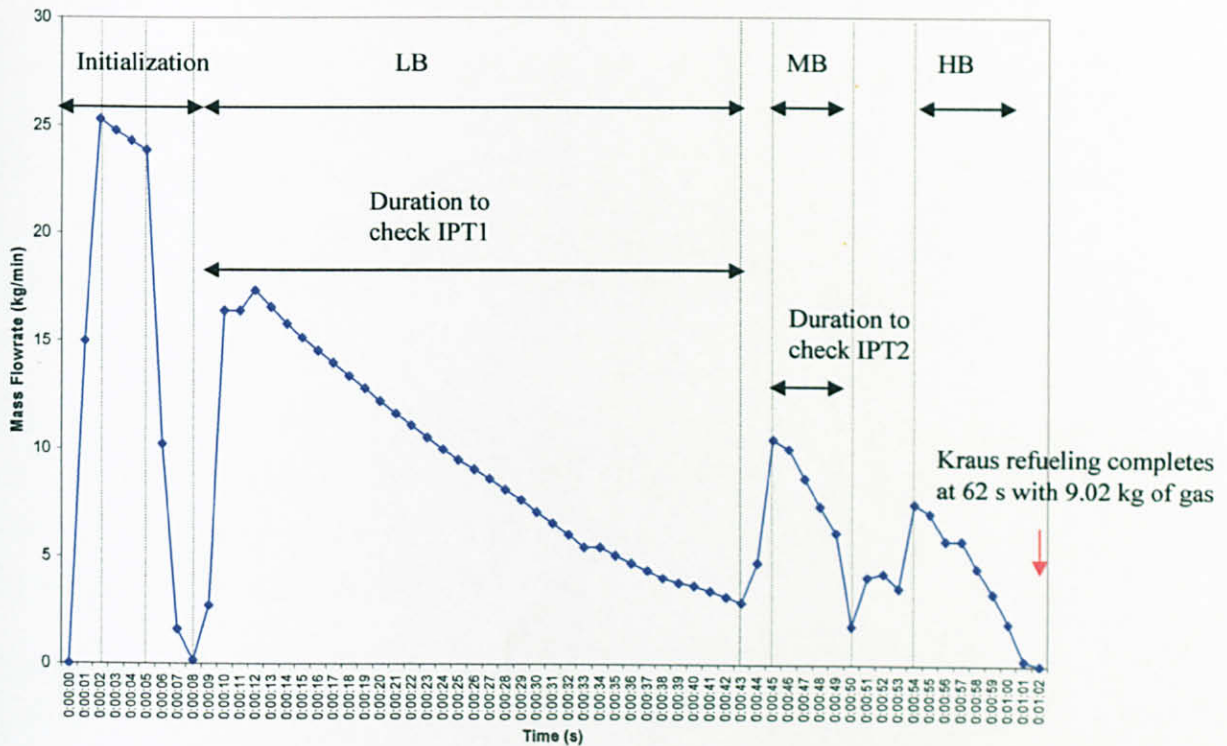


Figure 3.28: Graph of mass flowrate for Kraus refueling

When the Kraus refueling is initiated from the control panel of NGV test rig: the low bank, medium bank and high bank valves are opened for four seconds. If the flow of the natural gas is not detected for the first twenty seconds, the process is automatically stopped and deemed complete. If the flow is detected within four seconds, all valves are closed and the fill pressure is checked to know whether the initial pressure is equal to or higher than 90% of the final pressure. In Malaysia, the final pressure for NGV refueling is standardized at 3000 psig [5].

If the fill pressure is less than 90% of the final pressure, the refueling begins by opening the low bank valve. Within this refueling period, the fill pressure and the 'IPTP1' values are continuously checked. 'IPTP1' is the sequencing threshold point at which the flow has dropped significant enough for the switch over to the medium bank to take place. If the flowrate is less than 'IPTP1' and the final pressure are not yet reached, the medium bank valve is opened.

During this refueling period, the fill pressure and the 'IPTP2' value are continuously checked. 'IPTP2' is the sequencing threshold point at which the flow has dropped significant enough for the next switch over to the high bank to take place. If the flowrate is less than 'IPTP2' value and the final pressure is not yet reached, the high bank valve is opened. The flow is checked again whether it has reached the minimum flow value and the final pressure.

This sequence of switch-over continues until the highest pressure source is reached. At this point, the refueling will automatically stopped when the flow of natural gas into the vehicle storage has reached to a specified minimum value. All the valves will then be closed and the refueling process ceased.

The descriptions of NGV refueling for TOC and Kraus could also be simplified in flowcharts as shown by Figure 3.29 and 3.30. The flowchart for Kraus refueling is based on [37]. By comparing graph of mass flowrate for TOC with current NGV refueling i.e., Kraus, it is verified that TOC refueling time is shorter than Kraus refueling i.e., time optimal. Noted that, the refueling time for TOC i.e., 50 seconds shown by Figure 3.26 is shorter compared to Kraus i.e., 62 seconds shown by Figure 3.28.

This observation verifies that TOC could reduce or optimize current refueling time i.e., current congestion problem in the country as stated in the problem statement and could be developed as an efficient method for NGV refueling. However, several experiments need to be done to investigate the effect of TOC with respect to total mass of natural gas stored which is explained in the following chapter.



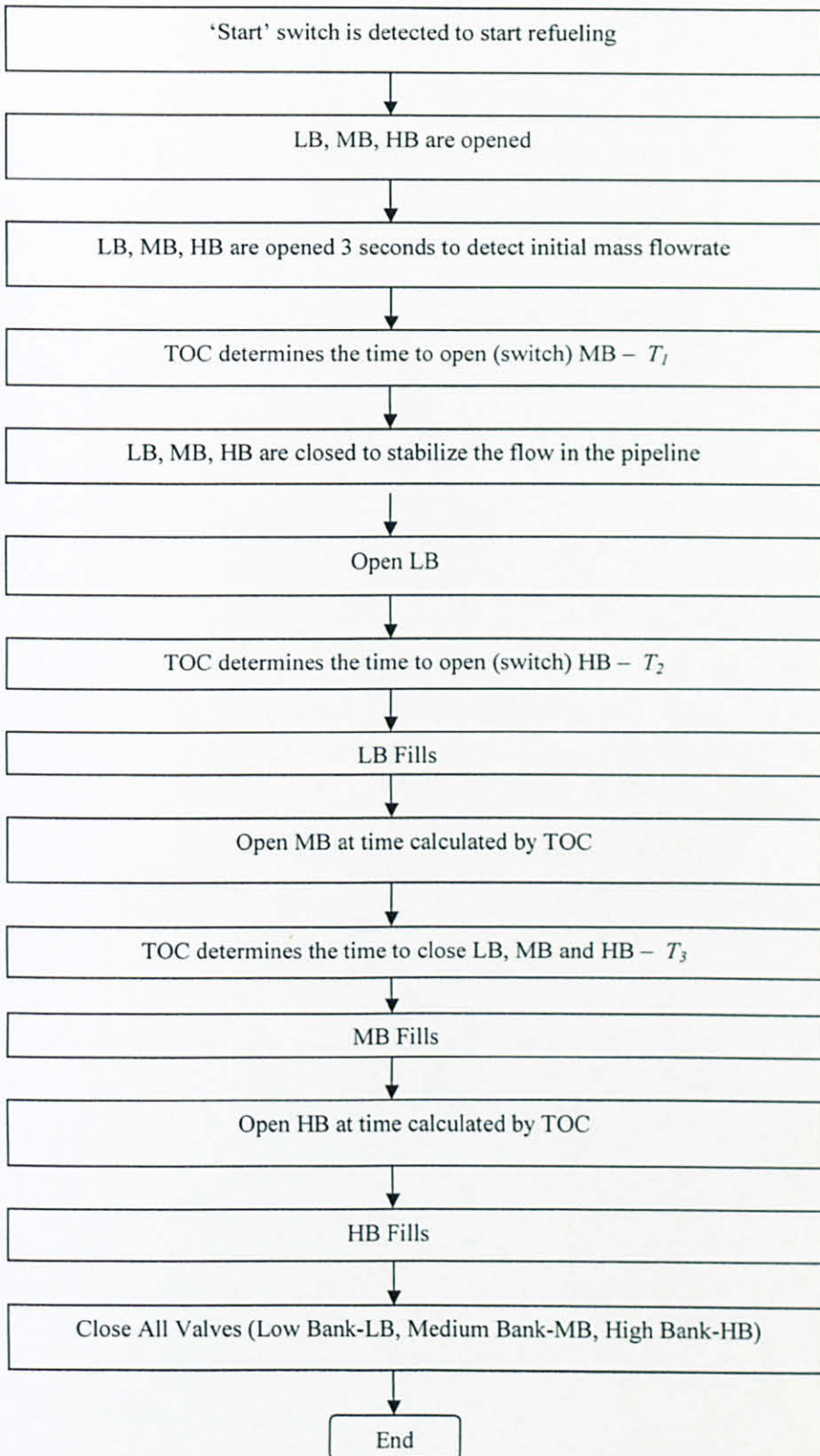


Figure 3.29: Flowchart of TOC refueling algorithm

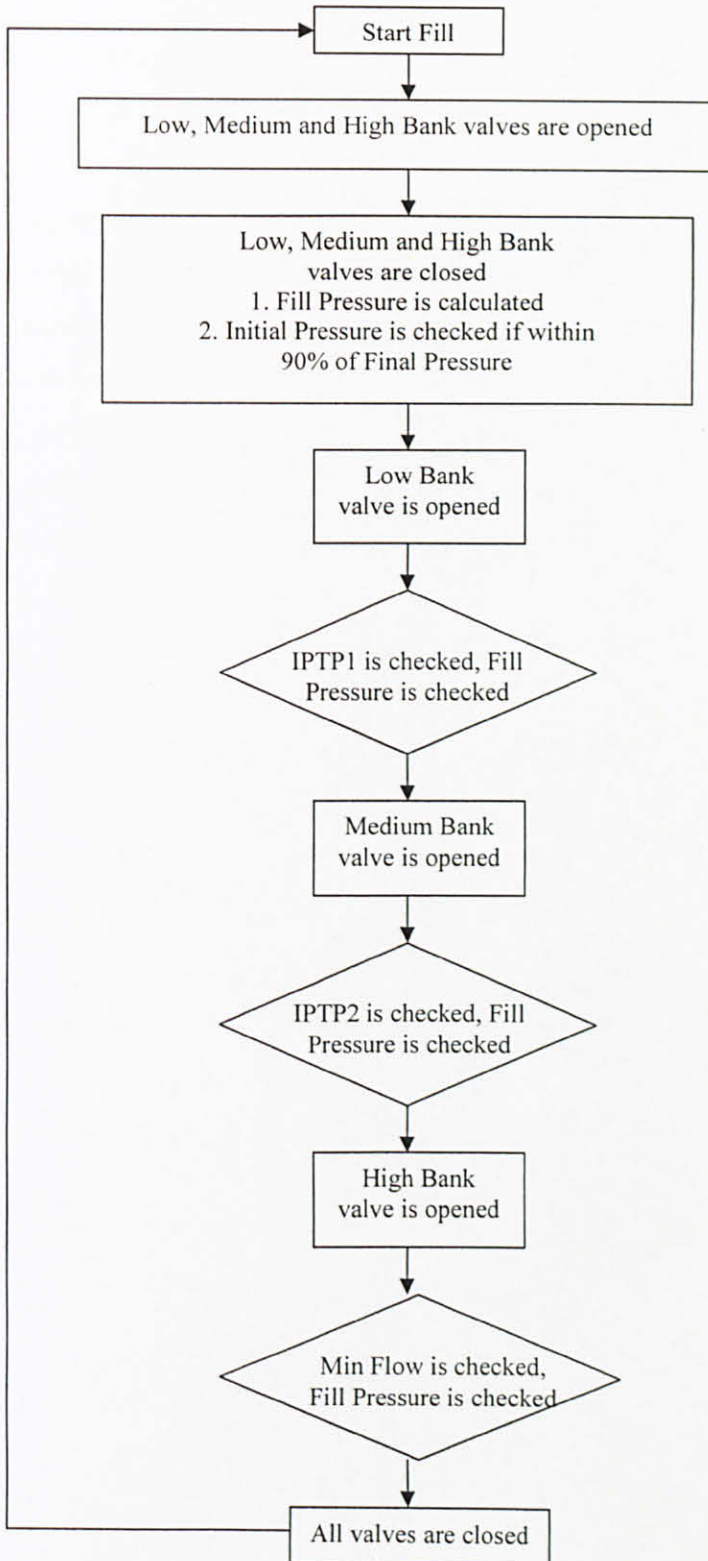


Figure 3.30: Flowchart of Kraus refueling algorithm [37]

### 3.7 Summary

Chapter 3 introduces the conceptual model of applying TOC in NGV refueling system with multi-level pressure source. The TOC is used as a basis in NGV refueling algorithm by determining the optimal switching time for the switch-over to take place or in other words, until the pressure inside the storage banks reaches the pressure inside the receiver tank. The TOC refueling algorithm is developed using mass and mass flowrate as state variables and measurement is made using a coriolis flowmeter. The model validation and verification of switching algorithm for NGV refueling is solved using a forced trajectory simulated using Matlab Simulink. In order to implement TOC refueling algorithm in actual NGV refueling process, a fully instrumented NGV laboratory test facility is designed and constructed to enable a simulated TOC filling to be performed over a wide range of initial pressures. The development of NGV test rig consists of three main parts: the NGV test rig, the Data Acquisition (DAQ) & Control System using FieldPoint and the LabVIEW programming model. The NGV test rig is designed such that it is able to replicate the actual filling condition of existing refueling station. The TOC refueling algorithm is developed using LabVIEW programming and embedded inside FieldPoint, before it is tested in the test rig. Graph based on mass flowrate for TOC refueling is compared with graph based on mass flowrate from a commercially NGV refueling i.e., Kraus to validate TOC as a suitable method for NGV refueling. From the comparison of mass flowrates, it shows that TOC could be developed as an efficient method to improve NGV refueling time. However, several experiments need to be done to investigate the effect of TOC with respect to total mass stored as described in the following chapter.

## **CHAPTER 4**

### **RESULTS AND DISCUSSION**

This chapter concentrates on discussion of TOC and Kraus refueling experiments conducted on NGV test rig. Since mass flowrate is applied in development of TOC refueling algorithm, graph based on mass flowrate is used to analyze the experiments which could be summarized into three areas: Performance of valves switching and refueling time transitions; Performance of refueling using various initial pressures inside receiver tank; Performance of refueling using multi-pressure storage source.

#### **4.1 Introduction**

In order to evaluate TOC refueling, a comparison is made with commercially available NGV refueling i.e., Kraus refueling. Each of experiments is summarized into two models: the first model is valuation for TOC refueling and the second model is valuation for Kraus refueling. The following section describes the first area of experiments i.e., performance of valves switching and refueling time transitions.

#### **4.2 Performance of valves switching and refueling time transitions**

Figure 4.1 and Figure 4.2 show graphs based on mass flowrate for TOC and Kraus refueling. Noted that, the shape of mass flowrates is identical which is shown by 4 stages of refueling process. Apart of that, each of them is separated with 4 different heights of spikes which lengths between them are varied. The position and length between spikes are defined as 'time of switching' and 'refueling time transition' which would be analyzed further in the following section.

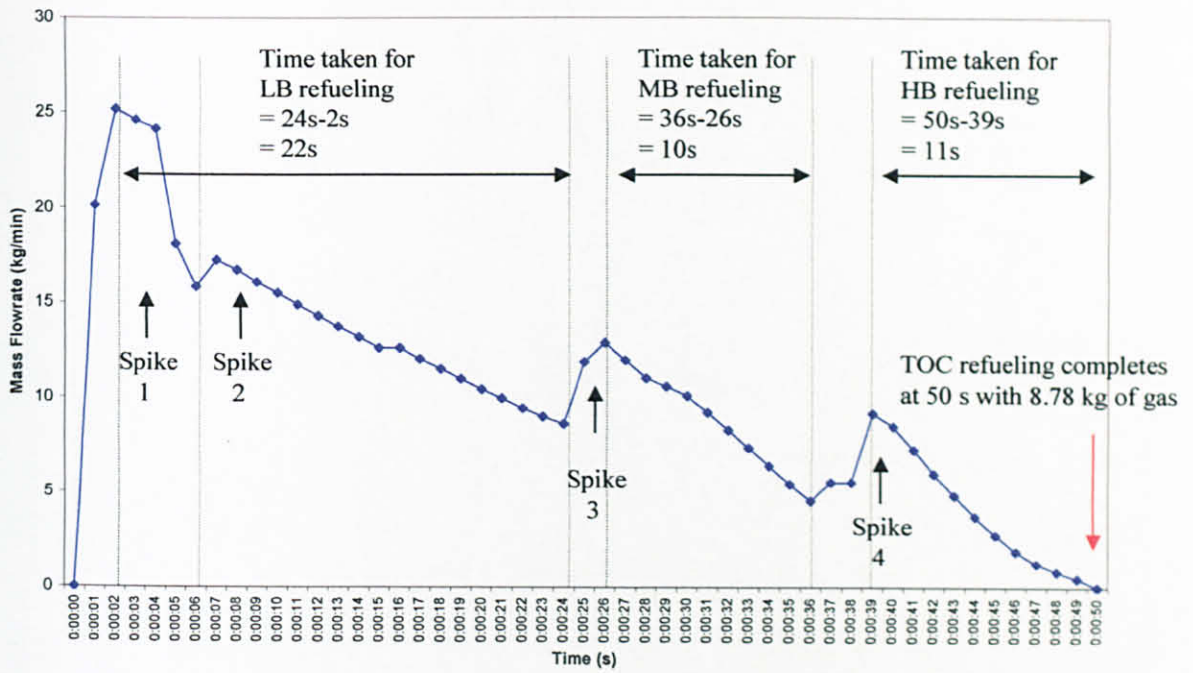


Figure 4.1: Graph of mass flowrate for TOC refueling

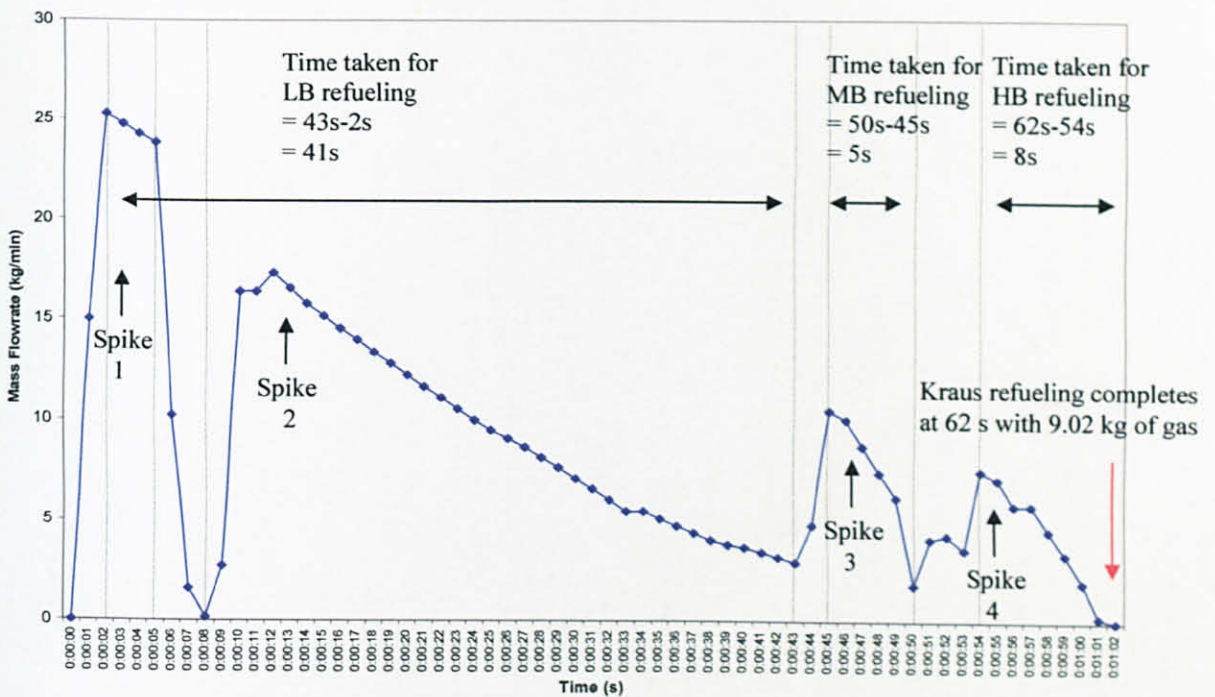


Figure 4.2: Graph of mass flowrate for Kraus refueling

### 4.2.1 Comparison of NGV refueling performance for Experiment 1

Table 4.1 shows comparison for valves switching time, whilst Table 4.2 shows comparison for refueling time transitions. Results show that total time for switch-over and total refueling time transitions taken by TOC refueling are faster and shorter than Kraus refueling.

Table 4.1: Comparison of refueling performance based on valves switching time

Type of NGV refueling algorithm	Time for LB switch-over (s)	Time for MB switch-over (s)	Time for HB switch-over (s)	Total time (s)
<i>TOC</i> (Figure 4.1)	6	24	36	66
<i>Kraus</i> (Figure 4.2)	8	43	50	101
AVERAGE	7	33.5	43	83.5

Table 4.2: Comparison of refueling performance based on refueling time transitions

Type of NGV refueling algorithm	Time taken for LB refueling (s)	Time taken for MB refueling (s)	Time taken for HB refueling (s)	Total time (s)
<i>TOC</i> (Figure 4.1)	22	10	11	33
<i>Kraus</i> (Figure 4.2)	41	5	8	54
AVERAGE	31.5	7.5	9.5	43.5

Based on Figure 4.1, actual refueling time taken and total mass stored until TOC refueling completes are 50 s and 8.78 kg, respectively. Whilst, based on Figure 4.2, actual refueling time taken and total mass stored until Kraus refueling completes are 62 s and 9.02 kg, respectively. Results show that although TOC refueling could minimize refueling time taken, total mass stored would drop compared to Kraus refueling. Reason for the losses are because one performance index of optimal control theory is used i.e., time optimal. To compensate for that losses another performance index need to be combined i.e., fuel optimal as explained in the next chapter. This issue has brought to discussion on performance measures based on two significant consequences i.e., refueling time taken and total mass stored. Discussion would address several issues for various initial pressures inside the receiver tank. The following section describes the second area of experiments.

### **4.3 Performance of refueling by varying initial pressure inside receiver tank**

Sections 4.1 and 4.2 analysed trends when applying either Kraus or TOC refueling, by evaluating time of valves switching and refueling time transitions, respectively. This section is dedicated to analysis of second area of experiments. Initial conditions of experiments are storage pressures tanks are set to 3600 psig, whilst initial pressure inside receiver tank varies from 20 to 2000 psig. Performance of refueling is measured based on refueling time and total mass stored. Values for initial pressure i.e., 20 to 2000 psig are based on Figure 2.9 which simulate various initial pressures for NGV vehicles in Malaysia coming for refueling. The following section describes the first model of the experiment i.e., TOC refueling.

#### ***4.3.1 Test model 2(a): Performance of TOC refueling***

Results of experiments are divided into two sections: the first section is results when initial pressure ranges from 20 to 100 psig, whilst the second section is results when initial pressures ranges from 200 to 2000 psig. Results are divided into two sections because mass flowrates are similar when initial pressure ranges from 20 to 100 psig, but vary when initial pressure ranges from 200 to 2000 psig.

Figure 4.3 shows results of mass flowrates when initial pressure ranges from 20 to 100 psig, whilst Table 4.3 shows results of refueling time and total mass stored. In the following section, Figure 4.4 shows results of mass flowrates when initial pressure ranges from 200 to 2000 psig, whilst Table 4.4 shows results of refueling time and total mass stored. Based on Table 4.3 and Table 4.4, performance measures for TOC refueling is investigated by comparing refueling time with respect to total mass stored.

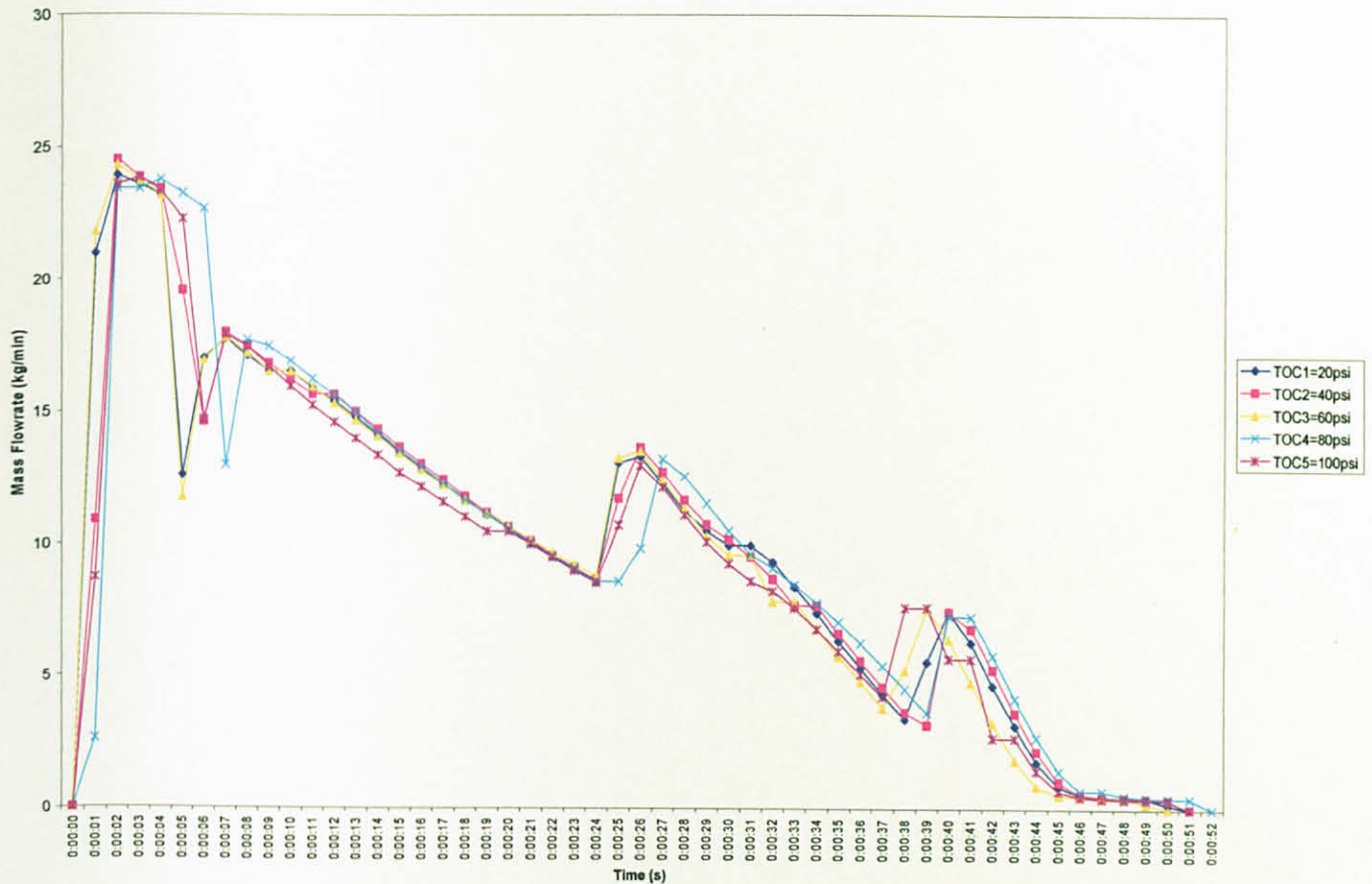


Figure 4.3: Graph of mass flowrate for TOC refueling with all storage pressures set to 3600 psig and receiver tank varies from 20 to 100 psig

Table 4.3: Total time taken and total mass stored for TOC refueling with all storage pressures set to 3600 psig and receiver tank varies from 20 to 100 psig

Experiment	Initial Pressure of receiver tank	Actual initial pressure of receiver tank	Total time taken	Total mass stored
	(psig)	(psig)	(s)	(kg)
TOC1	20	19.24	51.00	8.58
TOC2	40	40.60	51.00	8.53
TOC3	60	60.30	50.00	8.47
TOC4	80	79.66	51.00	8.57
TOC5	100	99.10	50.00	8.25
AVERAGE	60	59.78	50.65	8.48



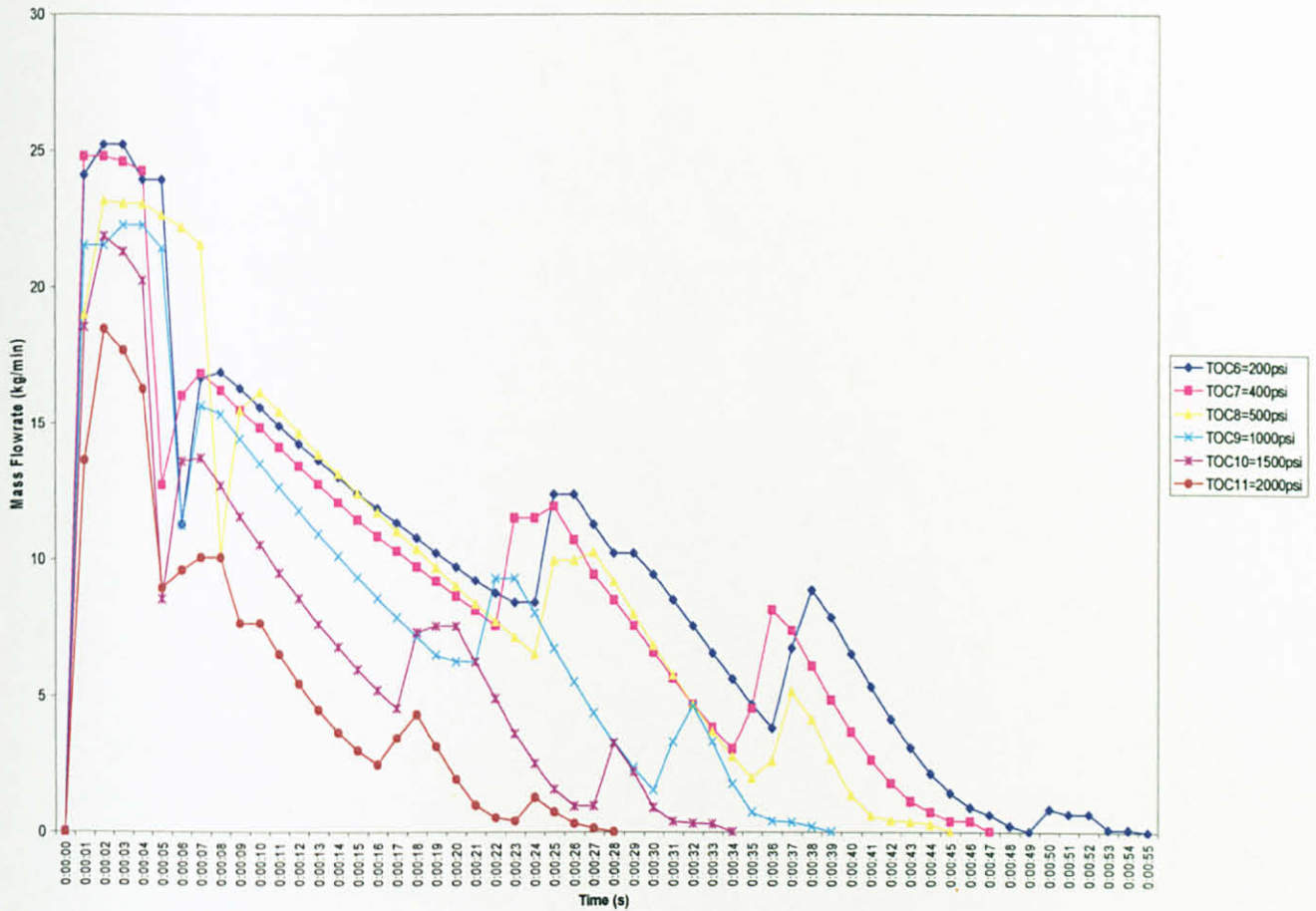


Figure 4.4: Graph of mass flowrate for TOC refueling with all storage pressures set to 3600 psig and receiver tank varies from 200 to 2000 psig

Table 4.4: Total time taken and total mass stored for TOC refueling with all storage pressures set to 3600 psig and receiver tank varies from 200 to 2000 psig

Experiment	Initial Pressure of receiver tank	Actual initial pressure of receiver tank	Total time taken	Total mass stored
	(psig)	(psig)	(s)	(kg)
TOC6	200	196.73	55.00	8.49
TOC7	400	407.02	47.00	7.60
TOC8	500	512.17	45.00	7.31
TOC9	1000	1036.64	41.00	5.80
TOC10	1500	1490.43	34.00	4.19
TOC11	2000	1994.70	28.00	2.72
AVERAGE	933.33	939.62	41.70	6.02

Based on Figure 4.3 and Figure 4.4, it is verified that TOC refueling could complete NGV refueling for initial pressure ranges from 20 to 2000 psig. Several observations could be made based on results from mass flowrates. One of the interesting results is behaviour of valves switching and refueling time transitions. Both of them are not changing when initial pressure ranges from 20 to 100 psig i.e., TOC1 to TOC5, but reduce faster and shorter when initial pressure ranges from 200 to 2000 psig i.e., TOC6 to TOC11.

Based on Table 4.3, when initial pressure ranges from 20 to 100 psig i.e., TOC1 to TOC5, average refueling time and total mass stored for TOC refueling are 50.65 seconds and 8.48 kg, respectively. However, based on Table 4.4, when initial pressure ranges from 200 to 2000 psig i.e., TOC6 to TOC11, refueling time and total mass stored would drop significantly with average values of 41.70 seconds and 6.02 kg, respectively. In order to evaluate performance for TOC refueling, there is need to make a comparison with performance contributed by commercial refueling i.e., Kraus refueling. The following section describes the second model of experiment i.e., Kraus refueling.

#### ***4.3.2 Test model 2(b): Performance of Kraus refueling***

Initial conditions for Kraus refueling experiment are similar with initial conditions for TOC refueling experiment discussed in the previous section i.e., storage pressure tanks are set to 3600 psig, whilst initial pressure varies from 20 to 2000 psig. Results are divided into two sections to compare results of Kraus refueling with Figure 4.3 and Figure 4.4 i.e., results of TOC refueling.

Figure 4.5 shows results of mass flowrates when initial pressure ranges from 20 to 100 psig, whilst Table 4.5 shows results of refueling time and total mass stored. In the following section, Figure 4.6 shows results of mass flowrates when initial pressure ranges from 200 to 2000 psig, whilst Table 4.6 shows results of refueling time and total mass stored.

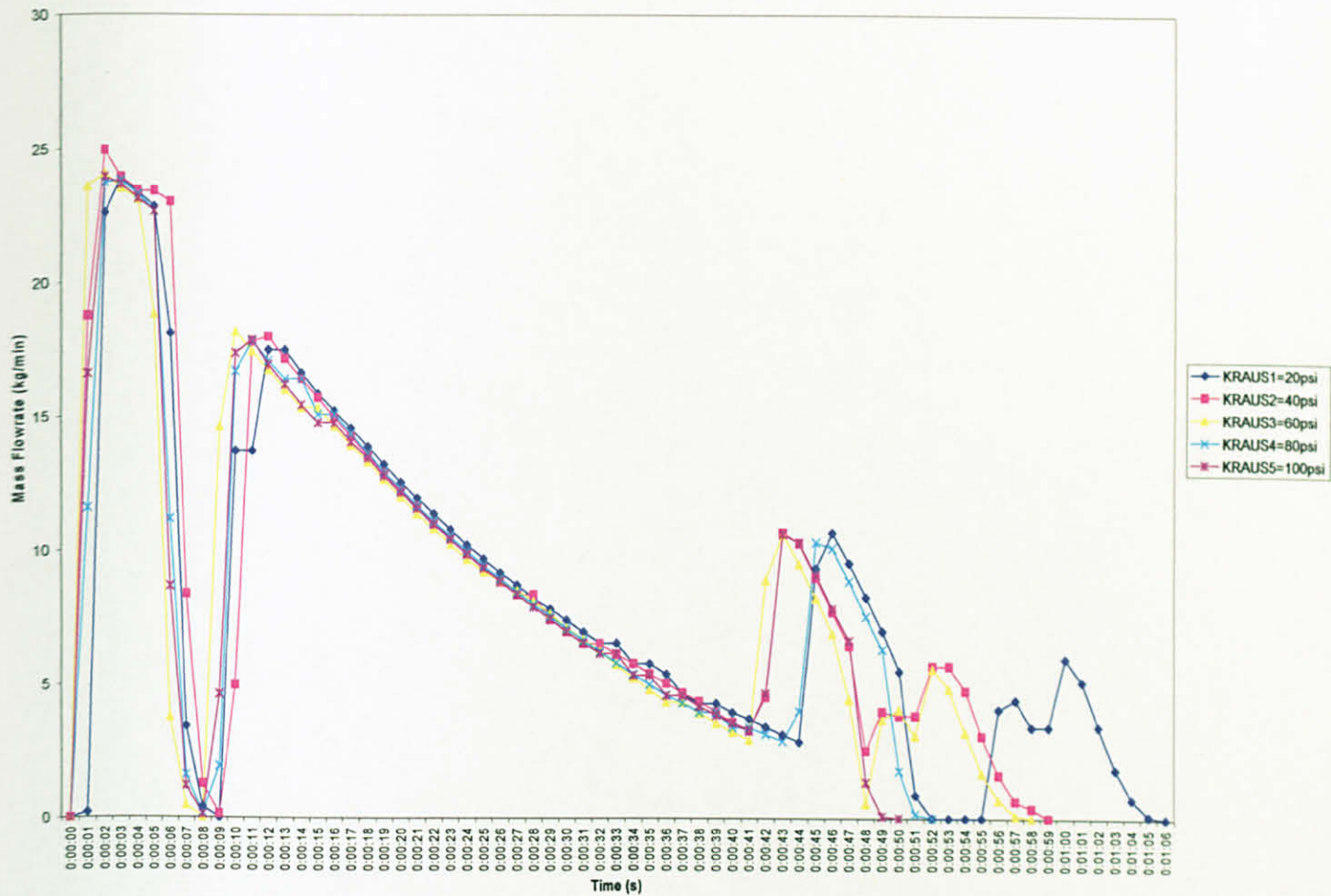


Figure 4.5: Graph of mass flowrate for Kraus refueling with all storage pressures set to 3600 psig and receiver tank varies from 20 to 100 psig

Table 4.5: Total time taken and total mass stored for Kraus refueling with all storage pressures set to 3600 psig and receiver tank varies from 20 to 100 psig

Experiment	Initial Pressure of receiver tank	Actual initial pressure of receiver tank	Total time taken	Total mass stored
	(psig)	(psig)	(s)	(kg)
Kraus1	20	21.58	66.00	8.76
Kraus2	40	40.94	59.00	8.96
Kraus3	60	59.88	58.00	8.61
Kraus4	80	87.42	52.00	8.14
Kraus5	100	99.52	51.00	8.11
AVERAGE	60	61.87	57.20	8.52

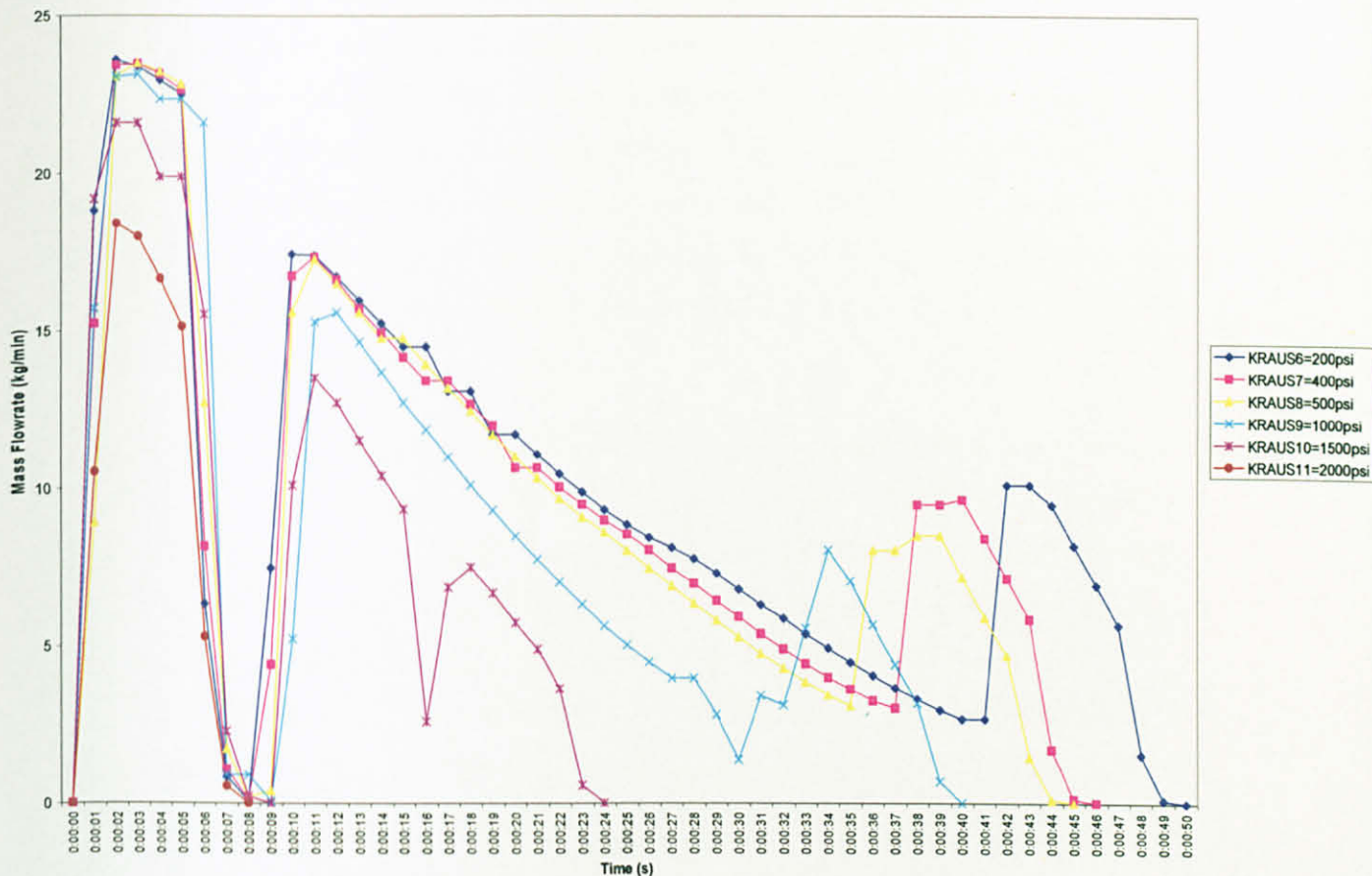


Figure 4.6: Graph of mass flowrate for Kraus refueling with all storage pressures set to 3600 psig and receiver tank varies from 200 to 2000 psig

Table 4.6: Total time taken and total mass stored for Kraus refueling with all storage pressures set to 3600 psig and receiver tank varies from 200 to 2000 psig

Experiment	Initial Pressure of receiver tank	Actual initial pressure of receiver tank	Total time taken	Total mass stored
	(psig)	(psig)	(s)	(kg)
Kraus6	200	200.91	50	7.89
Kraus7	400	379.48	46	7.37
Kraus8	500	514.09	45	7.04
Kraus9	1000	1001.67	40	5.79
Kraus10	1500	1489.76	24	3.77
Kraus11	2000	1981.43	8	1.41
AVERAGE	933.33	927.89	35.50	5.55

Several observations could be made from the second model of experiment. Noted that, when initial pressure is increased, valves switching and refueling time transitions became faster and shorter for whole initial pressure values used in this experiment. Noted that, three spikes occur for initial pressure ranges from 20 to 60 psig i.e., Kraus1 to Kraus3, indicates that refueling is done from three banks. However, only two spikes occur when initial pressure ranges from 80 to 1500 psig i.e., Kraus4 to Kraus10, indicates that refueling is done from low and medium bank, which the low bank refueling time is longer than the medium bank.

The longer refueling time transition at low bank shows that Kraus refueling fully utilizes pressure source at low bank to complete NGV refueling. Interestingly, when initial pressure is 2000 psig i.e., Kraus11, only one spike occurs which is in the initialization stage, indicates that mass flowrate is not sufficient for Kraus to start NGV refueling. Similar spike is experienced when initial pressure is greater than 2000 psig i.e., 2000 to 3000 psig, indicates that Kraus would not start the NGV refueling if initial pressure is greater than 2000 psig. Based on Table 4.5 and 4.6, performance for Kraus refueling is investigated by comparing refueling time with respect to total mass stored for whole initial pressure values used in this experiment.

Based on Table 4.5, when initial pressure ranges from 20 to 100 psig i.e., Kraus1 to Kraus5, refueling time and total mass stored would drop significantly with average values of 57.2 seconds and 8.52 kg. Whilst, when initial pressure ranges from 200 psig to 2000 psig i.e., Kraus6 to Kraus11, refueling time and total mass stored would drop significantly with average values of 35.5 seconds and 5.55 kg, respectively. The following section discusses comparison of refueling performance between TOC and Kraus refueling.

### 4.3.3 Comparison of NGV refueling performance for Experiment 2

This section summarizes results between TOC and Kraus refueling for initial pressure ranges from 20 to 100 psig, whilst the following section shows results for initial pressure ranges from 200 to 2000 psig. Table 4.7 to Table 4.10 show results based on two performance measures i.e., refueling time and total mass stored.

Table 4.7: Analysis of comparison for total time taken between Kraus and TOC refueling when initial pressure inside receiver tank varies from 20 to 100 psig

Initial pressure of receiver tank (psig)	Total time taken by Kraus (s)	Total time taken by TOC (s)	Difference between Kraus to TOC (s)	Percentage of Improvement (%)
20	66.00	51.00	+15.00	+22.73
40	59.00	51.00	+8.00	+13.56
60	58.00	50.00	+8.00	+13.79
80	52.00	51.00	+1.00	+1.92
100	51.00	50.00	+1.00	+1.96
AVERAGE	57.20	50.60	+6.60	+10.79

Table 4.8: Analysis of comparison for total mass stored between Kraus and TOC refueling when initial pressure inside receiver tank varies from 20 to 100 psig

Initial pressure of receiver tank (psig)	Total mass stored by Kraus (kg)	Total mass stored by TOC (kg)	Difference between Kraus To TOC (kg)	Percentage of Improvement (%)
20	8.76	8.58	-0.18	-2.05
40	8.96	8.53	-0.43	-4.80
60	8.61	8.47	-0.14	-1.63
80	8.14	8.57	+0.43	+5.28
100	8.11	8.25	+0.14	+1.73
AVERAGE	8.52	8.48	-0.04	-0.29

For initial pressures ranges from 20 to 100 psig, results indicate that TOC refueling time would be faster than Kraus with a average difference is 6.60 seconds and a average total mass loss is only 0.04 kg, respectively.

However, for initial pressures ranges from 200 to 2000 psig, results show that TOC refueling time would be slower than Kraus with average difference is 6.17 seconds but total mass stored would increase with average values is 0.47 kg, respectively.

Table 4.9: Analysis of comparison for total time taken between Kraus and TOC refueling when initial pressure inside receiver tank varied from 200 to 2000 psig

Initial pressure of receiver tank	Total time taken by Kraus	Total time taken by TOC	Difference between Kraus to TOC	Percentage of Improvement
(psig)	(s)	(s)	(s)	(%)
200	50.00	55.00	-5.00	-10.00
400	46.00	47.00	-1.00	-2.17
500	45.00	45.00	0.00	0.00
1000	40.00	41.00	-1.00	-2.50
1500	24.00	34.00	-10.00	-41.67
2000	8.00	28.00	-20.00	-250.00
AVERAGE	35.50	41.70	-6.17	-51.06

Table 4.10: Analysis of comparison for total mass stored between Kraus and TOC refueling when initial pressure inside receiver tank varies from 200 to 2000 psig

Initial pressure of receiver tank	Total mass stored by Kraus	Total mass stored by TOC	Difference between Kraus to TOC	Percentage of Improvement
(psig)	(kg)	(kg)	(kg)	(%)
200	7.89	8.49	+0.60	+7.60
400	7.37	7.60	+0.23	+3.12
500	7.04	7.31	+0.27	+3.84
1000	5.79	5.80	+0.01	+0.17
1500	3.77	4.19	+0.42	+11.14
2000	1.41	2.72	+1.31	+92.90
AVERAGE	5.55	6.02	+0.47	+19.80

The results verify that for initial pressure ranges from 20 to 100 psig, TOC is better in term of refueling time, whilst for initial pressure ranges from 200 to 2000 psig, Kraus is better in term of total mass stored. No conclusion can be made yet to determine which refueling is better for NGV refueling using multi-pressure storage source. Therefore, another comparison is needed by investigating TOC and Kraus refueling in the third area of experiments i.e., performance of refueling using multi-pressure storage source.

#### **4.4 Performance of refueling using multi-pressure storage source**

Sections 4.2 has been to analyzing trends when applying either TOC or Kraus refueling, by evaluating time of valves switching and refueling time transitions. Whilst, section 4.3 has been to evaluating performance of TOC and Kraus refueling using various initial pressures inside receiver tank. This section is dedicated to analyze the third area of experiments by evaluating performance of TOC and Kraus refueling using multi-pressure storage source tank. In this experiment, storage pressures at low bank, medium bank and high bank are set to pressure ranges from 290 to 2000 psig, 1450 to 3000 psig and 3000 to 3600 psig, respectively, whilst, initial pressure at receiver tank is set initially at 20 psig. The following section describes the first model of experiment.

##### ***4.4.1 Test model 3(a): Performance of TOC refueling***

Figure 4.7 shows results of mass flowrates when storage banks are set at three different pressures i.e., 290-1450-3600 psig, 1000-2000-3000 psig and 2000-3000-3600 psig, whilst Table 4.11 shows results of refueling time and total mass stored. Based on Figure 4.7, it is verified that TOC refueling could complete NGV refueling using multi-pressure storage source. Several observations could be made based on Figure 4.7. One of the interesting results is valves switching and refueling time transitions became faster and shorter when lower pressure source is used. Noted that, when pressure at storage banks are 290-1450-3600 psig, a delay occur before the low bank.



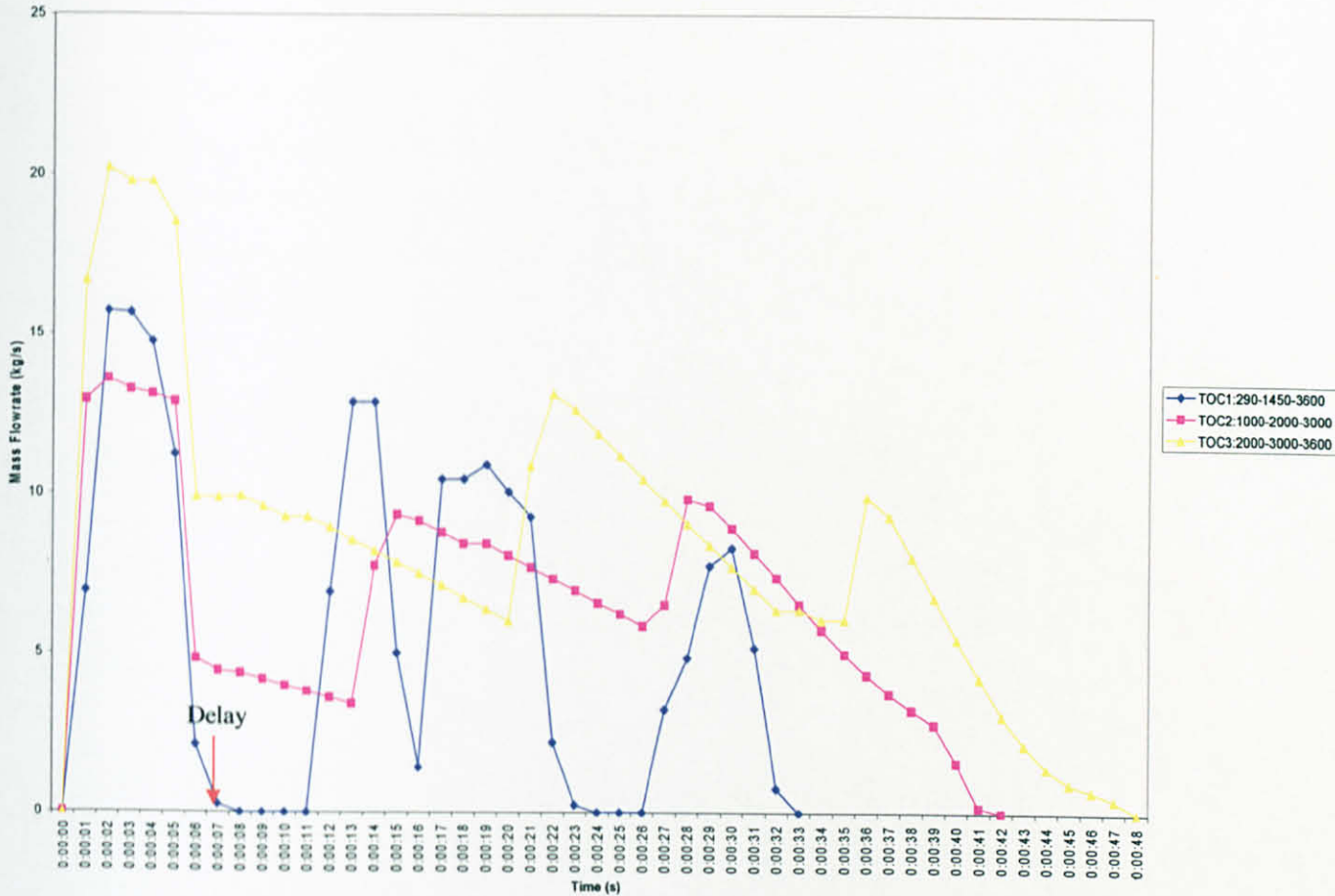


Figure 4.7: Graph of mass flowrate for TOC refueling using different storage pressures with receiver tank initially at 20 psig

Table 4.11: Total time taken and total mass stored for TOC refueling using different storage pressures with receiver tank initially at 20 psig

Initial Pressure of Low Bank, Medium Bank and High Bank (psig)	Actual Initial Pressure of Low Bank, Medium Bank, and High Bank (psig)	Initial Pressure of Receiver tank (psig)	Actual Initial Pressure of Receiver tank (psig)	Total time taken (s)	Total mass stored (kg)
290-1450-3600	296.45-1445.61-3567.52	20	18.66	38.00	3.16
1000-2000-3000	994.41-1996.62-2998.49	20	17.82	42.00	4.71
2000-3000-3600	1980.43-3039.97-3527.30	20	17.99	48.00	6.82
AVERAGE	1090.43-2160.73-3364.44	20	18.16	42.67	4.90

The delay indicates that mass flowrate is not sufficient to start refueling from low bank due to smaller pressure difference between low bank and receiver tank. Thus, the phenomenon is represented by a delay as shown by Figure 4.7. When there is sufficient mass flowrate, a spike occurs to continue TOC refueling from the low bank. However, when pressure source at storage banks are 1000-2000-3000 psig and 2000-3000-3600 psig, spikes occur as usual since mass flowrate is sufficient for TOC refueling to start refueling from all the banks.

Based on Table 4.11, the fastest refueling time that could be achieved by TOC is 38 seconds and the maximum total mass that could be stored is 6.82 kg, respectively. Whilst, average values for refueling time taken and total mass stored are 42.67 seconds and 4.90 kg, respectively. In order to evaluate performance of refueling time and total mass stored for TOC refueling, there is need to make a comparison with Kraus refueling. The following section describes the second model of experiment.

#### ***4.4.2 Test model 3(b): Performance of Kraus refueling***

In the following section, Figure 4.8 shows results of mass flowrates for Kraus refueling when storage banks are set to different pressure, whilst Table 4.12 shows results of refueling time and total mass stored. When storage banks are set to 290-1450-3600 psig, similar observation could be made for Kraus refueling in term of spike occurrence. Noted that, when pressure source is lower i.e., 290 psig, pressure difference is too smaller for natural gas to flow, therefore a delay occurs before the low bank. When mass flowrate is sufficient, refueling starts from the low bank again which could be seen from a spike occurred after the delay. Noted that, when storage banks are set to 290-1450-3600 psig, Kraus refueling uses only two banks to complete NGV refueling i.e., the low bank and the medium bank which could be seen from two spikes, not including spike at the initialization stage. However, when storage tanks are set to 1000-2000-3000 psig or 2000-3000-3600 psig, three spikes occur indicating that Kraus refueling uses the low bank, medium bank and high bank to complete NGV refueling.

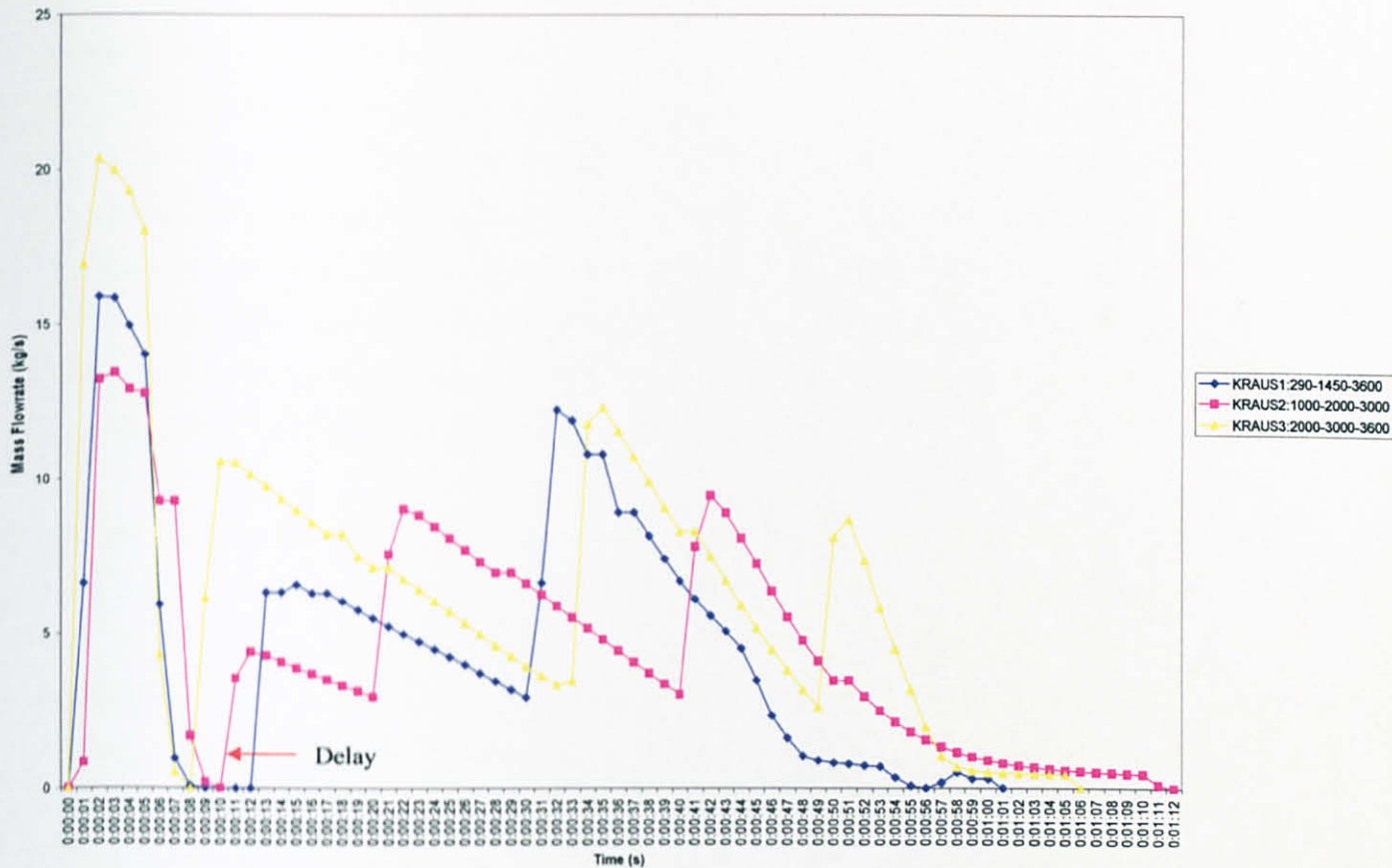


Figure 4.8: Graph of mass flowrate for Kraus refueling using different storage pressures with receiver tank initially at 20 psig

Table 4.12: Total time taken and total mass stored for Kraus refueling using different storage pressures with receiver tank initially at 20 psig

Initial Pressure of Low Bank, Medium Bank and High Bank	Actual Initial Pressure of Low Bank, Medium Bank, and High Bank	Initial Pressure of Receiver tank	Actual Initial Pressure of Receiver tank	Total time taken	Total mass stored
(psig)	(psig)	(psig)	(psig)	(s)	(kg)
290-1450-3600	288.44-1451.62-3594.31	20.00	18.91	66	4.87
1000-2000-3000	989.49-1939.12-2984.31	20.00	17.49	72	5.41
2000-3000-3600	2082.40-3073.26-3560.68	20.00	19.57	66	7.27
AVERAGE	1120.11-2154.67-3379.77	20.00	18.66	68	5.85

Based on Table 4.12, the results imply that the fastest refueling time that could be achieved by Kraus is 66 seconds and the maximum total mass that could be stored is 7.27 kg. Whilst, average values for refueling time and total mass stored are 68 seconds and 5.85 kg, respectively. Results indicate that valves switching and refueling time transitions for Kraus refueling are becoming faster and shorter if suitable arrangement of pressure sources are used. Major impact that could be identified by Kraus refueling using different pressure storage source is from the results shown by Table 4.12. Noted that, there are two observations that prove performance of Kraus refueling is inaccurate if applied in NGV refueling using multi-pressure storage source.

Firstly, the refueling time is similar for storage banks set to 2000-3000-3600 psig and 290-1450-3600 psig i.e., 66 seconds, but the total mass is different i.e., 7.27 kg and 4.87 kg. Secondly, when storage banks set to 1000-2000-3000 psig, refueling time would be longer i.e., 72 seconds and total mass stored drop tremendously i.e., 5.41 kg compared to storage banks set to 2000-3000-3600 psig, which has shorter refueling time i.e., 66 seconds and higher total mass stored i.e., 7.27 kg. These results show that performance of Kraus refueling is vague and not suitable to be implemented in NGV refueling using multi-pressure storage source.

Results from this experiment have described clearly performance of TOC and Kraus refueling using multi-pressure storage source, which TOC refueling has major advantage in term of refueling time compared to Kraus refueling. The following section discusses comparison between TOC and Kraus refueling.

#### 4.4.3 Comparison of NGV refueling performance for Experiment 3

Table 4.13 and Table 4.14 show results of refueling time and total mass stored between Kraus and TOC refueling when storage banks set to different pressure values, whilst initial pressure inside receiver tank is set initially at 20 psig.

Table 4.13: Analysis of comparison for total time taken between Kraus and TOC refueling using different storage pressures with receiver tank initially at 20 psig

Pressure at Low Bank, Medium Bank and High Bank (psig)	Total time taken by Kraus (s)	Total time taken by TOC (s)	Difference between Kraus to TOC (s)	Percentage of Improvement (%)
290-1450-3600	66.00	38.00	28.00	+42.42
1000-2000-3000	72.00	42.00	30.00	+41.67
2000-3000-3600	66.00	48.00	18.00	+27.27
AVERAGE	68.00	42.67	25.33	+37.12

Table 4.14: Analysis of comparison for total mass stored between Kraus and TOC refueling using different storage pressures with receiver tank initially at 20 psig

Pressure at Low Bank, Medium Bank and High Bank (psig)	Total mass stored by Kraus (kg)	Total mass stored by TOC (kg)	Difference between Kraus to TOC (kg)	Percentage of Improvement (%)
290-1450-3600	4.87	3.16	1.71	-35.11
1000-2000-3000	5.41	4.71	0.70	-12.94
2000-3000-3600	7.27	6.82	0.45	-6.19
AVERAGE	5.85	4.90	0.95	-18.08

Based on Table 4.13 and Table 4.14, the results show that TOC refueling time is much faster than Kraus refueling with average difference is 25.33 seconds and total mass loss is only 0.95 kg. Based on Table 4.12 and discussion from the previous section, it is verified that Kraus refueling is inaccurate and not suitable for NGV refueling using multi-pressure storage source. In conclusion, this experiment validates that TOC refueling is the suitable method for NGV refueling using multi-pressure storage source as proposed by Radhakrishnan et al. [4].

## 4.5 Summary

Results of experiments described in this chapter are based on two criterions, i.e., refueling time and total mass of natural gas stored. These become performance measures to compare with other NGV refueling currently applied in commercial NGV dispenser i.e., Kraus refueling. Three experiments are conducted to evaluate performance of TOC and Kraus refueling: the first experiment is performance of valves switching and refueling time transitions; the second experiment is performance of refueling when storage pressures are set to 3600 psig whilst receiver tank is varied from 20 to 2000 psig; the third experiment is performance of refueling when storage pressures are set to different pressures while receiver tank initially at 20 psig. The results from the third experiment verifies the viability of TOC compared to Kraus refueling to be used as a switching controller in NGV refueling using multi-pressure storage source, which average difference for refueling time and total mass loss is 25.33 seconds and 0.95 kg, respectively. Reason for losses are because one performance index of optimal control theory is used i.e., time optimal. To compensate for that losses another performance index need to be used i.e., fuel optimal by determining optimal total mass with respect to time as proposed in the next chapter.

## **CHAPTER 5**

### **CONCLUSION**

#### **5.1 Conclusion**

The aim of this thesis has been to design and implement switching time strategies for an NGV refueling system that would provide a minimum switching time and a faster filling rate for NGV refueling using multi-pressure storage source.

It discusses fundamental issues in development of simulation model for an NGV refueling system and methodology for optimization of the switching; and has covered two main issues: development of model and experimental design. In particular, it has been organized to answer questions such as,

- what optimization method is required to produce an optimized switching time for storage banks.
- how to implement method and build a simulation model for optimization purpose.
- how to specify problems and scenarios to be analyzed (the relevant experimental design), and
- how to extract useful information for comparisons.

In a survey, it was found that initial pressure inside NGV vehicle that came for refueling in Klang Valley varies from 20 to 2000 psig, where most of them came with an empty tank or in some cases, the initial pressure was less than 20 psig. Hence, the scope of this research work is to design a switching algorithm for an NGV refueling controller that is able to perform effectively in these conditions.

Results from experiments have shown that refueling algorithm developed from this work is capable of providing switching strategy for NGV refueling with multi-pressure storage source by determining the optimum time to switch between NGV storage banks, reducing the filling time of NGV and increasing the filling capacity at storage aboard of NGV. By implementing TOC refueling algorithm in actual NGV refueling station, it is expected to provide savings in term of time consumed by NGV vehicle owners and could resolve congestion problem at NGV refueling station within the country.

The main contributions of this work are:

- The detailed comparisons of three criteria (the amount of time for refueling with a multi-level pressure source, the filling time, and the filling capacity) for an NGV refueling system were given. The TOC algorithm, which has not been reported elsewhere to be used in an NGV refueling station has been shown to have several advantages compares to other existing refueling method i.e., Kraus.
- As existing method applied in NGV refueling system in the country is not able to reduce NGV congestion problem, this work demonstrated steps taken in analyzing and developing an optimized switching strategies for an NGV refueling system using the well established technique of optimal control theory and validating the results on actual multi-stage NGV test rig. One of the promising results is faster refueling time with minimal loss of natural gas stored in receiver tank i.e., NGV vehicle.

## 5.2 Direction for Future Work

It is important to point out that not all locations of NGV refueling station in Malaysia are congested with NGV vehicles. The most congested area is particularly refueling stations in Klang Valley which TOC refueling strategy could be introduced to reduce the refueling time. Time Optimal Control, as suggested in this work may provide optimum refueling time but that does not mean it is sufficient to optimize the overall architecture of NGV refueling system i.e., the multi-pressure storage source and the energy consumptions by the NGV compressor.



It has been mentioned in Chapter 4 that although TOC refueling could minimize refueling time, the total mass would drop slightly compared to Kraus refueling. The drop in the total mass would have been contributed by hardware used such as data acquisition loop rate, delayed signal from transmitters and other disturbances occurred during the experiments. Since in this work only one performance index has been considered, an improved TOC is anticipated if additional performance indices could be implemented.

At this point, at least two other optimal controls need to be analyzed: first the Fuel Optimal Control i.e., for controlling the distance traveled based on minimal fuel on car storage or total mass stored in NGV, and second the Energy Optimal Control which is ideal for controlling NGV compressor efficiency with minimal energy utilization. The conceptual design of NGV refueling station for these optimization problems are shown by Figure 5.1.

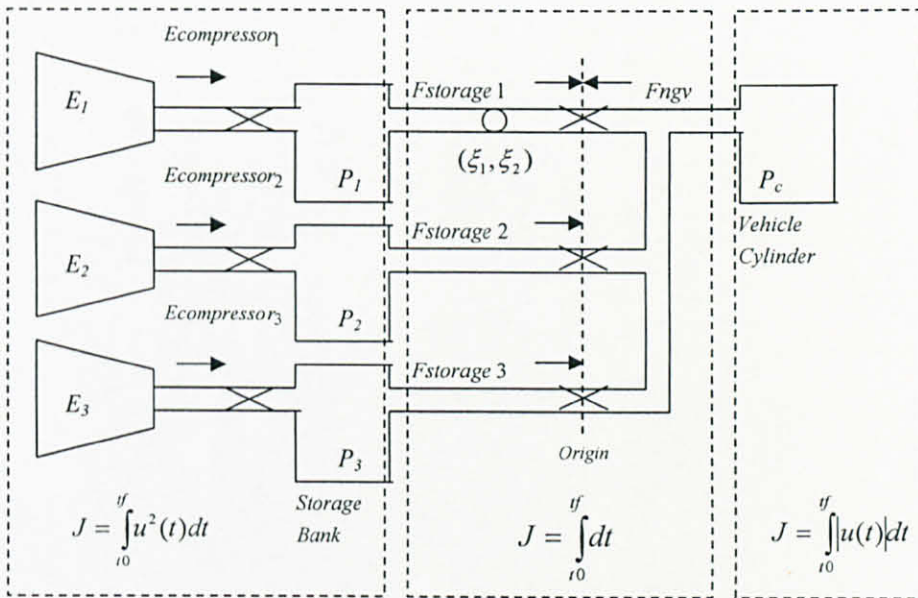


Figure 5.1: Optimization study for NGV refueling system

- Fuel Optimal Control systems arise in NGV where the vehicle is controlled by thrusts and torques. The inputs like thrusts are due to the burning of fuel of mass. Hence, the natural question is whether the mass from the NGV vehicle can be controlled to minimize the fuel consumption. Let  $u(t)$  be the thrust of an NGV engine and assume that the magnitude  $|u(t)|$  of the thrust is proportional to the rate of fuel consumption. In order to minimize the total expenditure of fuel, the performance index can be formulated as

$$J = \int_{t_0}^{t_f} |u(t)| dt \quad (5.1)$$

- For Energy Optimal Control systems, the performance measure is often formulated as the energy of an electrical system. For example, if  $u(t)$  is the voltage input to a field circuit in a typical constant armature-current, field controlled positional control system, with negligible field inductance and a unit field resistance, the total energy to the field circuit is (power is  $u^2(t)/R_f$ , where,  $R_f = 1$  is the field resistance)

$$J = \int_{t_0}^{t_f} u^2(t) dt \quad (5.2)$$

For NGV congestion problem, the suitable solution for optimal control is combination of time and energy optimal which time optimal would make refueling time faster, whilst energy optimal would make energy consumed by NGV compressor minimal, in order to maintain higher pressure at storage banks and continuous pressure difference with NGV vehicles. If station is in normal condition, the preferable solution is combination of time and fuel optimal which time optimal would make refueling time faster, whilst fuel optimal would make total mass loss minimal, in order to achieve higher filling capacity.

The work presented in this thesis has contributed to an improved switching time, and may be up to some extent the congestion problem of NGV refueling stations. Even though the approach presented here offers some promising results, much work remains to be done to produce global optimization that includes other variables i.e., Fuel and Energy Optimal Control.

## REFERENCES

1. Gas Malaysia Sdn. Bhd. Homepage.  
URL: <http://www.gasmalaysia.com>. (Jan 1, 2005)
2. *The Guidelines on Natural Gas for Vehicle (NGV)*, Petronas NGV Sdn Bhd (2004)
3. M.G. Daud, *Experiences and Challenges in the Implementation of NGV/CNG As a Clean Fuel of Choice for Malaysian Transportation Sector*, The paper presented in ANGVA 2005 Conference, Kuala Lumpur, July 2005.
4. V.R. Radhakrishnan, N.A. Hisam, M.I.A. Mutalib, M.N. Abdullah "*Mathematical Model of the Refueling System of a Compressed NGV*" The paper presented in ANGVA 2004 Conf, Buenos Aires, Oct, 2004
5. Code of Practice for CNG Compressor Refueling Stations: On-Site Storage and Location of Equipment, MS 1204: 2001, Department Of Standards Malaysia
6. Wednesday, February 11, 2004, Article taken from AAM "*Drive*" Autoworld Magazine January/February 2004.
7. Jordair CNG Technical Exchange Presentation, p.7 - 9  
URL: [http://www.jordair.ca/P\\_CNG\\_Tech\\_2.htm](http://www.jordair.ca/P_CNG_Tech_2.htm) (Jun 7, 2003)
8. M.Schuker, "*Experiences and Challenges in CNG Measurement – The Case for Coriolis Flow Meter*" The paper presented in ANGVA 2005, Kuala Lumpur, July 2005.
9. G. Thomas, J.W.Goulding, and C. Munteanu, "*Measurement, Approval and Verification of CNG Dispensers*", KT11 Report, p. 10  
URL: <http://www.nwml.gov.uk/legis/refs/kt11.pdf> (July 7, 2004)
10. Naidu, D.S "*Optimal Control Systems*" CRC Press, Boca Raton, Florida, 2003

11. Kuo, B. Yackel, R. and Singh, G., "*Time-optimal control of a stepping motor*" IEEE Trans on Automatic Control, Vol. 14, Issue. 6, pp. 747- 749, Dec 1969
12. J. Chang and J.H.Chow, "*Time-optimal control of power systems requiring multiple switchings of series capacitors*" IEEE Trans on Power Systems, Vol. 13, Issue. 2, pp. 367-373, 1998
13. M. G. Park and N.Z Cho, "*Time-optimal control of nuclear reactor power with adaptive proportional -integral-feed forward gains*", IEEE Trans on Nuclear Science, Vol.40, Issue.3, pp. 266-270, Jun 1993
14. Danbury, R.N. "*Near time-optimal control of nonlinear servomechanisms*" IEEE Proceedings in Control Theory and Applications, Vol. 141, Issue. 3, pp.145 - 153, May 1994
15. Moon, M.S., VanLandingham, H.F. and Beliveau, Y.J. "*Expert rule based time optimal control of crane loads*" The paper appeared in Proceedings of the 1996 IEEE on Control Application, pp. 602-607, Sept 1996
16. Turnau, A., Korytowski, A. and Szymkat, M, "*Time optimal control for the pendulum-cart system in real-time*", Proceedings of the 1999 IEEE International Conference on Control Applications, Vol. 2, pp. 1249-1254, 1999
17. Furuta, K. Xu, Y. and Gabasov, R., "*Computation of time optimal swing up control of single pendulum*" The paper appeared in Industrial Electronics Society, IECON '99 Proceedings, Vol. 3, pp.1165-1170, 1999
18. Eker, J. and Malmborg, J. "*Design and implementation of a hybrid control strategy*" The paper appeared in Control Systems Magazine, IEEE Trans, Vol. 19, Issue. 4, pp. 12-21, Aug 1999
19. Heckenthaler, T and Engell, S "*Approximately time-optimal fuzzy control of a two-tank system*" The paper appeared in Control Systems Magazine, IEEE Trans, Vol. 14, Issue. 3, pp. 24-30, Jun 1994

20. Walther, U. Georgiou, T.T. and Tannenbaum, A. "*On the computation of switching surfaces in optimal control: a Grobner basis approach*" IEEE Trans on Automatic Control, Vol.46, Issue. 4, pp. 534-540, Apr 2001
21. Hol, C.W.J., van Willigenburg, L.G., van Henten, E.J. and van Straten, G. "*A new optimization algorithm for singular and non-singular digital time-optimal control of robots*", Proceedings of the 2001 ICRA IEEE International Conference on Robotics and Automation, Vol. 2, pp. 1136 – 1141, 2001
22. Galicki, M. "*Time-optimal controls of kinematically redundant manipulators with geometric constraints*" IEEE Trans on Robotics and Automation, Vol.16, Issue. 1, pp. 89-93, Feb 2000
23. Reynolds, N.C and Meckl, P.H "*Hybrid optimization scheme for time-optimal control*" Proceedings in American Control Conference, Vol. 5, pp. 3421 – 3426, June 2001
24. Penev, B.G and Christov, N.D. "A fast time-optimal control synthesis algorithm for a class of linear systems" Proceedings of the 2005 on American Control Conference, Vol. 2, pp. 883 - 888, June 2005
25. Melsa, J. and Schultz, D. "A closed-loop, approximately time-optimal control method for linear systems" IEEE Transactions on Automatic Control, Vol. 12, Issue.1, pp. 94-97, Feb 1967
26. Zhiqiang Gao, "*On discrete time optimal control: a closed-form solution*" The paper appeared in: Proceedings of the 2004 on American Control Conference, Vol. 1, pp. 52-58, July 2004
27. Ailon, A. and Langholz, G, "A study of controllability and time-optimal control of a robot model with drive train compliances and actuator dynamics" IEEE Trans on Automatic Control, Vol. 33, Issue. 9, pp. 852 – 856, Sept. 1988
28. Newman, W.S. "*Robust near time-optimal control*" IEEE Trans on Automatic Control, Vol. 35, Issue. 7, pp. 841 – 844, July 1990
29. Shiller, Z., "*On singular time-optimal control along specified paths*", IEEE Trans on Robotics and Automation, Vol. 10, Issue. 4, pp. 561 – 566, Aug. 1994

30. Ebrahimi, A., Moosavian, S.A.A. and Mirshams, M. "*Minimum-time optimal control of flexible spacecraft for rotational maneuvering*" Proceedings of the 2004 IEEE International Conference on Control Applications, Vol. 2, pp.961-966, Sept 2004
31. Sakagami, N. and Kawamura, S., "*Time optimal control for underwater Robot manipulators based on iterative learning control and time-scale transformation*" The paper appeared in OCEANS 2003 Proceedings, Vol.3, pp.1180-1186, Sept. 2003
32. Brown, R.H., Zhu, Y. and Feng, X. "*A new relaxation algorithm for the time optimal control problem of step motors*" The paper appeared in Proceedings of the 28th IEEE Conference on Decision and Control, Vol. 1, pp. 907-908, Dec 1989
33. Clark, M. and Stark, L., "*Time optimal behavior of human saccadic eye movement*" IEEE Transactions on Automatic Control, Vol. 20, Issue 3, pp. 345-348, Jun 1975
34. Steiner, G. Watzonig, D. Schweighofer, B. "*Time optimal control of ultrasonic transducers for improved multiple object recognition*" The paper appeared in Robot Sensing, 2004, pp. 69-73, 2004
35. Furukawa, T.; Durrant-Whyte, H.F.; Dissanayake, G. and Sukkarieh, S.; "*The coordination of multiple UAVs for engaging multiple targets in a time-optimal manner*" The paper appeared in Intelligent Robots and Systems, 2003 (IROS 2003), Vol. 1, pp. 36-41, Oct. 2003
36. M. Athans and P. Falb. "*Optimal Control: An Introduction to the Theory and Its Applications*" McGraw Hill, New York, NY, 1966
37. Kraus Global Inc Homepage  
URL: <http://www.krausglobal.com> (Nov 27, 2005)
38. National Instruments Homepage  
URL: <http://www.ni.com> (Dec 20, 2005)

## APPENDIX

### Description for Process & Instrumentation Diagram (P&ID)

To have better understanding on the process flow of the test rig, a Process and Instrumentation Diagram (P&ID) is included as shown in Figure A1. As can be observed from the figure, materials or equipments are presented by tag numbers. These tag numbers will be defined individually in the process explanation and can be referred from Table A1. There are 4 types of flowmeters installed in the dispensing system which are Coriolis **B310**, Turbine **B320**, Differential Pressure **B330** and Vortex **B340** with Coriolis flowmeter acting as the reference flowmeter. At any time, only Coriolis and any one of the three flowmeters could be used. Data from all flowmeters are electronically retrieved and stored in a data acquisition system **YC01**. The recycle system is to recover and recycle the natural gas from car storage into the supply storage system. The system consists of two timed-filled compressors **B470** and **B480**. It is expected a small amount of natural gas from car storage will be lost during each experiment trial. Thus, the system is equipped with make-up cylinders **B270** to compensate for the losses. The supply storage system consists of nine 55 liters cylindrical tanks altogether with maximum pressure at 3600 psig (at 70 °C) and they are all placed in one rack. These tanks are sub-divided into three different bank systems, low bank (LB) **B280**, medium bank (MB) **B290** and high bank (HB) **B300**. LB, MB and HB systems have 4, 3 and 2 cylindrical tanks respectively. All of these tanks have the same pressure of 3600 psig when they are fully occupied by natural gas. What differentiate these tanks are their functions and number of tanks. To dispense natural gas to vehicle tank **B260**, nozzle **B250** is connected to receptacle that is located at the cylinder's neck. After that, the switch on display panel is turned to 'ON' position. Next, the nozzle valve **B250** is turned to 180 degree to 'ON' position. When the dispensing occurs, the **B240** hose should not be connected to the vehicle tank. The hose is only connected to **B070** and **B110** valves when recycling system is operated. The pressure, temperature and mass of natural gas are measured using transmitters **B390**, **B450**, and **B460** as shown in the diagram. These transmitters will then send input signal to the data acquisition system **YC01**.

## Refueling and Recycling Process

At the very beginning of the dispensing, natural gas from low bank **B280** flows to the vehicle tank **B260**. The gas flows due to differential pressure between the tanks. The gas will continue to flow until pressure in the vehicle tank **B260** approach the pressure in the low bank **B280**. Then the flow will switch to medium bank **B290** to continue refueling until pressure in the vehicle tank **B260** approach the pressure in the medium bank **B290**. Lastly, the flow will switch to high bank **B300** to perform the same task until the vehicle tank **B260** reaches its maximum capacity. These filling processes are controlled by solenoid valves which get input signal from control system **YC01**. The natural gas will flow through Coriolis flowmeter **B310** and sends the measured value to the data acquisition system **YC01** using pressure transmitter **B350**. Coriolis flowmeter is generally regarded as a master flowmeter because it offers greatest accuracy and reliability under the exacting measurement conditions for determining mass of Compressed Natural Gas (CNG) compared to other volumetric flowmeters which are Turbine **B 320**, Differential P ressure **B 330** and Vortex **B 340**. Since the flowmeters are installed parallel to each other, the natural gas flows only through any one of these flowmeters. Finally the natural gas will flows through flexible hose **B230** and nozzle **B250** into the vehicle tank. After the refueling process, recycling system is used to empty the vehicle cylinder **B260** by transferring the gas to the storage cylinders **B280**, **B290** and **B300**. This is done via timed-filled compressor that has inlet and discharge pressure of 1.25 psig and 3600 psig respectively. Once empty, the compressor **B470** or **B480** will stop before the next sampling process could take place. To operate the recycling system, flexible hose **B240** is connected to temporary storage tank **B270**. One end of high pressure flexible hose is coupled to ball valve **B070** located at bottom neck of the vehicle tank **B260** while the other end is connected to inlet of check valve **B110**. After that, both valves **B070** and **B060** are turned to 'ON' position. Natural gas will flow to the temporary storage tanks **B270** before it is stored back to low bank **B280**, medium bank **B290** and high bank **B300** until all pressures approach the pressure value set at control system **YC01**.





ITEM	DESCRIPTION	QTY	MATERIAL/SPECIFICATION
B010	VALVE, BALL	3	PARKER P/N: HPB6S8A
B020	VALVE, BALL	8	PARKER P/N: HPB6S8FF
B030	VALVE, BALL	2	KITZ BRASS 150PSIG MAWP
B040	VALVE, BALL	1	SWAGELOK P/N: SS-63TS8
B050	VALVE, BALL	3	SWAGELOK P/N: SS-33VF4
B060	VALVE, BALL	1	SWAGELOK P/N: SS-83KS8
B070	VALVE, BALL	1	OASIS P/N: BV506-NT
B075	VALVE, BALL	4	PARKER P/N: 4A-B2LJ2-SSP
B080	VALVE, BALL PNEUMATIC	3	PARKER P/N: 8A-B8LJ2-SSP-62AC-3
B090	VALVE, BALL PNEUMATIC	2	PARKER P/N: 8F-B8LJ2-SSP-62AC-3
B100	VALVE, CHECK	3	PARKER P/N: 8A-C8L-1-SS
B110	VALVE, CHECK	3	SWAGELOK P/N: SS-CHS16-1
B120	VALVE, CHECK	2	SWAGELOK P/N: SS-CHS4-1
B130	VALVE, CHECK	4	PARKER P/N: 4A-C4L-1-SS
B140	VALVE, NEEDLE	1	AGCO-P/N: H5RIC-22
B150	VALVE, NEEDLE	1	SWAGELOK P/N: SS-1RS4
B160	VALVE, NEEDLE	3	PARKER P/N: 4A-V4LN-SS
B170	VALVE, RELIEF	1	SWAGELOK P/N: SS-4R3A1 SET @ 3750PSIG
B180	VALVE, RELIEF	3	SWAGELOK P/N: SS-4R3A SET @ 3950PSIG
B185	VALVE, RELIEF	1	SWAGELOK P/N: SS-RL4M8F8 SET @ 100PSIG
B190	VALVE, REGULATOR	1	JORDAN P/N: JHR Cv=0.6 SET @ 150PSIG
B200	VALVE, REGULATOR	1	JORDAN P/N: JHR Cv=0.6 SET @ 30 PSIG
B210	VALVE, REGULATOR	1	JORDAN P/N: MARK608 5/16" OR SET @ 7" H2O
B220	VALVE, REGULATOR	1	JORDAN P/N: MARK608 5/16" OR SET @ 35" H2O
B230	HOSE, FLEXIBLE	1	SWAGELOK P/N: SS-NGS6-NN-120X
B240	HOSE, FLEXIBLE	1	PARKER P/N: 5CNG0101-16-16-16-120
B250	NOZZLE	1	SWAGELOK P/N: SS-83XKF4
B260	CYLINDER, NGV	1	EKC 1x55LWC 3600PSIG
B270	CYLINDER, NGV	1	EKC 3x55LWC 3600PSIG
B280	CYLINDER, NGV	1	EKC 4x55LWC 3600PSIG LOW BANK
B290	CYLINDER, NGV	1	EKC 3x55LWC 3600PSIG MEDIUM BANK
B300	CYLINDER, NGV	1	EKC 2x55LWC 3600PSIG HIGH BANK
B310	FLOW, SENSOR CORIOLIS	1	MICROMOTION P/N: CNG050S239NCAZEZZZ
B320	FLOW, SENSOR TURBINE	1	HOFFER P/N: 3/ 4x3 /4-25-CB-1RPR-MS-CE
B330	FLOW, SENSOR ORIFICE	1	ENDRESS + HAUSER P/N: DN25 PN250
B340	FLOW, SENSOR VORTEX	1	ENDRESS + HAUSER P/N: 70HS25-D0D20B100
B350	FLOW, TRANSMITTER CORIOLIS	1	MICROMOTION P/N: 2700111BBFEZZZ
B360	FLOW, TRANSMITTER TURBINE	1	HOFFER P/N: HIT2A-3-B-C-X-FX
B370	FLOW, TRANSMITTER ORIFICE	1	ENDRESS + HAUSER P/N: PMD235-MB588EM3C
B380	FLOW, TRANSMITTER VORTEX	1	ENDRESS + HAUSER P/N: 70HS25-D0D20B1B100
B390	PRESSURE, TRANSMITTER	3	ENDRESS + HAUSER P/N: PMP731-I33Z1M21X1
B400	PRESSURE, TRANSMITTER	2	MURPHY P/N: PXMS-6000
B410	PRESSURE, TRANSMITTER	5	MURPHY P/N: PXMS-5000
B420	PRESSURE, GAUGE	1	SWAGELOK
B430	PRESSURE, GAUGE	4	SWAGELOK
B440	PRESSURE, GAUGE	2	ASHCROFT 2-1/2" DIAL 0-60" H2O
B450	TEMPERATURE, TRANSMITTER	3	ENDRESS + HAUSER P/N: TMT162-E21231AAA
B460	LOAD CELL	1	METTLER TOLEDO EX APPROVED, 0-150KG
B470	COMPRESSOR, TIME FILLED	1	FUEL MAKER P/N: FMQ-2-36
B480	COMPRESSOR, TIME FILLED	1	FUEL MAKER P/N: FMQ-8-36
YC-01	DISPENSER REGISTER	1	KRAUS P/N: 09 N28AGUCGMS-D
YC-02	DATA ACQUISITION SYSTEM	1	NATIONAL INSTRUMENTS FIELDPOINT

Table A: Bill of Material